To Carolyn

BLOOD FLOW IN NARROW CAPILLARIES

BY

JAMES MEREDITH FITZ-GERALD

IMPERIAL COLLEGE

A thesis submitted in fulfilment of the requirements for the degree of Doctor of Philosophy of the University of London.

November, 1969.

Abstract

This thesis discusses several aspects of the problem of the mechanics of blood flow in narrow capillaries. In Chapter I an historical development is presented, including theoretical and experimental work on blood rheology, vessel morphology, red cell mechanics and flow properties of blood components.

Chapter II contains a description of the mechanics of red cell motion, in terms of a lubrication concept. It is shown that enhanced resistances to motion are expected, which depend non-linearly on the applied pressure gradient. The elastic properties of the red cell itself are examined, and included in the theory.

In Chapter III, these theoretical results are expressed in more direct, physiologically-relevant forms, and their implication for capillary flow phenomena are explored. Topics discussed include vasomotion and autoregulation, patchy filling of pulmonary networks, and the non-uniform viscosity of blood in narrow capillaries.

An analysis of plasma flow in the spaces between red cells is given in Chapter IV. Analytic solutions for the velocity field are obtained, and compared with previous numerical results. The relevance of these flow patterns to mass transport phenomena is discussed.

Finally, Chapter V briefly describes a model experiment designed to test the theory of Chapter II. Model red cells, consisting of fluid-filled latex membranes, were forced down a perspex tube. The prediction of enhanced, non-linear resistances was confirmed, and observation of some of the plasma flow patterns found in Chapter IV was also possible.

Acknowledgements

I have great pleasure in expressing my gratitude to Professor M.J. Lighthill for his constant advice and assistance. Under his guidance, I have been introduced to an intensely interesting field of research; without his interest and encouragement, the work of this thesis would not have been possible.

I am deeply indebted also to Dr. C.G. Caro, for many stimulating discussions on the physiological aspects of the work, for his generous personal assistance, and for making available the facilities of the Physiological Flow Studies Unit, Imperial College, for experimental research.

The generosity of the Trustees of the Gowrie Scholarship Trust Fund, in the award of a Major Hore-Ruthven Travelling Scholarship, is gratefully acknowledged.

Finally, my thanks are due to my wife, for her assistance in the preparation of the thesis; her patience and understanding have never faltered.

Table of Contents

Chapter		Page
I	The Development of the Problem	1.
II	Mechanics of Red Cell Motion through Very Narrow Capillaries	20.
III	Implications of a Theory of Erythrocyte Motion in Narrow Capillaries	89.
IV	Plasma Flow in Inter-Erythrocyte Spaces	120.
V	A Model Capillary Flow Experiment	147.

Chapter I

'The Development of the Problem'

Although the existance of capillaries in the circulation was discovered by Malpighi almost two hundred and fifty years ago, no serious study was made of them until the work of August Krogh, in the early 1920's. He investigated capillary flow patterns, discussed the behaviour of blood in the capillaries (red cell deformation and plasma 'skimming', for example), and extended Starling's (1896) concepts of the exchange of gases, water and metabolites, through the capillary wall, between blood and tissue. This latter work was done in collaboration with his wife, Marie Krogh, and was influential, in particular, in establishing the physical diffusion concept of oxygen supply in the lungs, rather than the earlier, erroneous, 'secretion' theory.

Krogh's work was chiefly qualitative and descriptive, and until the 1960's, little was done towards an understanding of the quantitative, mechanical aspects of capillary flow. A partial exception was the work of Fahreus and Lindquist (19) on the viscosity of blood in narrow tubes; they found that the viscosity apparently decreased as the diameter of the tube decreased. Although this

theory recognized that blood does not behave as a Newtonian fluid, and used the two-phase nature of blood to explain this qualitatively, it suggested that flows in narrow vessels may be explained using a concept of a non-Newtonian system, whose viscosity depends in some way on the vessel diameter.

It is now recognized that such a straightforward, rheological approach is inadequate for an accurate description of the flow properties of whole blood. In any detailed, dynamical discussion of flow phenomena, it is necessary to regard the blood as a suspension of 'formed elements', chiefly erythrocytes, in the plasma; furthermore, it is essential to include as a cornerstone of any theory the ease of deformation of the red cells. Recent filmed studies, for example by Goldsmith and Mason (1968) and by Monro (1966), have demonstrated the importance of red cell deformability for blood flow in small vessels (say 20-40 microns), and near the walls of larger ones. The inwardly-directed pressure on the cells caused by asymmetric distribution of 'flailing' collisions in space-dependent shearing flows (which, together with a resultant 'lift' on individual bodies, is thought to be responsible for the axial concentration phenomenon), is more effective for flexible than for rigid particles.

For flow in narrow capillaries, it is perhaps even more essential to include the flexibility of red cells as a central theme of any investigation of the mechanics. In some cases, the capillary diameter is smaller than that of the undistorted erythrocyte, which must be deformed (possibly accompanied by capillary deformation) even to allow it to fit inside. It must therefore be expected that the elastic properties of the cell play a significant role in determining the charactistics of the motion. Gabe and Zatz (1968) have demonstrated that plasma behaves as a Newtonian fluid to very good accuracy, so that the Navier-Stokes equations may be used to describe the flow of plasma around the erythrocytes. The Reynolds' number for plasma under capillary flow conditions is very small, of the order of 10^{-2} or 10^{-3}; the motion is therefore governed by a balance between pressure gradient and viscous forces; inertial terms in the equations of motion may be ignored. Theoretical attacks based on this concept of a two-phase system supported by a Newtonian fluid seem to offer the best hope for an adequate discussion of capillary dynamics, and recent work on these lines will be discussed below.

A well-known experimental study of the physics of narrow-capillary flow was made by Prothero and Burton

(1961, 1962a and b), with two principal techniques: measurement of blood flow through artificial capillaries, and modelling of the flow on a larger scale using dimensional similarity. They also studied the ease of passage of red cells through millipore filters. These classical experiments represented a substantial contribution to the understanding of the problems of capillary dynamics, and a significant attempt to gain insight into the physical characteristics of a physiological phenomenon. With work of such a pioneering nature, it was perhaps inevitable that the full significance of various parameters of the system should not have been realized, particularly since the magnitude of some of the effects are quite surprising in comparison with what might be expected from more familiar situations. The work is of sufficient importance to merit a fairly detailed discussion.

The model experiments were intended principally to investigate mass transfer between blood and surrounding tissue, as influenced by the 'bolus' flow of plasma between successive red cells in narrow capillaries; they utilized heat transfer to water containing trains of bubbles to simulate such conditions, and care was taken to maintain the Peclet number (which determines the relative importance of diffusion and convection) at the correct

value. Unfortunately, it was not possible to reproduce the in vivo value of the Reynolds' number, which was of order 10 in the experiments. This is some three orders of magnitude too large, and it might be inferred that artifacts may have been introduced into their results by excessive inertial effects in the bolus flow. Further, the hydrodynamic boundary conditions at an air-water interface are different from those at a solid boundary. Direct application of the quantitative results to the capillaries, therefore, should perhaps be made with some caution. A more detailed discussion of mass transfer phenomena in the capillaries is given in Chapter IV.

It was also inferred from the model experiments that although the resistance of the fluid bolus was increased by the toroidal motion, the overall resistances of cell-plasma trains in capillaries should be less than that given by Poiseuille's law, mainly because the viscocity of plasma is much less than a typical viscosity for whole blood. These results were apparently confirmed by studies of blood flow in micropipettes of average diameter 8.4 microns, but tapering at the ends to as little as 5 microns. Resistances corresponding to effective viscosities of the order of 30% higher than that of plasma (considerably lower than typical values for blood) were

obtained, and it was inferred that the resistance offered by the red cells, even in a deformed, compressed state in narrow capillaries, was negligible; variation in resistance was chiefly due to changes in the flow in the plasma 'bolus' separating successive red cells. Studies using millipore filters showed that red cells would readily pass through fine filters (5 microns effective pore diameter) under very small pressure differences; this was interpreted as confirmation of the negligible red cell resistance (Burton 1966).

Limitations in flow measuring technique (for these extremely small flow rates) meant that the smallest usable velocity was of the order of 30 cms/sec, rather than the 100-1000 microns/sec found in living capillaries of similar dimensions; this was a consequence of the necessity for using tube diameters in the same size range as the red cell. Two possible sources of error are introduced into the interpretation of the results. Firstly, the Reynolds' number is again some three orders of magnitude too large, so that inertial effects may produce artifacts, particularly in the development of the toroidal motion in the plasma bolus. Secondly, the relatively enormous shear rates in the blood at these velocities may well have so deformed the flexible red cells that their effect-

ive diameter was considerably less than that normally found; and the results could be interpreted as being typical of flow in somewhat larger capillaries. It is interesting that Whitmore (1967) pointed out the agreement between the results of Prothero and Burton and his theoretical predictions for capillaries of diameter larger than the effective diameter of the red cell; Whitmore's theory is discussed below. Similar considerations apply to the millipore filter experiments, and these are considered in more detail in Chapter III.

Subsequent work by Rand and Burton (1964) investigated the mechanical properties of red cells, in particular of the cell membranes. They measured the flexibility, or 'deformability', of cells in response to distorting forces, and found that this was due to a combination of elasticity and bending moment. The experiments also showed that erythrocyte deformations involve principally a change of shape, and that surface area and volume do not change appreciably; indeed, an increase of only 10% in surface area was found to cause haemolysis (cell rupture). Fung (1966) made a theoretical study of possible modes of deformation available to red cells (isochoric and applicable), and also pointed out that, in contrast, the walls of systemic capillaries, at least, are much less compli-

ant than are red cells.

This question of capillary deformation is very interesting, and quite controversial. Fung's calculations are based on a 'tunnel in a gel' concept; however, in the pulmonary circulation at least, the capillaries are contained in very thin membranes, and have relatively unsupported walls. Glazier et al. (1963) have demonstrated that the mean diameter of such capillaries varies with the transmural pressure, and it is known that under zero flow conditions the walls of pulmonary capillaries may collapse, although the absence of smooth muscle in capillaries means that this must be a passive rather than an active phenomenon. Krogh's work showed that under certain circumstances capillary elasticity may be of importance for pressure-flow relationships; on the other hand, Burton (1966) has found no observable deformation in systemic capillaries after the introduction of high-pressure air bubbles. The problem of whether capillary deformation affects flow characteristics is further discussed in Chapter II.

Another phenomenon which must be considered in a discussion of dynamics in capillaries is that of loss or gain of fluid through the endothelium by filtration. Although Starling's original model involving diffusion

under the combined action of fluid and osmotic pressure differences has been shown to be only a crude approximation to the actual mechanism, it is still accepted that a proportion of plasma, perhaps as much as 10% of the total, moves out of the capillary in the proximal region, and returns in the distal region; a small fraction, perhaps 0.5%, is removed in the lymph circulation. The effect of this fluid exchange might well be of significance for flow mechanics, and is considered in the final section of Chapter II.

An important theoretical contribution was made by Whitmore (1967), who studied the flow of a two-phase system in tubes of capillary dimensions. Two models were used: a 'shearing-core' model for large capillaries, and an 'axial train' model for capillaries sufficiently small that the red cells travel in single file along the axis of the lumen. The behaviour of particles, both rigid and deformable, in sheared-core flows has been studied experimentally and theoretically by Goldsmith and Mason (1964); they described the distribution of forces on the particles, and showed that a tendency towards axial concentration is to be expected. The results of the two theories were matched graphically in the intermediate region (capillaries of diameter in the range 12-20 microns). Whitmore

found that for the model, the Fahreus-Lindquist viscosity-reducing mechanism ceases to apply for capillaries smaller than about 15 microns, where the effective viscosity was about half that of whole blood. The viscosity then increased, rapidly below about 10 microns, where the value was about equal to that for whole blood. The position of the (local) viscosity minimum depended on the velocity; the possibility of cells 'curling' in the sheared plasma is introduced, and an 'effective cell diameter' is used in the calculations, although no attempt is made to relate this to the unstressed cell diameter. No mention is made of local cell membrane deformation, but the importance of 'leak-back' of plasma past the cells is brought out. The theory is considered not to apply to vessels whose diameters approach that of the stressed red cells (below 8 microns, say), because of a failure of the assumptions beyond that point.

It should perhaps be mentioned that cinematographic evidence does not, on the whole, support the 'axial train' concept for vessels of diameter greater than about 10 microns; cell deformation in larger vessels permits a 'sheared core' type of flow. Detailed application of Whitmore's results to <u>in vivo</u> phenomena is therefore inadvisable; the overall concept, however, of a gradual

transition from sheared-core to axial-train behaviour in narrow capillaries is very valuable, and provides a link between theories based on the Fahreus-Lindquist effect and the present work on lubricated motion in very narrow capillaries.

The notion of leakback, or relative movement of the plasma back past the cells, is connected with the difference in mean velocity between cells and plasma; cells travel faster in the capillary than does the plasma. Some of this effect may be due to a type of pericapillary flow, in which plasma moves along an annular space outside the lumen, somewhat more slowly than does the blood inside; such a theory is discussed, for example, by Howe and Schaeffer (1967). Leakback, however, must also play a part in creating the velocity difference, and in the case of very narrow capillaries, Lighthill (1968) has mentioned the possible importance of leakback in promoting mass transfer to the endothelium.

Further theoretical contributions have been made. Wang and Skalak (1968) considered the movement of rigid spherical particles along closely-fitting, fluid-filled tubes, for diameter ratios between about 0.2 and 0.8. Bloor (1968) treated the flow patterns in the motion of rigid cylindrical particles in a tube, and although he

found resistances higher than those for the supporting fluid alone, no mention was made of the possible effects of red cell elasticity on the pressure-flow relationships. Bloor's work, however, was principally concerned with fluid motions in the spaces between particles, discussed more fully in Chapter IV.

Omission of elastic effects from a model of red cell motion in narrow capillaries introduces at least one severe defect; it ignores the necessity for a normal force to be sustained at the rim of the erythrocyte to produce deformation, and the effect this will have on the mechanics. Thus in Bloor's work, for example, simple Couette flow was assumed between the rigid cylinders and the tube wall. A more realistic approach utilizes viscous forces to balance the required normal force; such a system is provided by a modified form of hydrodynamic lubrication. The classical theory may be coupled with an equation describing the distortion produced in the red cell membrane (and possibly in the capillary wall) by the lubrication pressures. The complete process is therefore envisaged as one of elastohydrodynamic lubrication.

The necessity for such a treatment was first realized by Lighthill (1968, 1969), who gave an important theoretical discussion of the problem. In his paper on the

lubricated motion of elastic pellets in elastic tubes, he proposed a model which, although employing some fairly crude approximations, retained all the essential physical features of red cell movement. The results of the discussion indicated the important characteristics of elastic-pellet motion; perhaps the most significant concerned the comparatively large resistances offered, under certain circumstances, by the pellet-fluid system in narrow tubes. Predicted velocities were smaller, for a given pressure gradient, than those for a hypothetical, corresponding homogeneous fluid having the same bulk viscosity as the two-phase system. These velocities depended non-linearly on the pressure gradient, and lubrication film thickness was also found to depend on velocity. The possibility of 'seize-up' due to lubrication failure at low film thicknesses (low velocity) was introduced.

The potential importance of Lighthill's results for problems of capillary flow suggested that a detailed study, employing more sophisticated mathematical models, would be valuable. The second chapter presents a discussion of such a study, in the form of a paper published in Proc. Roy. Soc, B. An analysis of the work of Lighthill is made, with a view to determining the most desirable features to include in the new model. A theory of lub-

rigorous motion of an axisymmetric elastic pellet is presented, and the elastic behaviour of a fairly realistic red cell model is discussed. The theoretical results are then applied to the basic problem of the form of the pressure-flow relationship for a capillary, and tentative quantitative predictions are made. Later sections extend the theory to cases where non-axisymmetric pellets and porous tubes are included.

The third chapter, comprising a paper accepted for publication by the Journal of Applied Physiology, seeks to enlarge on the physiological aspects of the work. A summary of the mathematical theory is given, emphasizing the features which have particular significance for capillary flow problems. The theoretical results are expressed in directly applicable forms, and several flow phenomena are discussed in the light of the predictions. In view of the paucity of observational data in some cases, the agreement with *in vivo* experiment is quite satisfactory. The topics discussed comprise pressure-flow relationships in the capillaries, perfusion control, vasomotion and autoregulation, pulmonary capillary networks, and apparent viscosity; comparison is made wherever possible with recent experimental work.

The importance of the thin lubrication layer for

the transport of gases (O_2 and CO_2), nutrients and metabolites between red cell, plasma and endothelium has been mentioned by Lighthill (1968). However, a considerable portion of the red cell surface is exposed to plasma which is comparatively distant from the endothelium, and transfer to and from these regions may be influenced to some extent by the patterns of flow in the bolus separating successive red cells. The effect depends on the relative importance of convection and diffusion, expressed by the Péclét number Ua/κ; this determines the manner in which the distribution of concentration occurs in the fluid. The significance of convection for mass-transport may be quantified in terms of a Nusselt number, which measures the enhancement by convection of transfer to a surface. A discussion of the magnitudes of these parameters for various blood components is given in Chapter IV. Prothero and Burton (1961) have shown, for example, that the Péclét number for oxygen is of order unity, and demonstrated in a model experiment that convection could considerably enhance transfer; the possible limitations of that experiment have already been discussed.

A complete treatment of gas uptake or release by the blood would be very complex, involving diffusion in the alveolus, in the alveolar wall, across the endothel-

ium, in the plasma, across the red cell membrane, in the red cell itself, where non-linear second-order chemical reactions further complicate the analysis; and then release involving these processes in reverse to the systemic capillary endothelium, together with an equation such as that of Krogh-Erlang for oxygen supply and consumption in the tissues. An important step in the understanding of the process, however, is to investigate the effect of flow regimes in the plasma.

Prothero and Burton's suggestion of a circulating bolus flow has prompted several numerical solutions of the equations of motion for flow between successive obstacles in pipe flow. Bugliarello et al. (1966) used a very simplified model with a jump singularity in the stream function at the point where the 'red cell' met the 'capillary wall'; and although their numerical technique used only a small number of mesh points, the streamlines obtained agreed well with the postulated flow of Prothero and Burton. Calculations of a similar nature, but with much higher accuracy, were made by Gross (1967); again the toroidal flow pattern was obtained.

Bloor examined the case of rigid cylinders moving in a closely-fitting tube. Using the velocity profile of the known Couette flow in the narrow gap as a boundary

condition for the flow in the fluid-filled spaces between the two cylinders, he found numerical solutions for various inter-cylinder distances. While his results agreed with those of Bugliarello and Gross for spacings of the same order of size as the tube diameter, he found that the toroidal circulations broke up into two or more concentric toroids as the spacing decreased. It is interesting that no evidence of such a phenomenon was obtained even from the accurate computations of Gross.

An analytic solution was obtained by Wang and Skalak (1969) for flow in a fluid-filled tube containing a row of solid spheres. They used periodic solutions of the biharmonic equations in combinations with certain singular solutions to form functions which satisfied the boundary conditions on the tube; linear combinations of these new functions were then used to satisfy the boundary conditions on the spheres. Again the basic toroidal motion in the fluid between the spheres was obtained. Their method was valid, however, only for spheres whose diameter was somewhat smaller than that of the tube - convergence became inconveniently slow for diameter ratios greater than about 0.8. Like Bloor, they did not include any mention of elastic effects in their model.

The difficulty of obtaining a single, overall sol-

ution in the limiting case where pellet diameter is very nearly equal to tube diameter was overcome by Bloor essentially by matching a solution obtained analytically in the narrow, constricted region with a numerical one in the non-constricted section. In Chapter IV, a similar technique is used to obtain an analytic solution for the flow in the inter-erythrocyte spaces. These spaces are assumed to be finite, fluid-filled cylinders; the ends represent the red cell faces, except for a narrow gap at the tube wall, where the velocity profile is assumed known from the lubrication theory of Chapter II.

A series of eigenfunctions, satisfying the boundary conditions on the tube wall, is obtained for the stream function; these are then superimposed on the basic Poiseuille solution to fit the boundary conditions at the red cell faces. Streamlines are plotted for typical situations. An interesting feature of the solution obtained is the existence of a highly-sheared region adjacent to the tube wall; this effect is virtually independent of both cell spacing and the thickness of the lubrication film. The high-shear zone extends some distance across the red cell face; and some of the streamlines of the flow intrude into the entry and exit portions of the lubrication layer. The significance of these flow characteristics is discussed

with relation to the mass transfer problem.

Finally, in Chapter V, a description is given of a model experiment designed to test the findings of the lubrication theory of pellet motion. Fluid-filled, latex models of red cells are forced along an oil-filled perspex tube by applied pressure differences, and pressure-flow relationships are obtained. The results confirm the enhanced, non-linear resistances predicted for such a system, and observations of small particles suspended in the fluid also allow qualitative confirmation of the flow patterns predicted for inter-pellet regions.

References

Bloor, M.I.G. 1968 Phys. Med. Biol., 13, 443.

Bugliarello, G., H.J. Day, A. Brant, A.J. Eggenburger & G.C.C. Hsiao 1966 Proc. First Int. Conf. Haemorheology, Reykjavik, p305 (Pergamon, 1968).

Burton, A.C. 1966 Federation Proc., 25, 1753.

Fahreus, R. & T. Lindquist 1931 Amer. J. Physiol., 96, 562.

Fitz-Gerald, J.M. 1969 Proc. Roy. Soc. B (in the press).

Fitz-Gerald, J.M. 1969 J. Appl. Physiol. (in the press).

Fung, Y-C. 1966 Federation Proc., 25, 1761.

Gabe, I.S. & L. Zatz 1968 Biorheology, 5, 86.

Glazier, J.B., J.M.B. Hughes, J.E. Maloney & J.B. West 1968 CIBA Symposium on Circulatory and Respiratory Mass Transport, London (Churchill, 1969).

Goldsmith, H.L. & S.G. Mason 1966 Proc. First Int. Conf. Haemorheology, Reykjavik, p237 (Pergamon, 1968).

Gross, J.F. 1969 Euromech 12, Jablonna.

Howe, J.T. & Y.S. Schaeffer 1967 Circulation Res., XXI, 925.

Krogh, A. 'The Anatomy and Physiology of Capillaries' (Hafner, 1930).

Lighthill, M.J. 1968 J. Fluid Mech., 34, 113.

Lighthill, M.J. 1968 CIBA Symposium on Circulatory and Respiratory Mass Transport, London (Churchill, 1969).

Monro, P.A.G. 1963 Biorheology, 1, 239.

Prothero, J. & A.C. Burton 1961 Biophys. J., 1, 565.

Rand, R.P. & A.C. Burton 1964 Biophys. J., 4, 115.

Starling, E.H. 1896 J. Physiol., London, 19, 312.

Wang, H. & R. Skalak 1969 J. Fluid Mech., 38, 75.

Whitmore, R.L. 1967 J. Appl. Physiol., 22, 767.

Chapter II

'Mechanics of Red Cell Motion through Very Narrow Capillaries'

Abstract

In a recent paper, Lighthill (1968) has formulated a model of compressible pellet movement through narrow, fluid-filled, elastic tubes; the model involves a thin lubricating layer of fluid between the pellet and the wall, and the results obtained are expressed in the form of relationships between various velocity, resistance, clearance, and lubrication-film thickness parameters. An important biological motivation for this work was the problem of movement of red blood cells through narrow capillaries. The present paper examines in detail the approximations and assumptions of Lighthill's model, and extends the investigation in several directions. Firstly, the elastic behaviour of the pellet is discussed with particular relevance to the red cell, which is considered to consist of a fluid-filled, flexible membrane. It is shown, in particular, that as the velocity of such a red cell in a capillary increases, the consequent increase in viscous drag on the rim tends to 'bow' the cell, and allow it to fit more easily into a capillary of given diameter.

Further, the modulus of elastic response to the non-uniform lubrication pressures around the rim is shown to depend on the membrane's 'resistance to deformation' and the geometry of the cell.

Next, a model of axisymmetric pellet flow through a tube is set up. Results are expressed in terms of clearance and resistance experienced by the pellet, for various velocities and film thicknesses typical of capillary flows. Much greater resistances than those estimated by Lighthill are obtained; for normal flow in capillaries of 5-7 microns diameter, these range from 4.5 to 7 times that expected for a corresponding Poiseuille fluid flow with whole-blood viscosity. It is not suggested that these results are true of all capillaries, or of a capillary network, but only of those very narrow capillaries in the diameter range being considered. Of equal importance is the non-linear dependence of resistance on velocity. The red cell velocity falls off very rapidly as the pressure gradient is reduced; this is discussed in detail with reference to the phenomenon of autoregulation.

Finally, the effects of asymmetry and tube porosity are considered. It is shown that deviations from axisymmetry tend to be reduced by pressures developed in the fluid; this is due to the compressible nature of the pell-

cts, and means that the results obtained for capillary flow are reasonably valid even for configurations in which the red cells may not be axisymmetric. Leakage of plasma through the walls of the capillary is shown not to affect the flow characteristics of a capillary to any great extent, or to significantly increase the possibility of seizing-up of the flow due to failure of lubrication at small film thicknesses.

Introduction

In a recent paper (henceforth referred to as [1]), Lighthill (1968) has discussed the behaviour of tightly-fitting pellets of solid matter, possibly elastic, being forced along possibly distensible tubes by pressure gradients in the fluid with which, in addition to the pellets, the tubes are filled. The principal biological motivation for this investigation was the movement of blood through very narrow capillaries; considerations of the relative dimensions, and direct observations, show that the flow must involve the passage of individual red cells along the capillary, separated by what Burton (1964) has called a 'bolus' of viscous fluid (the plasma). In addition, it must be expected that some deformation of the cells, and possibly of the capillary, must occur to allow passage of the cells through the tube.

Accordingly, a highly simplified model involving elasto-hydrodynamic lubrication of the cells by the plasma was set up; the model retained, however, certain features of the system considered essential for any realistic discussion of the problem. The purpose of this paper is to examine the problem in detail using more complex models, as suggested in the introduction to [1]. Results obtained in the present investigation fit into the same general qual-

itative pattern as Lighthill's, but produce substantial quantitative modification of certain of Lighthill's conclusions; in particular, under certain circumstances very high resistances, much greater than those experienced in purely fluid flow, are predicted; in addition, some interesting new phenomena are brought to light.

1. Discussion of the approximations

We shall first set out the basic principles of the elasto-hydrodynamic lubrication theory; in this context, we shall then discuss the geometrical and elastic assumptions and approximations used in [1], and the mathematical characteristics of the model so obtained; an assessment of the relative accuracy of the approximations made will be useful in determining the desirable features for a more refined physical model. The tube and pellet are initially supposed axisymmetrical (but see section 4, where effects of asymmetry are considered), with the maximum diameter of the pellet taking at the downstream pressure a value differing from that of the tube by a small fraction (positive or negative); it is assumed that only those regions where the gap (between pellet and tube) is small significantly affect the elastic and hydrodynamic processes. In all of what follows, 'downstream' will refer to that portion of

the tube into which the pellet is moving, regardless of the fluid behaviour in any coordinate system which may be introduced. Further, the shape of the pellet is taken to be that of some simple mathematical function (a parabola was used in [1]), with curvature appropriate to the physiological (or physical) system under discussion. The tube wall is assumed to be non-porous, while the elastic behaviour of both pellet and tube is expressed by some dependence of radial displacement on the pressure distribution in the lubrication film.

We shall be interested in determining expressions for the pressure, fluid velocity, and gap profile under various circumstances, and deriving from these expressions functional relationships between quantities which govern the physical characteristics of the system. For example, we shall want to know how the resistance of the pellets to the driving pressure gradient depends on the velocity of the pellets, and on the relative sizes of pellet and tube. It would also be useful to obtain information on typical thicknesses found for the lubrication film, and how much fluid leaks back past the pellet during the motion. Such knowledge may then be used to gain insight into the mechanics of, say, red cell motion in narrow capillaries; in this paper, we shall be particularly interested in any

special advantages which the microcirculation morphology has in comparison with other possible systems.

Under these assumptions, we may set up a continuity equation for flow in the gap; then, making the usual assumption of lubrication theory, that inertial forces may be ignored, we obtain from the Navier-Stokes equations an expression for longitudinal velocity, assuming also that pressure is independent of position in any plane normal to the tube's axis. Introducing the leakback Q, defined as the nett flux backwards (per unit length of undistorted tube circumference) past any plane normal to the axis in a coordinate system where the pellet is stationary, we obtain a Reynolds' equation for the lubrication flow as

$$\frac{1}{\mu}\cdot\frac{dp}{dx} = f(U,Q,R(x),h(x),r_o) \qquad (1.1)$$

where U is the velocity of the pellet along the tube, R(x) the pellet radius, h(x) the gap thickness, r_o the tube radius, μ the viscosity, and x is the longitudinal coordinate; the function f is the resultant of two pressure gradients, one due to the relative motion of the tube and pellet, and the other to the presence of a nett flux of fluid through the gap.

Suppose, now, that a reference pressure p_o exists, such that if this pressure were acting in the lubrication region, the radius of tube and pellet would be equal (due

to elastic distortion); this pressure will obviously be dependent on the initial clearance between pellet and tube, and will be discussed more fully later. We may represent the pellet profile under the action of this pressure as $r = c(x)$, and the tube radius as r_o. If the pellet is symmetric about $x = 0$, clearly $c(0) = r_o$ by the above definition of reference pressure. In what follows, we shall define r_o as the 'undistorted tube radius', so that 'distortion' will refer to elastic displacements caused by pressures generated in the lubrication film. Under the action of such a (non-uniform) pressure, we may express the pellet radius as

$$R(x) = c(x) - l_1(p - p_o) \qquad (1.2)$$

where $l_1(p(x))$ denotes the functional dependence on pressure mentioned above. Similarly, we may express the tube radius as

$$r(x) = r_o + l_2(p - p_o)$$

where l_2 also denotes some functional dependence. Various authors, e.g. Fung (1966), have pointed out that, in the systemic capillaries, the compliance of the wall and surrounding tissue is expected to be orders of magnitude less than that of the red cell; and in fact no distortion of the wall is observed even with the introduction of high-press-

ure bubbles into systemic capillaries (Burton 1966). In the analysis of section 4, we shall therefore ignore tube compliance, although retaining it in the present section to show briefly how it could be included in the theory if necessary. It may be suggested that since most pulmonary capillaries are not surrounded by relatively inelastic tissue (in the septa of the alveoli), capillary compliance may become important in this case. Glazier et al (1968) found, however, that a pressure of 50 cm of water (approx.) is needed to fully expand the capillaries; pressure increases in the lubrication films are much less than this, and although the figure was obtained on the basis of average measurements (so that it is not evident that the same pressure changes are needed to expand any one capillary), it is still by no means certain that pulmonary capillary compliance is sufficiently large to be significant for our purposes. It will also be convenient to have defined the gap thickness,

$$h(x) = r_o - c(x) + l_1(p - p_o) + l_2(p - p_o) \quad (1.3)$$

If we are now given, say, the downstream value of the pressure, then we may solve the coupled equations (1.1), (1.2) and (1.3) to find the pressure distribution and gap profile. Unfortunately, this solution involves the leak-back Q, a priori unknown; but, as Lighthill has pointed

out, a further condition, that of balance between driving forces and viscous resistance acting on the pellet, is available to determine the value of Q. The viscous drag per unit area, parallel to the tube axis, is given by

$$\tau = \mu \frac{\partial u}{\partial r} \qquad (1.4)$$

where r is the radial coordinate; the viscous resistance on the pellet is therefore

$$2\pi \int R(x).\tau(x).dx$$

where the integration is over the length of the pellet. If we now assume that a uniform pressure difference Δp acts over a frontal area on the pellet equal to the cross-sectional area of the tube, then the driving force on the pellet will be $\Delta p.\pi r_o^2$. The statement of equality of forces now becomes

$$\Delta p.\pi r_o^2 = 2\pi \int R.\tau.dx \qquad (1.5)$$

It may be argued, with justification, that the l.h.s. is only an approximate expression for the driving force; Δp will actually vary over the pellet faces, and the area of application will not be exactly πr_o^2; but it must be pointed out that since we expect most of the pressure variation to occur in the thin lubrication region, Δp will be nearly constant over most of the frontal area; furthermore, in the application of the theory to actual physiological

problems (such as capillary flow), we shall be able to use only a fairly crude approximation to the undistorted pellet profile c(x), so that the use of a more exact, complex form for the driving force does not seem justified. This argument, based on the availability of only very approximate data for the situations in which we shall be applying the theory, is a very pertinent one, and will be involved later when discussions of the elastic behaviour are made.

Evidently, we may use directly the equations derived above to determine various parameters of interest; such an analysis, however, would be cumbersome, in that a large number of calculations would need to be performed in order to obtain useful ranges of definition for these parameters. It is convenient to outline at this point the further approximations and assumptions made in Lighthill's preliminary study; we will also discuss the mathematical simplicity introduced when non-dimensional variables are used; this elegance does not depend to a great extent on the simplifying approximations, and is clearly a desirable feature to retain in any more sophisticated model. In the case where the film thickness in the region of interest is very much smaller than the tube radius, it is assumed in [1] that, to a first approximation, the wall may be con-

sidered to be locally plane; the corresponding equations are those obtained for two-dimensional Cartesian coordinates, using a boundary-layer-type normal coordinate y. Lighthill in fact finds that equations (1.1) and (1.4) reduce to

$$\frac{dp}{dx} = -\frac{6\mu U}{h^2} + \frac{12\mu Q}{h^3} \qquad (1.6)$$

and

$$\tau = -\frac{2\mu U}{h} + \frac{6\mu Q}{h^2} \qquad (1.7)$$

respectively. A further assumption is made about the elastic behaviour of tube and pellet: the radial displacement is supposed to depend linearly on the local pressure at any point, with elastic compliances α and β respectively. Further, the gap profile under the reference pressure is assumed parabolic, with curvature κ at the point of contact; equation (1.3) then becomes

$$h(x) = \tfrac{1}{2}\kappa x^2 + (\alpha+\beta)(p - p_o) \qquad (1.8)$$

It is shown in [1] that a suitable scheme of non-dimensionalization is:

$$H = \frac{h}{2Q/U}, \qquad P = \frac{(\alpha+\beta)(p - p_o)}{2Q/U}, \qquad X = \frac{\kappa^{\frac{1}{2}} x}{(2Q/U)^{\frac{1}{2}}}$$

The quantity $2Q/U$ is a typical gap thickness, at the point where the pressure has a maximum. Lighthill now points out that since we expect almost all of the pressure fluct-

uations to occur in the region of constriction, then we will probably not introduce too great an error by replacing the ends of the pellet by upstream and downstream infinity, so that equations (1.6), (1.7) and (1.5) now become in non-dimensional form

$$\frac{dP}{dX} = L\left(H^{-3} - H^{-2}\right) \qquad (1.9)$$

$$H = \tfrac{1}{2}X^2 + P \qquad (1.10)$$

$$P(-\infty) - P(\infty) = IC \int_{-\infty}^{\infty} \left(H^{-2} - \tfrac{2}{3}H^{-1}\right) dX \qquad (1.11)$$

where L is the non-dimensional parameter

$$\frac{6\mu U}{(2Q/U)^{5/4}\kappa^{1/4}}$$

and C is the ratio of typical gap size to tube radius, $2Q/Ur_o$. The equation (1.9) is shown to have the extremely convenient property, that the value taken by the solution at $+\infty$ is very insensitive to the value taken at $-\infty$, particularly for larger values of L; this means that if (1.9) is integrated from left to right in the usual sense, the downstream pressure obtained will be almost independent of the upstream pressure chosen. In view of this stability, and also of the expectation that the nett pressure drop will be small compared with the size of the fluctuations in the gap (i.e. both sides of equation (1.11) will be small as well as positive), Lighthill assumes that the solution

determined by the computationally convenient criterion

$$P(\infty) = P(-\infty) = b(L), \text{ say,} \qquad (1.12)$$

will be a useful zero order approximation to the true solution, for a given value of L; using this solution he then obtains a first order approximation to the pressure difference, from (1.11), as

$$LC \int_{-\infty}^{\infty} (H^{-2} - \tfrac{2}{3}H^{-1})\,dX = LCf(L) \qquad (1.13)$$

These are the values used in [1] for the non-dimensional downstream pressure and pressure difference (although Lighthill points out that they may be used as the initial values of an iteration procedure based on (1.9) and (1.11). In particular, for small values of L (which are shown in [1] to correspond to positive clearances), b(L) and f(L) are obtained by asymptotic methods to be of the form

$$b(L) = 0.75 - 0.1313L^2$$

$$f(L) = 0.0657L^2 \qquad \text{as } L \to 0$$

It is important to realize that in the above analysis, three separate major approximations have been made: (i) that the equation (1.9) is sufficiently accurate in the region of interest (that is, that the transverse curvatures of tube and pellet may be ignored); (ii) that the ends of the pellet may be replaced by upstream and

downstream infinity; (iii) that the condition (1.7) is a sufficiently accurate criterion to determine the downstream value of the pressure. For small L the theory derived from these assumptions gives the rather implausible result, that the frictional resistance is extremely small. This corresponds to conditions of relatively large positive clearance, where we might expect the resistance to tend to that experienced by a simple Poiseuille flow along the tube. We now show that the discrepancy is chiefly due, in fact, to a breakdown of assumption (ii); although this is sufficiently accurate for determining the upstream or downstream pressure, the error introduced during the computation of the pressure difference is considerable.

Suppose that the pellet actually extends to a point where, say, $h = r_o$; i.e. where $H = 1/C$. Assume for the moment that past this point $P = P(\infty) = b(L)$, and that this is true on both sides of the pellet. Then the drag, as given by (1.8) will be in error by

$$2LC \int_G^\infty (H^{-2} - \tfrac{2}{3}H^{-1})\,dX$$

where G is the value of X for which $H = 1/C$, and is given by (1.10) as $[2(1/C - b(L)]^{\frac{1}{2}}$. Integration gives this to be

$$2LC\left\{\sqrt{\frac{2}{b(L)}}\left(\frac{2}{b(L)} - \frac{2}{3}\right)\left(\frac{\pi}{2} - \tan^{-1}\sqrt{\frac{1/C - b(L)}{b(L)}}\right) - \frac{C\sqrt{2(1/C - b(L)}}{2\,b(L)}\right\}$$

For small L we may use $b(L) = 0.75 - 0.1313L^2$, whence the

error becomes

$$-1.886LC^{\frac{3}{2}} + 0.708LC^{\frac{5}{2}} - 0.124L^{3}C^{\frac{5}{2}} + 0.038L^{5}C^{\frac{5}{2}} \quad \ldots\ldots$$

Since L and C are both small, we may ignore the latter terms, and consider only the first. Clearly, if we denote the corrected pressure difference by $LCf_c(L)$, then

$$f_c(L) = f(L) + 1.886C^{\frac{1}{2}}$$

Thus even for C as small as 0.01 and L as large as 1, the value of f(L), computed as $0.0657L^2$, has an error of almost 300%. Of course, P does not remain constant in the whole of the interval $[G,\infty]$; it actually decreases slowly. However, even if we take $P(\infty) = 0$ for the whole of the region of integration, the leading term in the error expression, $(-1.886LC^{\frac{1}{2}})$, is not affected; this shows that the major error does in fact occur in assumption (ii) above. The corresponding correction to b(L) for the downstream value of the pressure is much smaller: an analysis similar to that given above shows that

$$P(G) = P(\infty) + 0.471LC^{\frac{3}{2}},$$

an error of approximately 8% even for the relatively adverse values L = 0.5, C = 0.05. We might expect, therefore, that the breakdown of assumption (ii) will not greatly affect the value of the downstream pressure obtained using (1.12). This does not guarantee the accuracy of this value,

however, since it depends on the validity of assumption (iii); and although the same stability of solution is found in this paper for integration from left to right, the greatly increased pressure differences found cast doubts upon the accuracy of this assumption.

In this paper, then, noting the error occasioned in the drag by the neglect of terms of small order in C, we give in section 3 a reformulation of the mathematical statement in terms of cylindrical coordinates, taking into account the curvature of tube and pellet. The finite limits (-g,g) are used for the extent of the pellet, and a more realistic, elliptic profile is assumed for the pellet in the absence of the lubrication pressures. In the analysis, tube elasticity will be ignored, a simplification prompted by the situation which obtains in the systemic capillaries; it is recognized, however, that in other cases, particularly in pulmonary capillaries, the compliance of the tube wall may be comparable with that of the pellet; this question will be more fully investigated later in this section in the discussion of the elastic assumptions. A satisfying feature of the Reynolds' equation obtained is that the pressure gradient tends to that predicted for simple Poiseuille flow, as X approaches the ends of the pellet. In view of the discussion of the validity of assumption (iii),

we shall determine the boundary conditions (for given values of L and C) on the pressure by an iteration principle based on an equation similar to (1.11), rather than by the simpler condition (1.12).

An explicit dependence of the downstream pressure on the value of C is found, in contrast to results of the earlier approximate theory. A striking feature of the results obtained is that the resistances experienced by the pellets are much higher than those found by Lighthill; in particular, even for small values of L (corresponding to positive clearance) and relatively large values of C (large film thickness), the resistance is still several times that for the same length of an equivalent Poiseuille flow. Otherwise, the results of individual calculations using particular values of L and C are qualitatively similar to those obtained in [1]; the same geometry of the lubrication film is found: a convergent entry region, a central elastically-dominated region of slowly varying thickness culminating in a 'necking' where the pressure reaches a minimum, and an exit region where the gap rapidly widens and the pressure climbs quickly to the upstream value. The same increase of resistance with decreasing film thickness and decreasing clearance is found, although this increase is more rapid than that found in [1], and rises to much higher levels.

The physical explanations for these phenomena are of course identical with those discussed in [1], and the reader is referred to the extremely lucid exposition in that paper.

2. The physical assumptions

It must be realized that there is an essential difference between approximations and assumptions being used in any model. Most of the previous discussion has been concerned with the approximations made in [1], and the need for refinement of these in a more detailed study; on the other hand, the decision to use an elliptic rather than a parabolic profile for the pellet in the undistorted state concerned a simplifying assumption made about the physical properties of the system we are modelling. We shall now examine the physical assumptions more closely, in particular those concerning elastic behaviour, axisymmetry, and tube porosity; this will be done where possible in the light of observational evidence from the microcirculation.

In this new model, we shall take a more sophisticated view of the elastic behaviour of the red cells. It will be recalled that Lighthill's simplified model involved pellets whose radius changed under the influence of an external pressure according to a linear stress-strain relationship; such a model is applicable to a situation where

purely compressible pellets pass down a possibly compressible tube. In such cases, a convenient reference pressure may be defined, as that which will cause sufficient compression to make the radius of the pellet equal to the radius of the tube. We shall in this paper, however, use concepts of reference pressure and elastic behaviour more applicable to the red blood cell. According to Rand and Burton (1964), the erythrocyte consists of an incompressible fluid enclosed by a slightly elastic, very flexible membrane supporting a small surface tension, in the form of a biconcave disc. As Fung (1966) has shown, such a structure can easily support increases in external pressure without altering its shape; the pressure changes are transmitted directly to the fluid inside the membrane. Isochoric, applicable deformations are permissible (essentially 'bending' without change of internal volume or surface area) but the membrane cannot withstand a great deal of stretching without haemolysis occuring. It is apparent that we cannot define a uniform 'reference pressure' at which the cell will be reduced to some requisite size, since such a uniform application of pressure cannot produce any change in the shape. The mechanism of deformation of the cell to allow passage through narrow capillaries is therefore one of response to a non-uniform distribution of forces.

Let us examine in detail the forces acting on a deformable pellet in a tube. Firstly, there is a pressure gradient driving the motion, producing pressures p_1 and p_2, say, acting on the downstream and upstream faces of the pellet; we ignore variations of pressure across the ends. The presence of the tube wall contributes to a viscous resistance, acting chiefly around the rim; further, the thin lubrication film between the pellet and tube necessitates an additional local pressure distribution along the rim. This may affect not only the local pellet profile, but also the mean pressure, which determines the pressure existing inside the pellet. We now consider the response of the pellet to these forces in a typical configuration in the tube.

If the pellet adopts a 'bullet-shaped' or 'parachute' form, the driving pressure difference and the viscous resistance form a 'bowing-stress' which bends the pellet as described above. The exact nature of the elastic response to this stress will be discussed below, but suppose for the moment that the radius of the pellet is reduced to a value $r_0 R_c$, where r_0 is the radius of the tube. This will be a function of the pressure difference $p(-g) - p(g)$, recalling that $-g, g$ represent the ends of the pellet; the functional dependence is formulated later (e.g. equation (3.1)). Here R_c is expressed in non-dimensional form, for later conven-

ience; it is a measure of the clearance the pellet would have in the tube without the action of the additional pressures generated in the lubricating film. If additional pressures are now applied around the rim of the pellet, further local deformations will take place: the curvature of the membrane will alter as a result of changes in the pressure difference across it. It is shown later that a linear dependence of local deformation on local pressure change may be used to a first approximation in certain cases. We may introduce the idea of a reference pressure p_o as that which will deform the pellet just sufficiently for it to fit the tube, when applied to the rim; clearly, this pressure will depend not only on the clearance, but also on the pellet. If we denote the compliance by β, representing the change in radius consequent on a unit change in pressure, then

$$\beta \left[p_o - \frac{p(g) + p(-g)}{2} \right] = (R_c - 1) r_o$$

is the equation determining the reference pressure. Clearly, $p_o - \frac{1}{2}(p(g) + p(-g))$ is the additional pressure which must be applied to the rim, once 'bowing' has occurred, to allow the pellet to fit inside the tube. As mentioned above, we shall discuss later the form of β, and arguments for using such a local Hooke's Law elastic approximation.

There seems to be no general agreement as to whether

in fact, this is the principal configuration observed during the flow of red cells in small capillaries. Examination of freeze-dried lung tissue, prepared as slides containing sections 2μm thick (by Dr. Hughes, of the Postgraduate Medical School, London) showed that the parachute configuration is typical of red cells in capillaries of 5-7 microns diameter, but that the so-called 'crepe-suzette' (or longitudinally rolled) shape, observed by Rand and Burton, seemed to predominate in smaller vessels. The analysis for such a case is much more difficult, and will not be attempted here. We merely point out that the equations governing the flow are the same in each case; the difficulty arises in the selection of suitable values for the clearance parameter under various conditions.

We may suppose that the pellet profile is given by $r = c(x)$ when the reference pressure is applied to the rim; we require that $c(0) = r_o$, say. Then under the action of a non-uniform pressure $p(x)$ generated in the lubrication film, the film thickness will be

$$h(x) = r_o - c(x) + \beta (p(x) - p_o) \qquad (2.1)$$

assuming the tube to be non-elastic. If the tube is also deformable (linearly) under the action of pressure changes, as may occur in other applications than capillary flows, the relation is

$$h(x) = r_o - c(x) + (\alpha + \beta)(p(x) - p_o)$$

where α is the elastic compliance of the tube. This, in conjunction with the Reynolds' equation for lubrication, enables us to find $p(x)$ and $h(x)$ in terms of various parameters. Clearly, the values of $p(x)$ and $h(x)$ corresponding, say, to a prescribed downstream pressure and a given velocity depend to a great extent on the interpretation of the reference pressure p_o. It is interesting that the equations for a purely compressible pellet are the same as those above, the difference being only in the concept of the reference pressure (an absolute constant in that case). The significance of this will be discussed in section 3, where a series of numerical solutions of the equations are obtained and analysed.

The other major geometric assumption made in [1] was that of axisymmetry of the tube and pellet. In section 4 the effect of relaxing this requirement is discussed; to make progress possible, attention is centred on systems where the departure from axisymmetry is small. Under these conditions, it is shown that we may ignore the effect of transverse pressure gradients; to a first approximation, we need only consider the quantities in equation (2.1) to depend parametrically on an azimuthal angle ϕ, say. A feature of the equations is that the flow rate $Q(\phi)$ must be deter-

mined from the condition that the pressure be independent of $\emptyset$ for large positive and negative X. An interesting result to appear is that the effect of the asymmetry decreases as L increases; i.e. as the clearance decreases, and eventually becomes negative, the pressure gradients tend to symmetrize the geometry of the pellet, rather than force fluid through the points of least resistance. A physical explanation for this depends on the assumption that transverse pressure gradients may be ignored. From this, it is clear that no redistribution of fluid around the rim is possible once the flow has commenced to pass the pellet. Hence points of greatest constriction (i.e. where the parameter has an effective maximum) must demand the greatest peak response to the pressure, in order to allow passage of the required amount of fluid; this reduces elastically the local peak constriction. It is shown in the numerical calculations of section 4 that the pellet tends to become more axisymmetrical as $L \to \infty$. The viscous resistances are increased slightly, and the pressure changes in the lubrication film are increased at the point of greatest asymmetry; but these results are relatively unimportant compared with that discussed above, which implies that any increased tendency towards seizing-up due to failure of lubrication at points of peak constriction is lessened at negative clearances, when such

considerations are likely to be of importance.

It must be emphasized that the behaviour predicted on the basis of this analysis is principally a consequence, not of the characteristic small-clearance erythrocyte-capillary relationship, but of the constrictability of the red cell. In fact, for the case of an asymmetric, rigid particle in a closely-fitting tube, it has been shown that quite a different situation exists - the particle tends to oscillate from side to side, possibly enhancing the additional film attenuation due to asymmetry. Related tendencies have been noted for the case of a rigid sphere in a cylindrical tube by Christopherson and Dowson (1964).

We shall now examine in more detail the elastic constants involved in the model. The elastic behaviour is extremely complex, and we can give at best only a very approximate treatment of the various factors involved. Although the equations which follow seem formally to give a reasonably exact description of the deforming processes, they must be considered to provide only order-of-magnitude information about the clearance and elastic compliance of an erythrocyte-like pellet, particularly in view of the paucity of relevant observational data for the red cell. It should be pointed out that the actual elastic model used does not affect the solution of the equations of motion

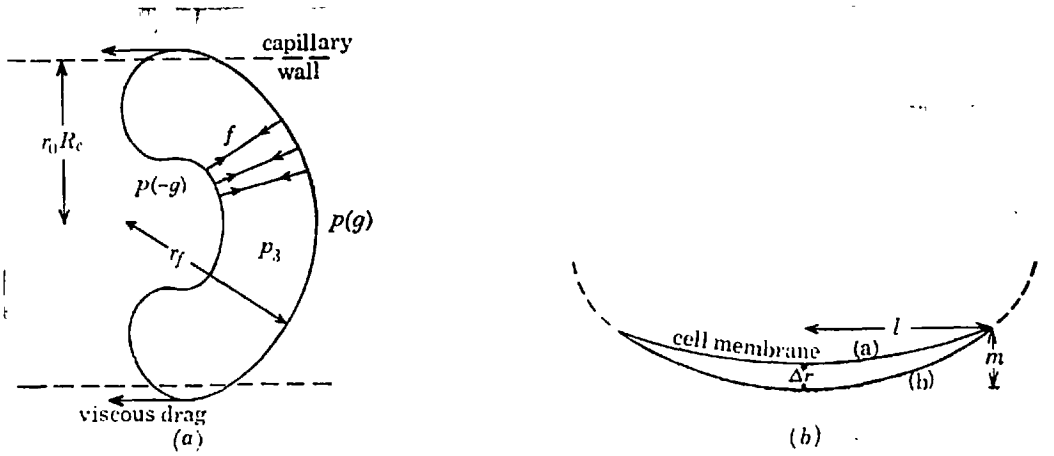


FIGURE 1 (*a*). Red cell configuration under action of 'bowing stress', (*b*) Effect of increasing rim pressure on red cell membrane.

(provided small local deformations are considered to depend linearly on the local pressure); the large-scale elastic effects must, however, be investigated if we are to obtain estimates of the values of the clearance and velocity parameters pertinent to red cell motion.

When the pellet is being deformed into the parachute shape described earlier, the forces acting, ignoring for the moment the lubrication pressures, are as shown in Fig. Ia, which is a longitudinal section containing the tube axis. Denote the radius of curvature of the left-hand membrane section by r_f, and that of the right-hand section by r_f/n; we might expect n in typical circumstances to be of order 2 or 3. There will be contributions from both faces to the 'bending resistance'; on the basis of recent observations, Burton (1968) attributes this coupling to long-chain fibrous bonds across the concave portion of the red cell, although there is no general agreement about this. (Canham, for example, has shown that the biconcavity may be explained in terms of an extremum principle for surface and bending energies.) We shall use the Burton hypothesis, since it allows a simple mathematical discussion. Suppose that these bonds exert a force f per unit area on the interior of both faces. Then the well-known equation for the pressure difference across a curved membrane gives for the downstream side

$$p_s - f - p(g) = S\left(\frac{2}{r_f}\right)$$

where p_s is the internal pressure, $p(g)$ the downstream pressure, and S the 'resistance to bending' measured by Burton and Rand (1964). We are assuming here that the surface forms part of a sphere, so that the two curvatures are the same. Similarly, for the right-hand wall

$$p(-g) - p_s + f = S\left(\frac{2n}{r_f}\right)$$

and addition gives

$$p(-g) - p(g) = \frac{2S}{r_f}(1 + n);$$

or, if we consider a non-dimensional pressure difference E, say,

$$E = \frac{\beta(p(-g) - p(g))}{r_o}$$

based on the modulus of elastic response to the lubrication pressures, then we have

$$r_f = \frac{2S(1 + n)\beta}{r_o E}$$

Suppose the arc-length of the left-hand wall section is a (typically 7.5 microns in the case of the rod cell); then the effective radius $r_o R_c$ is given by

$$r_o R_c = r_f \sin \frac{a}{2r_f} \qquad (2.2)$$

i.e. $$R_c = \frac{2S(1 + n)\beta}{r_o^2 E} \cdot \sin \frac{a r_o E}{4(1 + n)S\beta}$$

Previously, we showed that

$$\frac{\beta}{r_o}\left(p_o - \frac{p(g) + p(-g)}{2}\right) = R_c - 1 \; ; \qquad (2.3)$$

The L.H.S. is a non-dimensional parameter, which may be denoted by -F, say. Both E and F may be determined for any solution of the equations of motion discussed earlier; and for given values of the pellet size, tube radius, and elastic parameters, the equations (2.2) and (2.3) give an approximate value for the pressure drop compatible with the prescribed pellet velocity. Evidently, $r_o F$ is the excess of tube radius over pellet radius before effects of lubrication pressures are considered. We shall define F as the clearance for this configuration; for the rod cell we show in section 4 that values of F slightly less than zero are expected in narrow-capillary flow.

It remains to discuss the form of the parameter β and to examine the case for assuming a uniform, linear dependence of local deformation on pressure changes. The assumption consists of two parts: firstly, the assumption of linearity means essentially that we may express small changes in the azimuthal radius r_1 of the pellet as

$$-\delta r_1 = \left(-\frac{dr_1}{dp}\right)\delta p = \beta\, \delta p \qquad (2.4)$$

(noting that an increase in the pressure, δp, causes a decrease in r_1). We assert that we may ignore higher order

terms in this Maclaurin expansion for δr_1; in so far as the next term is concerned, this means that we neglect longitudinal stresses generated by non-uniform pressure and pellet radius. Such stresses may become of importance in any regions where the radius varies relatively rapidly, in particular the 'necking' predicted in the lubrication zone. We might, therefore, expect the linear theory to exaggerate such phenomena; the overall behaviour predicted should still be substantially correct.

Secondly, the assumption of uniformity means that $\frac{dr_1}{dp}$ is taken to be constant over the whole of the lubrication zone. In the case of the membrane model currently accepted for the red cell, $\frac{dr_1}{dp}$ will depend in a quite complicated way on both r_1 and r_2, the azimuthal and longitudinal radii of curvature. Since detailed information on the behaviour of $\frac{dr_1}{dp}$ would require a much greater knowledge of red cell mechanics than is supplied by the current form of the membrane model (which must be viewed as a general description only), it does not seem worthwhile to use a more complicated elastic model than a uniform linear one, although admittedly this must form a fairly crude approximation to the truth.

If we accept the elastic assumption, however, it is not too difficult to obtain a reasonable estimate of the

value of β. Denote by Δp the pressure difference across the membrane of the (erythrocyte-like) pellet; then

$$\Delta p = S\left(\frac{1}{r_1} + \frac{1}{r_2}\right)$$

Consider a small increase δp in the external pressure, corresponding to an equal decrease $-\delta p$ in the pressure difference. Suppose this 'pushes in' the rim membrane from position (a) on Fig. Ib to position (b), without affecting the position of the remainder of the membrane. Suppose for computational convenience these curves are circular arcs; then if ℓ and n are as shown, the longitudinal radius r_2 is given by

$$r_2 = \frac{n^2 + \ell^2}{2n} \approx \frac{\ell^2}{2n}$$

since $\ell \gg n$. If the pressure increase δp decreases r_1 by an amount δr_1 as shown, then r_2 becomes

$$r_2 + \delta r_2 = \frac{\ell^2}{2(n - \delta r_1)}$$

We then have

$$\Delta p - \delta p = S\left[\frac{1}{r_1 - \delta r_1} + \frac{2(n - \delta r_1)}{\ell^2}\right]$$

i.e.
$$-\delta p = S\left[\frac{1}{r_1^2} - \frac{2}{\ell^2}\right]\delta r_1$$

and this gives, using (2.4),

$$-\frac{\delta r_1}{\delta p} = \frac{r_1^2}{S} \Big/ \left(2\frac{r_1^2}{\ell^2} - 1\right) = \beta$$

For a red cell 2 microns thick, this would give values of

$\frac{dr_1}{dp}$ in the vicinity of $\frac{r_1^2}{15S}$ for capillaries of 5-7 microns diameter. In the absence of other data, then, this is the value we shall use when applying the results of the later calculations.

Finally, we turn to consideration of a model which allows leakage of fluid through the partially-permeable walls of the tube. The motivation for such a discussion comes from the observation that the walls of capillaries appear to allow transmigration of various components of plasma. The original hypothesis of Starling, that plasma diffused out near the proximal end, and returned near the distal end of capillaries, has recently been shown to be a very simplified approximation to the actual behaviour (e.g. Wiederheilm, 1966). It may still be postulated, however, (Zweifach and Intaglietta, 1966) that fluid movement through the capillary wall may be represented as

$$F.M. = \gamma \left[p_{pl} - \pi_{pl} - (p_t - \pi_t) \right] \qquad (2.6)$$

where γ is a diffusion coefficient (which may depend on chemical and physiological factors), p_{pl} is the mechanical pressure in the capillary lumen, π_{pl} is the colloid osmotic pressure there, and p_t, π_t are similar pressures in the surrounding tissue space. All of these pressures are much higher than the transient pressure increases mediated by the passage of the red cell, according to the lubrication theory;

consequently, it seems realistic to postulate merely a uniform loss of fluid along the whole extent of the lubrication film, rather than to introduce the needless complications of a minor additional loss dependent on small changes in the local pressure.

The amount of leakage experienced by the plasma film is uncertain; water loss is probably the main contributary factor to reduction of plasma volume in the lumen and absolute, quantative studies of water filtration are difficult (Wiederheilm, 1966). Some average values for filtration coefficients have been obtained for various tissues, for example by Landis (1927), Verney and Rushton (1950), and Verney (1951), ranging from 2.5×10^{-7} ml/sec/cm^2 wall area /cm H_2O filtration pressure (for mammalian muscular capillaries) to $3\text{-}6 \times 10^{-6}$ ml/sec/cm^2/cm H_2O (for mammalian glomerular capillaries). In the analysis of section 5, we shall use a value of 5.6×10^{-7} ml/sec/cm^2/cm H_2O (corresponding to .0056 μm^3/sec/μm^2/cm H_2O) obtained by Landis for frog mesentary capillary, which represents a mean value for the range of coefficients found; we shall, of course, also investigate the effect of larger and smaller coefficients. On the basis of recent studies by Guyton (1966) on interstitial fluid pressure in tissues, we find filtration pressures ranging from (approximately) 10 cm H_2O

at the proximal end of capillaries to -5 cm at the distal end (filtration pressure is the bracketted term in equation (2.6)). It appears that γ depends on position in the capillary, and that p_{pl} depends on time, due to the apparently random closing of the precapillary sphincters controlling perfusion. Measurements made by Zweifach and Intaglietta indicate that filtration outwards is the main process occurring during capillary perfusion; and that water tends to diffuse back in when the flow is interrupted. Furthermore, recent studies by Luft (1966) tend to support the hypothesis that egress of material from the capillaries occurs at the junctions between the endothelial cells, and is by no means evenly distributed over the capillary surface. To facilitate the formulation of a tractable mathematical model, however, we shall in section 5 postulate that a small amount of plasma is leaking out uniformly from the lubrication film so that the total flux of fluid past any cross-sectional plane in the capillary decreases towards the front (downstream) end of the red cell.

This loss of fluid from the plasma film appears potentially important because of the enhanced possibility of breakdown of lubrication it introduces. Lighthill pointed out that if the film thickness were reduced much below values characteristic of normal flow, the film might be

unable to sustain the high shears consequent on such a reduction, and 'seizing-up' might ensue. It seems likely that loss of fluid could contribute significantly to this effect: particularly, perhaps, in the region of the necking. In section 5 we examine the dependence of film thickness and resistance on the leakage rate, clearance, and pressure gradient. These are the local effects of wall porosity; the large scale dynamic effect, that of 'bunching' of red cells as fluid loss increases, has been considered elsewhere, for example by Zweifach and Intaglietta (1966), and will not be treated here. As might be expected, we find that, with a positive filtration pressure, the resistance at any given velocity is increased; or, more pertinently, for a given pressure gradient in a given size of tube, velocity is decreased in a region where leakage is occurring. Furthermore, film thicknesses are also reduced in such regions, leading to increased possibility of seizing-up of the flow if lubrication fails. As might also be expected, the effect is more apparent at lower velocities and smaller film thicknesses. It is interesting to note that these effects are suprisingly small (as shown by the computations of section 5); even the large filtration rates associated with glomerular capillaries, for example, do not appreciably interfere with the flow phenomena predicted for non-porous tube systems.

3. Mathematical formulation of the pellet motion

Consider an axisymmetric pellet of radius R(x), separated from a tube of radius r_o by a gap of thickness h(x). We shall choose a coordinate system stationary relative to the pellet, and assume that the tube wall is moving relative to the pellet with a velocity -U; x is measured as positive downstream from the point where the unstressed pellet has its maximum diameter. We shall investigate the dependence of h(x) and R(x) on the pressure, once the Reynolds' equation has been set up. As is usual in lubrication theories of this type, we assume the pressure to be independent of r in the region of interest, and that the flow is sufficiently slow for inertial terms to be ignored; the axial momentum equation becomes

$$\frac{dp}{dx} = \frac{\mu}{r}\frac{\partial}{\partial r}\left(r\frac{\partial u}{\partial r}\right)$$

where u(r,x) is the axial velocity. Integrating twice with respect to r, we obtain

$$u = \frac{1}{4\mu}\frac{dp}{dx}r^2 + A.\ln(r) + B$$

where A, B are functions of x determined by the boundary conditions. If we postulate the no-slip condition at the boundaries, and assume the walls to be non-porous, we find that u(r,x) becomes

$$u = \frac{1}{4\mu}\frac{dp}{dx}\left(r^2 - R^2 - \frac{2Rh + h^2}{\ln(1+h/R)}\ln\frac{r}{R}\right) - \frac{U\ln(r/R)}{\ln(1+h/R)} \qquad (3.1)$$

If we now integrate the continuity equation,

$$\frac{\partial}{\partial r}(rv) + \frac{\partial}{\partial x}(ru) = 0$$

once with respect to r, we obtain, using a well-known result on differentiation of integrals,

$$[rv]_R^{R+h} = -\frac{\partial}{\partial x}\int_R^{R+h} u.r.dr. + [r.u]_{R+h} = (R+h) \qquad (3.2)$$

Clearly, if the tube wall has an axial velocity -U, it must also at any point have a radial velocity $-U\frac{d}{dx}(R+h)$, where of course $\frac{d}{dx}(R+h)$ represents the slope of the tube wall with respect to the axis. Consequently, (3.2) simplifies to

$$\frac{\partial}{\partial x}\int_R^{R+h} u.r.dr = 0 \quad ;$$

and since the integral here represents the flux of fluid divided by 2π, we may integrate this to

$$\int_R^{R+h} u.r.dr = -r_o Q$$

where r_o is the undistorted tube radius, and Q is the backward flux per unit circumferential length of undistorted tube - the 'leakback' defined in section 1. If we use this equation in conjunction with (3.1) we obtain

$$\int_R^{R+h}\left\{\frac{1}{4\mu}\frac{dp}{dx}\left[r^2 - R^2 - \frac{2Rh+h^2}{\ln(1+h/R)}\ln\frac{r}{R}\right] - \frac{U.\ln(r/R)}{\ln(1+h/R)}\right\} r.dr = -r_o Q$$

We finally obtain the Reynolds' equation as

$$-\frac{1}{4\mu}\frac{dp}{dx}\cdot\frac{2Rh+h^2}{4}\left[2R^2+2Rh+h^2-\frac{2Rh+h^2}{\ln(1+h/R)}\right]$$

$$-U\left[\frac{(R+h)^2}{2}-\frac{2Rh+h^2}{4\ln(1+h/R)}\right]=-r_oQ \qquad (3.3)$$

Not surprisingly, in the limit as $h/R \to 0$ (very small gap thickness), the equation reduces to

$$\frac{dp}{dx} = -\frac{6\mu U}{h^2}+\frac{12\mu Q}{h^3} \qquad (3.4)$$

using also the limit $r_o/R \to 1$; this is the simplified boundary-layer equation used in [1]. On the other hand, as $R \to 0$ and $h \to r_o$, which occur past the ends of the pellet, the asymptotic form is

$$\frac{dp}{dx} = -\frac{8\mu U}{r_o^2}+\frac{16\mu U}{r_o^3} \qquad (3.5)$$

Thsi is the Poiseuille pressure gradient characteristic of simple pipe flow with mean velocity $(-U + 2Q/r_o)$; such a flow has a nett flux of $-\pi r_o^2 U + 2\pi r_o Q$, which is equal to the flux of pellet material past any point, less the leak-back; there is thus a satisfying agreement with the continuity requirements of the large-scale motion. It appears, therefore, that the Reynolds' equation (3.3) will provide a reasonably accurate description of the flow over the whole of the pellet; it forms, in fact, a matching of the asymptotic forms (3.4) and (3.5) in the entry region for the lubrication flow, where the gap thickness is of intermediate

size.

We shall consider a pellet with an elliptic profile at some reference pressure p_o (discussed in section 1), at which the maximum radius of the pellet is just equal to the unstressed tube radius. If the compliance of the pellet is β, we may express R(x) in the form

$$R(x) = r_o(1 - x^2\kappa/r_o)^{\frac{1}{2}} - \beta(p - p_o)$$

where κ is a measure of the curvature of the pellet at the point of constriction; the length of the pellet is given by $(r_o/\kappa)^{\frac{1}{2}}$. Similarly, if the compliance of the tube is α, its profile will be given by

$$R(x) + h(x) = r_o + \alpha(p - p_o)$$

whence

$$h(x) = r_o(1 - (1 - \kappa x^2/r_o)^{\frac{1}{2}}) + (\alpha + \beta)(p - p_o)$$

As in Lighthill's work, we notice that the dependence of film thickness on pressure depends only on the sum of the compliances; since, however, R(x) (in which β alone appears) occurs explicitly in the Reynolds' equation, we need to know α and β separately in this statement of the problem. As mentioned in the previous section, however, we may take α to be zero in the application of the theory to the systemic capillary flow model; we shall, therefore, ignore α in the following analysis, noting that computations could well be

undertaken with a non-zero value of α without further major complication.

The value of the leakback Q may be determined, once the downstream pressure has been prescribed, by the condition of equilibrium of forces on the pellet. The drag per unit area on the pellet is

$$\tau = -\mu \frac{dp}{dx}\Big|_{r=R}$$

$$= \frac{1}{4R}\cdot\frac{dp}{dx}\left[2R^2 - \frac{2Rh+h^2}{\ln(1+h/R)} + \frac{U}{R\ln(1+h/R)}\right] \quad (3.8)$$

where $\frac{dp}{dx}$ is given by (3.3). The total drag is

$$2\pi\int_{-g}^{g} R.\tau.dx$$

where g, $-g$ are the ends of the pellet. This must be balanced by the resultant pressure force; since we assume that over all of the frontal area of the pellet the downstream pressure is $p(g)$, and similarly for the upstream pressure $p(-g)$, we may take the pressure force to be

$$\pi r_o^2\left[p(-g) - p(g)\right]$$

(This approximation has been discussed in section 1.) We here define the downstream and upstream pressures to be those acting at the respective ends of the pellet. The equality of forces may be stated as

$$\pi r_o^2\left[p(-g) - p(g)\right] = 2\pi\int_{-g}^{g} R.\tau.dx \quad (3.9)$$

We shall take the value of $(-g)$ to be that which makes $R(x)$

vanish at the upstream pressure; since we expect relatively slow variation of pressure and gap width in the region around the ends of the pellet, such a choice of g should not introduce significant errors at the downstream end, even though R(g) will not be zero. We obtain

$$g = \left[r_o/\kappa - \beta^2(p(-g) - p_o)^2/(\kappa r_o)\right]^{\frac{1}{2}}$$

We shall now non-dimensionalize the equations, using the same scaling factors as in section 1; the equations become, on manipulation

$$\frac{dP}{dX} = \frac{2LC}{3}\cdot\frac{1}{H(1-\frac{1}{2}CH)}\cdot\left\{C-1-\frac{CH(2-CH)}{2.\ln(1-CH)}\right\}\cdot\left\{2-CH(2-CH)\,\frac{CH(2-CH)}{\ln(1-CH)}\right\}^{-1} \tag{3.10}$$

$$H(X) = P + \left[1 - (1 - CX^2)^{\frac{1}{2}}\right]/C \tag{3.11}$$

$$J(X) = R(X)/r_o = (1 - CX^2)^{\frac{1}{2}} - CP \tag{3.12}$$

(recalling that since we are ignoring elastic expansion of the tube, $J(X) = 1 - CH(X)$ in non-dimensional form). The equilibrium of force equation is

$$P(-G) - P(G) = \int_{-G}^{G}\left\{\frac{1}{2}\cdot\frac{dP}{dX}\left[2(1-CH)^2 + \frac{CH(2-CH)}{\ln(1-CH)}\right] - \frac{LC^2}{3.\ln(1-CH)}\right\}dX \tag{3.13}$$

where G is the non-dimensional equivalent of the distance g, and is given by

$$G = \left[1/C - C\left[P(-G)\right]^2\right]^{\frac{1}{2}}$$

Numerical solutions have been obtained for this set of equations for various values of L and C, using the condition (3.13) to determine the value of P(G) and the pressure difference ICf(L,C) for each set of values. This procedure differs from that advocated in the earlier discussion (where essentially L and P(G) were assumed known, and (3.13) used to determine C); as pointed out in section 1, however, it will be more convenient to obtain the results in this form, and interpret them in terms of more useful physical parameters later. Since we expect the most significant phenomena to occur near the middle point of the pellet, the numerical analysis was performed using the transformation $X = \tan\phi$, giving mesh points for a Runge-Kutta procedure which cluster around $X = 0$.

In view of the argument advanced in section 1 (regarding possible sources of error in the drag computatio using infinite limits), we expect the results obtained to deviate markedly from those of [1] for small values of L; for larger L, they should agree reasonably well. Further, the differences should tend to be accentuated by increasing C, and approach Lighthill's results more closely for $C \to 0$. This aspect of the solutions, typified by the non-dimensional value of the downstream pressure (denoted by b(L,C)) is

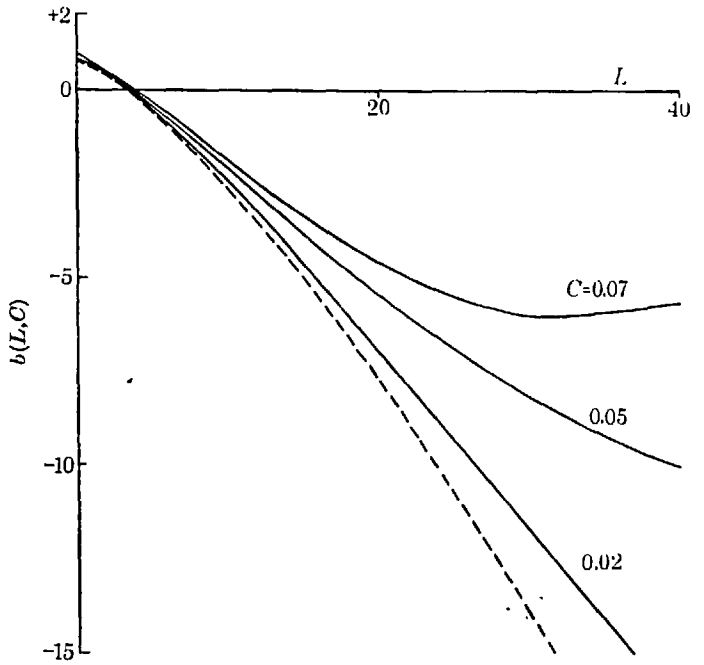


FIGURE 2. Plots of non-dimensional downstream pressure, $b(L, C)$ as a function of L, for various values of film thickness C. The broken line indicates the corresponding curve for Lighthill's approximate calculation.

shown graphically in Fig. 2. The corresponding curve for b(L) obtained in the approximate theory of [1] is shown as a broken line. As well as the expected deviations for different values of C from the approximate curve, we find a marked divergence as L approaches very large values, due to the effect of the very large resistances found under these conditions. Clearly, negative values of b(L,C) correspond to conditions where the downstream pressure is lower than the reference pressure although as pointed out earlier this does not necessarily correspond to negative clearance conditions.

It has not been thought necessary to include diagrams showing the variation of pressure and gap width in the lubrication film; a qualitative description was given in section 1, and it was noted there that such variations are very similar to those shown by Lighthill in [1].

As discussed earlier, it will be more useful for application of these results to actual physiological (and physical) problems to express the various quantities in terms of more realistic parameters of the motion, particularly since L and C involve quantities such as typical gap width and leakback, about which we wish to obtain information. Accordingly, we will now introduce additional velocity, clearance, and resistance parameters in a form

applicable to the relationships we wish to consider. These will be non-dimensional, but related to physically relevant scales.

Firstly, we introduce the parameter

$$\Lambda = \mu U \beta / r_o (\kappa r_o)^{\frac{1}{2}}$$

which measures pellet velocity on a scale depending only on the fluid viscosity and the geometry and elastic properties of the tube and pellet; next, a resistance parameter

$$D = \left[p(-\xi) - p(\xi) \right] r_o (\kappa r_o)^{\frac{1}{2}} / \mu U$$

is defined; this measures resistance on a scale of the resistance experienced by an equal length of tube containing an equivalent Poiseuille flow. Further, we shall require the clearance parameter F, whose derivation was foreshadowed in section 1:

$$F = \frac{\beta}{r_o} \left[\frac{p(\xi) + p(-\xi)}{2} - p_o \right]$$

where -F expresses the decrease produced in the maximum pellet radius when the pressure is increased from the mean driving pressure to the reference pressure, as a fraction of the tube radius. That this is a realistic measure of clearance has been discussed in section 1. Finally it will be useful, when actual evaluations are being made, to have defined the parameter E, also derived in section 1:

$$E = \beta/r_o \left[p(-g) - p(g)\right]$$

This measures the radius change which would be produced if the pressure at the rim were increased by an amount equal to the pressure drop across the pellet, also as a fraction of the tube radius. For the elastic model assumed here for the erythrocyte behaviour, E has no independent physical significance; it is merely a convenient non-dimensional measure of the pressure drop, in terms of the elastic properties of the pellet, and one which may easily be derived from the non-dimensional quantities obtained in the numerical analysis.

These are the same parameters as those used in [1], except for the clearance; Lighthill used a further parameter

$$B = \beta/r_o \left[p(g) - p_o\right]$$

We may easily show, however, that

$$F = B + \tfrac{1}{8}E$$

and since in [1] cases where E was of order 10^{-2} or less only were considered, the two clearance parameters are essentially equivalent. The interpretation, however, is not the same (and, of course, neither is the range of values found for the parameters); for although in the compressible model used in [1] a value of E much in excess of 10^{-2} was embarrassingly high when flow over a considerable length of

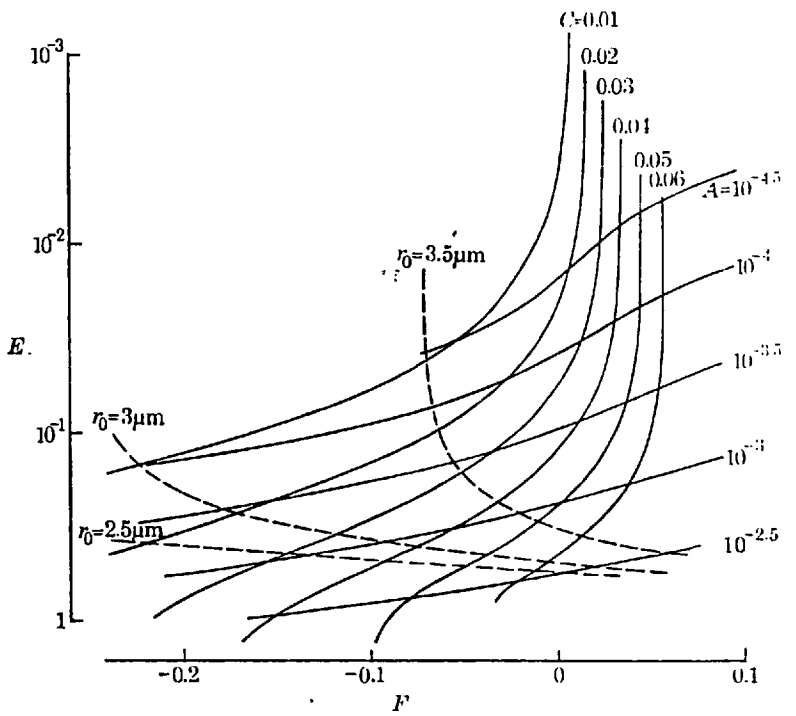


FIGURE 3. Curves of constant velocity parameter A and constant film thickness parameter C on an F–E diagram. The broken lines represent compatibility curves for a 7.5 μm red cell in capillaries of various radii.

tube was considered, the present model does not have this limitation. The comparison is further discussed below, in the light of red cell and capillary architecture.

A little algebraic manipulation easily shows that the four parameters A,D,E,F may be expressed in terms of L, C, b(L,C), f(L,C) as follows:

$$A = (LC^{\frac{5}{2}})/6 \qquad E = LC^{2} f(L,C)$$

$$D = 6C^{-\frac{1}{2}} f(L,C) \qquad F = Cb(L,C) + \tfrac{1}{2}E$$

We may now plot the various relationships between A,C,D,E and F; essentially, we have eliminated L from the results, and may now calculate any of the parameters in terms of two of the others, using the values obtained for b(L,C) and f(L,C) in the numerical analysis. For example, Fig. 3 shows sets of curves of constant A and constant C in terms of E and F. The broken curves indicate compatible values of E and F (for a deformable erythrocyte-like pellet) for several ratios of tube to pellet radius (assuming the latter to be fixed); these are obtained from equation (2.2) using numerical data appropriate to the red cell. As in [1], we find the typical gap width, expressed by the parameter C as a fraction of the tube radius, decreases as the velocity decreases, for a given value of the clearance. This is particularly noticeable under negative clearance conditions,

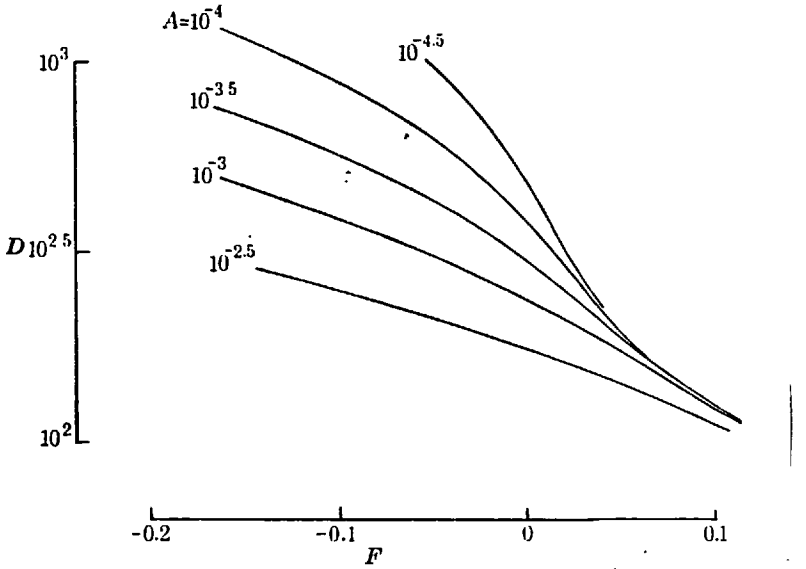


FIGURE 4. Plot of resistance parameter D as a function of clearance F for several values of the velocity parameter.

where the two sets of curves tend to become parallel; here we find that C varies as A^k, where k lies between about .45 and .55 (i.e. film thickness decreases approximately as the square root of the velocity), along compatibility curves of E and F for the red cell. Lighthill has pointed out that such decreases in film thickness could lead to seizing-up of the flow under low-velocity conditions; this has particular relevance to the capillary flow problem, and will be discussed later.

A second significant relationship is the dependence of the resistance parameter D on A for various clearances. The resistance experienced by Poiseuille flow with viscosity equal to that of the lubricating fluid corresponds to D = 16; consequently, the value of D expected if the pellet suspension were a fluid having viscosity, say, twice that of the lubricating fluid (a ratio applicable to whole blood and plasma) would be 32. Using these figures, we may use the D-A relationships to compare predicted resistances for pellet flow with those which would be found if the pellet-fluid system were replaced by a single fluid with viscosity comparable to that of the suspension in bulk. Accordingly, in Fig. 4 we plot constant-A curves on a D-F diagram. At relatively low values of A (as far as capillary flow is concerned), for example $10^{-4.5}$, the resistances are very much higher than

those expected for Poiseuille flow (with the same viscosity), particularly for negative clearances and small positive clearances; these low velocities correspond to very small film thicknesses, as shown in Fig. 3. Even for larger values of A, say 10^{-3}, and positive clearances, the resistances are still significantly higher than those for purely fluid flow. Furthermore, the pellet resistances do not increase as rapidly with velocity as do Poiseuille resistances; for a clearance of -0.1, for example, we find that D varies approximately as $A^{-.36}$. This means that if we define a 'resistivity for a given tube (assuming for the moment that the resistance is that of the pellets for the whole length of tube), as flow rate divided by pressure difference, then this will be a constant for fluid flow, but will be inversely proportional to approximately the cube root of the velocity for negative-clearance pellet flow. It is perhaps more illuminating to express these results as follows: for a given pressure drop across a length of tube, the mean velocity for pellet flow will be smaller than that for fluid flow; moreover, the pellet velocity will be more sensitive to changes in the pressure gradient than a corresponding fluid velocity. The importance of these non-linear effects produced by the presence of the pellets has been indicated by Lighthill in [1]. The dependence of resistances and film

thicknesses on velocity, under given clearance conditions, is due to the elastic effects; it is interesting to note that in Fig. 4 the curves converge on each other for positive clearances, where elastic control is expected to become progressively less important.

The relationships discussed above have considerable significance when interpreted in terms of capillary flow. Typical values of the various parameters will be necessary; we shall consider red cells of about 7.5 μm diameter, and capillaries of 5-8 microns diameter (for which the assumptions made about the mode of distortion of the red cell are likely to hold good). Rand and Burton (1964) give a figure of 0.0185 dyne/cm for the 'resistance to deformation' S, and plasma viscosity may be taken as 1.9 centipoise (Merrill and Folls, 1961). In section 2 we obtained an estimate of $r_1^2/15S$ for β, where r_1 is capillary radius. We might expect values of κr_o to be of order unity, and their square roots to be even closer to unity.

Consequently, we find that, for typical red cell velocities of the order of 100-200 μm/sec, the value of A is of the order of 10^{-3} on substituting the above values; similarly, the clearance-resistance compatibility relation (2.3), for a capillary of 6 microns diameter, is given by

$$1 - F = (.533/E).\sin(2.344E),$$

giving clearances of the order of -0.1 for the normal velocities mentioned above. (We have here taken the n of (2.3) to be 3). Larger and smaller clearances may, of course, be found for different-sized tubes (e.g. down to -0.6 for a capillary radius of 2.0 μ, and low red cell velocity). Under normal flow conditions in capillaries 5-7 μm in diameter, clearances are in the range -0.03 to -0.13. Compatibility curves for various capillary radii in this range are shown as broken lines in Fig. 3.

It must be pointed out that average resistance of a length of capillary will not be that found for individual red cells. Suppose for simplicity that red cells are interspersed with equal lengths of plasma; then we may take D as 16 for the plasma-filled parts of the capillary, and an average value of D (supposing we assume a particular value D_1 for a red cell in some situation) is then $\frac{1}{2}(D_1 + 16)$. Furthermore, if we wish to compare this resistance with that which would be expected if whole blood were a viscous fluid being forced along the capillary, we need to take into account the viscosity of whole blood; this is typically of the order of twice that of plasma alone, so that a comparative mean value of D is more like $\frac{1}{4}(D_1 + 16)$. On this argument, our spectacularly high resistances become smaller in practice; still, a value of D of 150 gives a resistance 2.5

times that calculated for viscous-fluid whole blood, while values of D of the order of 1000 correspond similarly to a resistance increased by a factor of 15. Perhaps of greater importance is the fact that these considerations do not affect the non-linear dependence of resistance on pressure gradient found above.

Let us now examine the characteristics of typical normal capillary flow. In a 6 μm capillary, for a cell velocity of 120 μm/sec (giving $A = 10^{-3}$ when $\kappa r_o = 0.5$) we have seen that a clearance of -0.1 would be expected. From Fig. 4, we see that this corresponds to a film thickness parameter of about 0.035; the lubrication film is therefore about 0.1 microns thick, and the leakback past the cell is 3.5% of the total flow. From Fig. 5 we obtain a corresponding value for D of 350, giving a mean resistance of about 5.5 times that for whole-blood Poiseuille flow. Similarly, for a 5 micron capillary, leakback is about 3.2% and mean resistance is about 7 times Poiseuille; film thickness is slightly less (.075 micron). On the other hand, for a 7 micron capillary, leakback is 4.5%, mean resistance 4.5 times Poiseuille, and film thickness is .16 microns. Clearly, we would expect to find that for narrower capillaries, velocities are comparatively much smaller than for corresponding Poiseuille flow.

Of course, these enhanced resistances do not necessarily mean a great contribution to the overall vascular resistance from the capillaries, since there are such a large number of them in parallel; it is thought, in fact, that systemic capillaries, for example, account for only about 20% of the resistance of the vascular bed. What is important here is the effect of the non-linearity of resistance on flow in each capillary. Suppose, for example, that in a capillary of 7 microns diameter, with a flow corresponding to $A = 10^{-3}$, the pressure drop across the ends is reduced by half, either by vasomotion or blockage. Then an examination of Fig. 3 shows that, if E is halved, the velocity parameter in this case falls to $10^{-3.5}$, which means that the velocity is reduced to one third of its original value; the film thickness also falls, from .16 microns to .1 microns. These tendencies are even more marked in smaller capillaries; for a lumen of 6 microns diameter, halving the pressure gradient reduces the velocity by a factor of 6, and the film thickness from .1 microns to .04 microns; while in a 5 micron capillary, the velocity is reduced by up to ten times, and film thickness falls to a value corresponding to C less than .01, i.e. less than .025 microns. The mean resistances are increased to 7.5, 18, and 40 times the Poiscuille value; these figures are obtained from Fig. 4, or

extrapolation from those curves, using the clearance and velocity data found from Fig. 3. (of course, these mean resistances could have been obtained directly from the values read off Fig. 4; for we see from the definitions of the various parameters that AD = E.)

In connection with these non-linear resistance effects, it is interesting to consider some recent work by Djojosugito et al. on blood viscosity; they found that the apparent viscosity of whole blood during perfusion of muscle increased (relative to that of a dextran-Tyrode solution) as flow rate decreased. It might be suggested that this effect is due, in part, to a markedly increased resistance in the capillary network of the muscle predicted for low flow velocities by the present theory.

Lighthill has mentioned the possible application of these results to control of perfusion by vasomotion in the arterioles and pre-capillaries. Constriction by the smooth muscle there reduces the pressure gradient in the perfused capillaries; we see that the sensitivity of the velocity to changes in pressure gradient rapidly reduces the flow rate. Further, the extremely thin lubrication films existing under low-velocity conditions suggest that breakdown of lubrication may occur, causing complete shutting-off of the flow without the necessity for complete occlusion of the

lumen of the pre-capillaries or arterioles. Such a process could explain phenomena concerned with other flow stoppages observed by, e.g. Burton (1966), and more recently the rapid cessation of flow at small positive vascular pressure differences observed in lung by Glazier, Hughes, Maloney and West (1968). Moreover, in pulmonary capillaries much less control of flow by arterioles occurs; the results of this theory could well provide an explanation for the resistance effects produced in the capillary 'marsh' of the lung. The perfusion process here, of course, may be further complicated by capillary compliance, and by the relation between vascular and alveolar pressures; this has been discussed in section 2.

The preceding discussion of sensitivity of control for pellet flow systems holds good whatever model of pellet elasticity is assumed (always provided that local small deformations depend linearly on pressure changes). It is interesting to consider differences in behaviour between systems containing, say, purely compressible pellets, and ones with erythrocyte-like pellets. Such a comparison may also throw some light on engineering applications, in particular the cleaning of pipes by forced passage of compressible pellets. The important factor here is the dependence of clearance on mean driving pressure at any point. For the distortable

erythrocyte, we have shown that the clearance depends only on the relative dimensions and the pressure drop across the pellet; on the other hand, the clearance for a compressible pellet depends directly on the absolute pressure. This means that for such a pellet the clearance decreases (and resistance increases) as the pellet moves along the tube. The parameter E has direct relevance here: it measures the change in clearance as the pellet moves a distance equal to its own length plus the length of the interspersing fluid (assuming negligible pressure drop in the fluid phase). Although the pellet could only expand until it reached its natural diameter if the lubrication pressures were removed, nevertheless the clearance parameter can go on decreasing indefinitely - it is a measure of the disparity between the mean driving pressure and the reference pressure. Consequently, for these systems the contribution to the resistance is greater from the downstream end of the tube (or tubes). Further, the possibility of 'sticking' when the film thickness becomes too small means that the downstream pressure must be kept above a certain level to avoid lubrication failure; this introduces a severe limitation on the flow rates which may be achieved for upstream pressures close to the lower limit for downstream pressure.

On the other hand, flow involving the 'bendable'

erythrocyte-like pellets shows much more uniformity and flexibility. Firstly, since the flow rate depends only on the gradient, and not on the absolute value, of the pressure, the rate of perfusion may be controlled with equal facility by pressure changes at either end of the system without introducing limitations on the flows that can be achieved. For the same reason, parts of a system having different tube lengths may be controlled uniformly at the one upstream pressure. Furthermore, since clearance, and hence resistance, of each pellet remains the same (in a uniform-velocity flow) at all parts of a tube, the pellets will all contribute equally to the total resistance of any given system. Consequently, control of the perfusion is effected at all points of a mesh by vasomotion at the upstream end (although the response depends on the local morphology). All of these features of red cell motion may have important applications when the phenomenon of autoregulation is being considered.

4. The non-axisymmetric case

We now consider a model where the pressures, velocities, and film thicknesses depend on two arguments: the axial coordinate x and an azimuthal angle ϕ. We make the usual lubrication assumptions, namely that pressure is independent of the coordinate measured across the film, and

that inertial forces may be ignored. The corresponding simplified Navier-Stokes equations are

$$\frac{\partial p}{\partial x} = +\frac{\mu}{r}\cdot\frac{\partial}{\partial r}\left(r\frac{\partial u}{\partial r}\right)$$

$$\frac{\partial p}{\partial \phi} = +\mu\frac{\partial}{\partial r}\left(r\frac{\partial w}{\partial r}\right) \qquad (4.1)$$

where u, w are the axial and azimuthal velocity components respectively. Integration with respect to r, and use of the boundary conditions

$$u = 0 \quad \text{on} \quad r = R, \qquad u = -U \quad \text{on} \quad r = R + h$$

$$w = 0 \quad \text{on} \quad r = R, \qquad w = 0 \quad \text{on} \quad r = R + h$$

now give

$$u = +\frac{1}{4\mu}\cdot\frac{\partial p}{\partial x}\left[r^2 - R^2 - \frac{2Rh+h^2}{\ln(1+h/R)}\ln\frac{r}{R}\right] - \frac{U.\ln(r/R)}{\ln(1+h/R)}$$

$$w = +\frac{1}{\mu}\cdot\frac{\partial p}{\partial \phi}\left[r - R - \frac{h.\ln(r/R)}{\ln(1+h/R)}\right] \qquad (4.2)$$

Integrating the continuity equation

$$\frac{\partial}{\partial r}(rv) = -r\frac{\partial u}{\partial x} - \frac{\partial w}{\partial \phi}$$

across the gap, we obtain

$$\left[rv\right]_R^{R+h} = -\frac{\partial}{\partial x}\int_R^{R+h} r.u.dr - \frac{\partial}{\partial \phi}\int_R^{R+h} w.dr + \left[ru\right]_{R+h}\cdot\frac{\partial}{\partial x}(R+h)$$

as in section 3; and we similarly simplify this to

$$\frac{\partial}{\partial x}\int_R^{R+h} r.u.dr + \frac{\partial}{\partial \phi}\int_R^{R+h} w.dr = 0 \qquad (4.3)$$

Substituting (4.2) in this gives a Reynolds' equation

$$\frac{\partial}{\partial x}\left\{\frac{1}{4\mu}\cdot\frac{\partial p}{\partial x}\cdot\frac{2Rh+h^2}{4}\cdot\left[2R^2+2Rh+h^2-\frac{2Rh+h^2}{\ln(1+h/R)}\right]-U\left[\frac{(R+h)^2}{2}\cdot\frac{2Rh+h^2}{\ln(1+h/R)}\right]\right\}$$

$$+\frac{\partial}{\partial\phi}\left\{\frac{1}{2\mu}\cdot\frac{\partial p}{\partial\phi}\left[2Rh+h^2-\frac{2h^2}{\ln(1+h/R)}\right]\right\}=0 \qquad (4.4)$$

This may be approximated to any desired accuracy by expansion of the logarithmic terms as Taylor series; we obtain, e.g.,

$$\frac{\partial}{\partial x}\left\{\frac{\partial p}{\partial x}\cdot\frac{Rh^3}{12}-\mu U\frac{Rh}{2}\right\}+\frac{\partial}{\partial\phi}\left\{\frac{\partial p}{\partial\phi}\cdot\frac{h^3}{12R}\right\}=0 \qquad (4.5)$$

as a first approximation corresponding to Lighthill's equation in the axisymmetric case. For clarity and simplicity of manipulation, we shall use this form, together with the simplified parabolic expression for the film thickness,

$$h = \beta(p-p_0)+\tfrac{1}{2}\kappa x^2$$

It has been shown that this should give a reasonably good approximation to the actual behaviour, provided that finite limits $(-g,g)$ are used for the ends of the pellet. In any case, we shall be interested only in the broad features of the flow (not in an exact solution) since the approximations we have made in setting up the asymmetric model must necessarily be fairly crude, in view of the comments made in section 1 on the paucity of observational data.

The elastic and geometric parameters of the model

are now functions of ϕ; accordingly, we may write

$$\beta = \beta_0 F_1(\phi)$$

$$K = K_0 F_2(\phi)$$

where $F_1(\phi)$, $F_2(\phi)$ are both unity; and the expression for film thickness is now

$$h(x,\phi) = \beta_0(\rho - \rho_0(\phi))\ F_1(\phi) + \tfrac{1}{2} K_0 F_2(\phi) x^2 \qquad (4.6)$$

Clearly, $F_1(\phi)$ and $F_2(\phi)$ are non-dimensional; notice also that the reference pressure ρ_0 may now be a function of ϕ. We may now express the flux $q(\phi)$ in terms of some reference value at $\phi = 0$:

$$q(\phi) = q_0 Q(\phi)$$

and non-dimensionalize as in section 1, using the reference values q_0, β_0, K_0 and $p_0(\phi)$. We obtain

$$h = \frac{2q_0}{U} H \ , \quad x = \left\{\frac{2q_0}{U K_0}\right\}^{\frac{1}{2}} X \ , \quad R = r_0 J(X) \ ,$$

$$p - \rho_0(0) = \frac{2q_0}{\beta_0 U} P(\phi) \ , \quad p_0(0) - \rho_0(\phi) = \frac{2q_0}{\beta_0 U} P_0(\phi)$$

Here $P_0(\phi)$ is a non-dimensional expression for the variation in reference pressure.

Equations (4.5) and (4.6) become

$$\frac{\partial}{\partial X}\left(J(X).H^3 \frac{\partial P}{\partial X} + LJH\right) + M \frac{\partial}{\partial \phi}\left(\frac{\partial P}{\partial \phi} \cdot \frac{H^3}{J}\right) = 0 \qquad (4.7)$$

$$H = F_1(\phi)\left[P + P_0(\phi)\right] + \tfrac{1}{2} F_2(\phi) X^2 \ , \qquad (4.8)$$

where L is defined as before, and $M = C/\kappa_0 r_0$; C is as before the ratio of a typical gap size $2q_0/U$ to the tube radius r_0. We have already shown that we expect $\kappa_0 r_0$ to be of order unity and C to be very small; we may therefore write

$$M \ll 1$$

This implies that we may neglect azimuthal pressure gradients in the Reynolds' equation (4.7) as a first approximation. Incidentally, this argument justifies a similar approximation made by Christopherson and Dowson (1959) for a model of a sphere moving through a closely-fitting tube; and the success of that model encourages us to make the simplification discussed above. We may now integrate (4.7) to obtain

$$\frac{dP}{dX} = L\left\{\frac{Q(\phi)}{H^3} - \frac{1}{H^2}\right\} \qquad (4.9)$$

where we have put $J(X) = 1$ as in the derivation of equation (3.4); this eliminates the singular behaviour which would otherwise occur at the ends of the pellet, where $J(X) = 0$ in the more exact model.

The flux function $Q(\phi)$ has not yet been prescribed; but if we use as a boundary condition $P(G) = b(L)$, say, independent of ϕ, then $Q(\phi)$ will be determined as that function which produces a value of $P(-G)$ also independent of ϕ. (Clearly, the upstream and downstream pressures cannot

depend on the azimuthal coordinate.) In fact, we shall determine b(L), for any L, as that value of P(G) which yields P(-G) = P(G) (an approximation discussed previously), at the reference point $\phi = 0$, say, where we define $Q(0) = 1$.

The principal reason for examining the non-axisymmetric case is to determine whether the asymmetries cause any additional local constriction of the lubrication layer; we shall, therefore, be interested in a local film thickness parameter $C(\phi)$, say. We may write

$$C(\phi) = \frac{2q_o Q(\phi)}{U r_o} ;$$

and since q_o, U, r_o, are all independent of ϕ, we may use the leakback function $Q(\phi)$ as a measure of C. This will be done in the computations which follow; the remarks made about the behaviour of Q may equally well be taken to refer to C.

Since we shall be interested in small deviations from axisymmetry, it is of interest to consider the relative magnitudes of the effects produced by the various possible asymmetries in the parameters. While small variations in κ and β may be expected to produce variations in Q of the same order of magnitude, small variations in the radius of the pellet can produce significant alterations in the clearance, since this is assumed to be small in any case. It might be expected, therefore, that such clearance variations will

produce large variations in the reference pressure needed to produce zero clearance; we shall in the computations consider only a modification in the pellet radius, to simplify the discussion of the results. A simple sinusoidal variation in the undistorted pellet radius is assumed, so that $P_o(\phi)$ is of the form $\frac{1}{2}T(\cos 2\phi - 1)$, where T is the 'degree of asymmetry', and represents the difference between the reference pressures (pressure required to distort the pellet just sufficiently for it to fit the tube) at the points of smallest and largest clearance. Since $P_o(\phi)$ is negative at $\phi = \frac{\pi}{2}$, we are decreasing the effective pressure available to produce elastic distortion; this is due, of course, to an increase in the reference level from which these 'distortion pressures' are measured. It might be expected that this rise in the reference pressure might equally be interpreted as a fall in the downstream pressure needed to satisfy the condition (1.7), consequent on an effective increase in the value of the parameter L if the leakback were assumed to remain constant (i.e. L is kept constant only by allowing the leakback to decrease): but although this gives an indication of how we expect the leakback to vary, it cannot be used as a computation technique, since the scaling factors for the non-dimensionalization all depend on the use of some constant leakback reference level

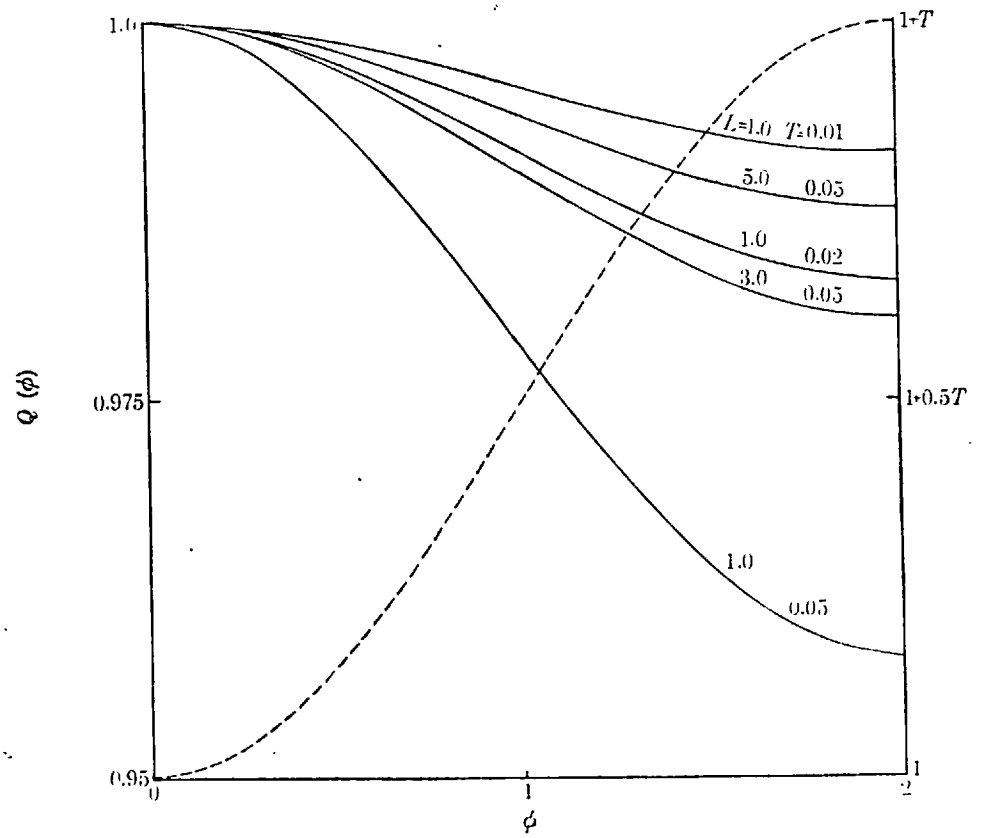


FIGURE 5. Variation of leakback with azimuthal angle for a non-axisymmetric pellet, for various values of L and T (the 'degree of asymmetry'). The broken line represents the corresponding variation in reference pressure, expressed as a ratio of the value at $\phi = 0$.

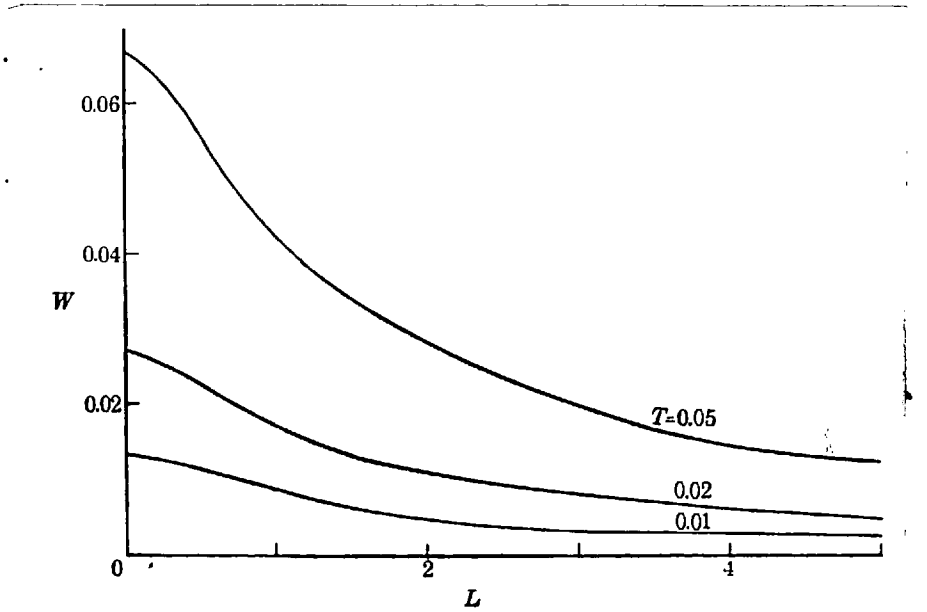


FIGURE 6. Decrease of W (asymmetry in leakback, $1-Q(\frac{1}{2}\pi)/Q(0)$) as L increases, for various values of T.

(which would not in this case exist).

As we expect, the leakback decreases as the reference pressure increases around the circumference of the pellet, and the maximum leakback defect is very nearly proportional to the degree of asymmetry for the values of T used; Fig. 5 shows some typical plots of the leakback function Q against $\emptyset$ for various degrees of asymmetry. The form of the reference pressure variation is also shown for comparison. Perhaps the most interesting feature of the results is that the maximum leakback defect decreases as L increases. As pointed out in section 2, this means that under conditions of negative clearance, when film constriction may possibly bring about failure of lubrication, any increased tendency in this regard caused by local asymmetries is reduced. If we define Γ as $1 - Q(\frac{\pi}{2})/Q(0)$, then Γ represents the amount of asymmetry induced in the leakback (and hence in the film thickness) by the asymmetry in the pellet shape; it will depend on T and L.In Fig. 6 we show how Γ decreases from a value of the order of T (for small-L flow), as L increases to values characteristic of normal blood flow; the tendency of the flow to symmetrize for larger values of L is clearly shown.

It was pointed out in section 2 that one of the most important consequences of these results (as far as this

theory is concerned), is that non-axisymmetric pellets may be treated with reasonably accuracy by an axisymmetric model, since the departures from axisymmetry are reduced by the flow. This, of course, extends the utility of the theory of section 3 for discussing capillary flow phenomena, where the pellets (red cells) are not always axisymmetric.

5. Tube porosity

In this final section we analyse a model in which leakage through the wall of the tube may occur. As discussed in the introductory outline of section 2, we shall consider that a local uniform loss of fluid occurs, the amount depending on the filtration coefficient λ and the mean filtration pressure, P_f say. For a tube of radius r_o, the fluid loss per unit length of tube is $\lambda P_f . 2\pi r_o$. If at any point the velocity of the pellets is U and the leakback is Q, then the total flux past that point is $\pi r_o^2 U - 2\pi r_o Q$; consequently, the fractional reduction in flux is $2\lambda P_f /(r_o U - 2Q)$ per unit length of tube, in the downstream direction. Further, since this result is also true of a coordinate system in which the pellets are stationary, the fractional reduction in leakback (which has been defined as the negative of the flux in such a system) is $-2\lambda/Q$, in the downstream direction. We shall denote this constant by $-k$.

If we consider a reference value of the leakback, Q_o, to be that which occurs at the midpoint of the pellet ($x = 0$), then the leakback at any point is $Q_o(1 + kx)$; we may define the parameter L in the non-dimensional form of the equations in terms of Q_o. Alternatively, we may define Q_o as the value at the upstream end of the pellet ($x = -g$), when the leakback is $Q_o\left[1 + k(x + g)\right]$; although this definition gives nominally different results in terms of the parameters L and C, the relations between the velocity, resistance and clearance parameters are found to be identical for the two formulations (as, indeed, we might expect). We shall, therefore, use the former definition in the following analysis.

If we write the leakback expression in terms of our non-dimensional variables, it becomes $Q_o(1 + KX)$, where K is the parameter

$$K = k(2Q_o/\kappa U)^{\frac{1}{2}} = 2\lambda P_f/\left[U(C\kappa r_o)^{\frac{1}{2}}\right]$$

In section 3 we showed that $U \approx 15(\kappa r_o)^{\frac{1}{2}} A$, and $A = LC^{5/2}/6$; further, it was found that κr_o is of the order of unity for erythrocyte-like pellets. We shall therefore use the formula

$$K = \frac{0.8\lambda P_f}{LC^3}$$

as our definition of the 'leakback reduction coefficient'.

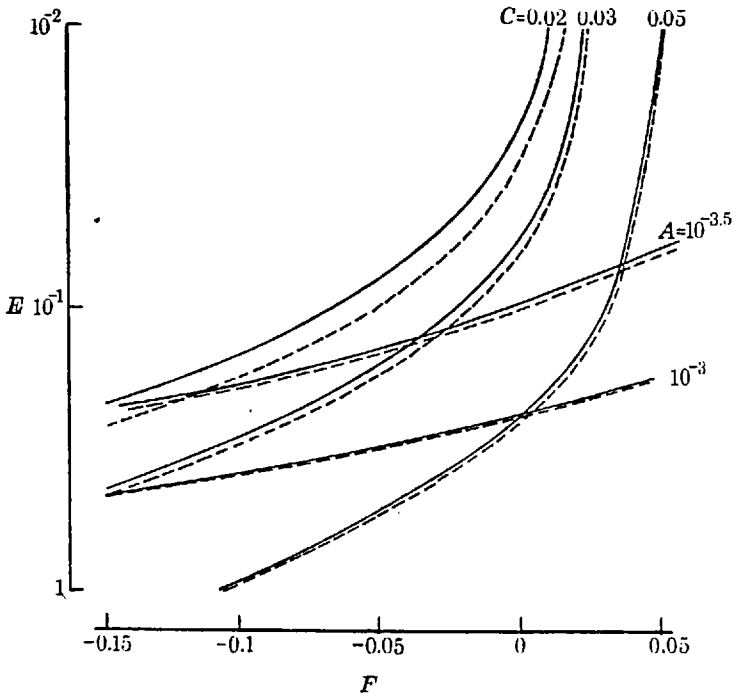


FIGURE 7. Effect of tube porosity on the curves of figure 3; the broken lines show the modification for a filtration constant λ of 0.0056 μ^3 s^{-1} μ^{-2}(cm H_2O)$^{-1}$ pressure, and a transcapillary pressure 10 cm H_2O.

If we now substitute the above form of the leakback into equation (3.3), we obtain a modified non-dimensional Reynolds' equation

$$\frac{dP}{dX} = \frac{2}{3}LC\left[C(1+KX)-\frac{1}{2}\frac{CH(2-CH)}{\ln(1-CH)}-1\right]\cdot\left(H-\tfrac{1}{2}CH^2\right)^{-1}\cdot \left[2-CH(2-CH)+\frac{CH(2-CH)}{\ln(1-CH)}\right]^{-1} \qquad (5.1)$$

while the equations (3.11), (3.12) and (3.13) remain unchanged. A similar series of computations to those of section 3 may now be performed for this modified equation, using the same techniques as those employed earlier. It is convenient to discuss the results in terms of the parameters A, C, E, and F defined in section 3.

As was foreshadowed in the discussion of section 2, we find that for a given clearance and pressure gradient, film thickness and velocity are both reduced. These effects are illustrated in the curves shown in Fig. 7. The broken lines represent curves of constant film thickness and velocity (using as coordinates clearance and resistance) in the absence of fluid leakage; the continuous lines represent the same curves with a filtration constant λ of .0056 μ^3/sec/μ^2/cm H_2O pressure (obtained for frog mesentery by Landis, 1927), and a transcapillary pressure of 10 cm H_2O. These values are merely representative of the range of conditions which obtain in various microcirculatory systems; the mag-

nitude of the effect naturally depends on the filtration constant, which may range in mammalian capillaries from .00025 (muscle) to .03 (glomerulus) $\mu^3/sec/\mu^2/cm\ H_2O$. Furthermore, the transcapillary pressure may become negative (at the distal end of capillaries); computations made with a value of -5 cm H_2O indicate that the reverse effect occurs under these inflow conditions, with magnitude approximately half that obtained above for outflow at 10 cm.

It is noticeable that, under conditions typical of normal flow in capillaries ($A = 10^{-3}$, $C = .035$) the effect of fluid loss is relatively small; the film thickness is reduced by less than 3%, and the velocity even less (for the filtration constant quoted). It is only for reduced velocity, film thickness, and pressure gradient that the effects become noticeable; we might expect the leakage to cause a rather more rapid cessation of flow on reduction of pressure than would be expected for a non-porous capillary, but not to affect normal flow to any great extent (unless, of course, abnormally high filtration rates occur, as in the case of capillary damage). Computations performed using a much larger filtration coefficient, such as is found in glomerular capillaries (.03 $\mu^3/sec/\mu^2/cm\ H_2O$) show that even for this fivefold increase in filtration, the film thickness reduction is only doubled. Perhaps this is the most

remarkable feature of this theory of porous capillary flow; the system is able to produce movement of metabolites by transport through the capillary walls, without interfering unduly with the pressure-flow characteristics of the microcirculation.

Acknowledgements

The author is deeply indebted to Professor M.J. Lighthill, without whose continued guidance, assistance and interest this work could not have been undertaken. He is also grateful to Dr. C.G. Caro for many informative discussions on the physiological aspects of the theory. The author would like to thank the Trustees of the Gowrie Scholarship Trust Fund for the financial support of a Gowrie Travelling Scholarship, during the tenure of which this work was undertaken.

References

Burton, A.C. 1966 Federation Proc., 25, 1753.

Christopherson, D.G. and Dowson, D. 1959 Proc. Roy. Soc. A, 251, 550.

Djojosugito, A.M., Folkow, B., Oberg, B. and White, S. (in the press).

Fung, Y-C. 1966 Federation Proc., 25, 1761.

Fung, Y-C. 1968 Appl. Mech. Rev., 21, 1, 1.

Glazier, J.B., Hughes, J.M.B., Maloney, J.E. and West, J.B. 1968 CIBA Conference on Mass Transport.

Guyton, A.C. 1963 Circulation Res., 12, 399.

Landis, E.M. 1927 Amer. J. Physiol., 82, 217.

Lighthill, M.J. 1968 J. Fluid Mech., 34, 113.

Luft, J.H. 1966 Federation Proc., 25, 1773.

Merrill, E.W. and Wells, R.E. 1964 Appl. Mech. Rev., 14, 9, 663.

Rand, R.P. and Burton, A.C. 1964 Biophysics J., 4, 115.

Verney, E.B. 1951 Dunham Lecture, Harvard University.

Verney, E.B. and Rushton, W.A.H. 1950 Proc. XVIII International Physiol. Congress.

Wiederhielm, C.A. 1966 Federation Proc., 25, 1789.

Zweifach, B.W. and Intaglietta, M. 1966 Federation Proc., 25, 1784.

Chapter III

'Implications of a Theory of Erythrocyte Motion in Narrow Capillaries'

Abstract

A theory of lubricated motion of deformable erythrocytes in very narrow capillaries is discussed, and applied to physiological phenomena. Velocities are smaller than expected if the pellet-fluid character of the motion is ignored; resistances are enhanced, and depend non-linearly on the velocity and capillary diameter. Film thickness decreases with decreasing velocity, and 'seize-up' may occur due to lubrication failure. The results are applied to phenomena such as perfusion control by vasomotion in arterioles, uneven filling of pulmonary capillary beds, non-linear apparent blood viscosity, and pressure-flow relationships in the capillaries. Approximate numerical values are obtained, and shown to be in reasonable agreement with observation.

Introduction

In a recent paper (6), the author presented a theoretical discussion of a model for red cell motion in narrow capillaries, and indicated possible applications of the theory. The aim of the present work is to review briefly, in as non-mathematical a manner as possible, the results of that theory; to convert these results to physiologically significant forms; and to explore the implications for various mechanical phenomena of the microcirculation, in the light of recent experimental findings. The numerical results given here are principally for illustrative purposes. Some necessarily crude approximations in the model make the quantitative predictions of perhaps uncertain accuracy; and it is the qualitative behaviour that is to be emphasized.

It is now generally accepted that blood in the capillaries cannot be regarded as a practically homogeneous fluid, but must in any dynamical consideration be treated as a suspension of solid bodies (the erythrocytes) in the plasma (9). Gabe and Zatz (11) have demonstrated that plasma behaves as a Newtonian fluid to good accuracy; furthermore, the Reynolds' number for plasma in capillaries is very small (10^{-2} or 10^{-3}), so that the plasma flow is governed by a balance between pressure gradient and

viscous forces - inertial contributions (dynamic head) may be ignored. An influential feature of the geometry is that the red cell diameters are comparable with those of the capillaries, as emphasized in the axial train concept of Whitmore (25). In some cases, the red cells are larger than the capillaries, and must deform in order to pass through. Other authors (1, 20, 23) have also discussed the theoretical behaviour of a series of fairly tightly-fitting solid bodies in fluid-filled tubes. These studies considered only rigid pellets, except for the comments of Whitmore on cell deformation in highly-sheared flows.

The currently-accepted erythrocyte model is that of a very flexible, slightly elastic membrane, supporting a small surface tension, in the form of a biconcave disc, 8 μm in diameter, and 2 μm thick at the rim, and containing an incompressible medium. (one hesitates to say 'liquid medium' until detailed information is available on erythrocyte internal structure.) Fung (10) has shown that such a structure can easily support changes in uniform pressure without deforming. An important consequence is that only non-uniform force distributions can cause deformation. There are two principal modes of deformation (15); 'bowing' produced by a combination of pressure gradient and viscous drag at the rim, and 'squashing' when

the rim is subject to local increased pressure (in a narrow capillary). In contrast, the walls of systemic capillaries are much less compliant (2, 10).

Lighthill (16) pointed out that, in narrow capillaries (whose diameters are equal to or less than red cell diameter), a lubricating film of plasma must be present between the cell rim and the endothelium, to permit free sliding of the cells. The relatively large pressures developed in the lubrication region will distort the cell membrane, and these elastic effects must be included in any dynamical treatment of narrow-capillary flow. Lighthill's investigations indicated that the resistance would be higher than for a corresponding homogeneous-fluid flow, and would depend non-linearly on velocity. Whitmore's concept of plasma 'leakback' (25) was extended to very narrow capillaries, and shown to be velocity dependent; it was postulated that this might have important consequences for the mass transport of gases. The thickness of the lubrication film decreases as velocity decreases, and this may lead, at very small film thicknesses, to a breakdown of the lubricating properties of the fluid, and a consequent sharp rise in resistance due to the development of frictional forces - a process referred to by Lighthill as 'seize-up'.

It is perhaps not immediently apparent that lubrication by plasma films is a necessary feature of red cell movement in narrow capillaries. There is, of course, justification for applying the well-known principles of lubrication theory to biological systems; such a treatment is a cornerstone of recent work on bone joints, for example (17); but it is not obvious that frictional forces would present a serious obstacle to the motion of erythrocytes in the absence of lubrication, since the cells are believed to be coated with layers of 'slippery' phospholipids. However, under normal circumstances there is probably no such thing as a dry membrane *in vivo*, and the presence of a fluid layer, presumably plasma, on the red cell membrane would constitute a lubrication film in the thin gap between cell and endothelium. Moreover, it may be argued that the phospholipids depend for their 'slipperiness' on the presence of fluid - Lighthill (15) has cited the analogy of the large frictional forces associated with a dry cake of soap. It is not envisaged that the mechanism of possible seize-up is one of complete removal of fluid from the gap, but rather of a breakdown of the lubricating properties of the film when some limiting thickness is reached; such behaviour has been observed, in a more classical context for thin-film sliding lubric-

ation (3), and more recently for low pressure gradient studies on blood (4), discussed in a later section.

Lubricated motion of an elastic pellet in a rigid tube

The equation governing the flow of fluid in a lubrication zone (the Reynolds' equation) is derived from the Navier-Stokes equations and the continuity condition (see (6)). Essentially, the pressure gradient along the zone (assumed constant for any cross section) is expressed in terms of the thickness of the lubrication film at any point. The equation also depends on the pellet velocity and on the volume flux of fluid past any cross-section (the 'leakback'). This is a priori unknown, but is uniquely determined by a second dynamical condition; the viscous drag on the pellet must just balance the 'driving force' of the applied pressure gradient. A third equation for the three unknowns (pressure, leakback and gap width) is the law of elastic compliance for the pellet. (In (6) a linear relationship was used, and shown to be a reasonable approximation for the red cell.) The gap width is expressed in terms of the undistorted geometry of tube and pellet, and the local deformation produced by the lubrication pressure.

The fluid pressures at the rim depend also on the

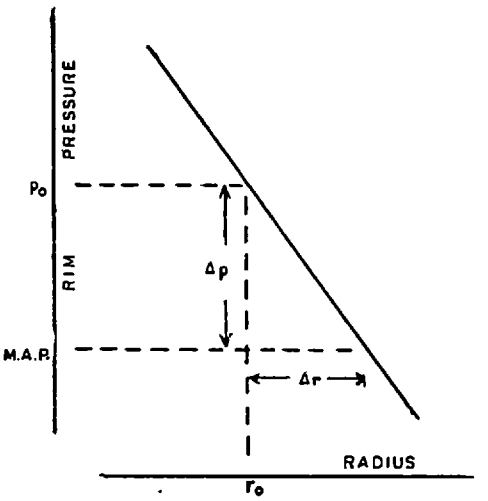


FIG. 1. Illustrating the concept of clearance. Δr is the radius increase caused by pressure reduction Δp from the reference level p to the mean ambient pressure MAP.

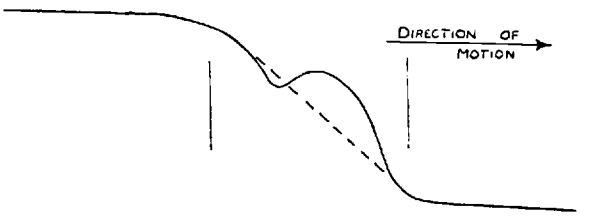


FIG. 2. Typical low-clearance pressure profile. Vertical lines mark the edges of the lubrication zone. Broken line indicates the mean pressure gradient in the zone.

amount of deformation necessary for the pellet to fit inside the tube. This is measured by the 'clearance' F of the pellet, defined as follows: suppose the rim pressure at the middle of the pellet is allowed to change from a reference level p_o (at which the pellet just fits inside the tube) to the 'mean ambient pressure', due to the applied pressure gradient (in the absence of any extra lubrication pressures). This will cause a change of pellet radius; the clearance is the negative of this radius change, expressed as a ratio of the tube radius. The concept is illustrated in Fig. 1; if Δp and Δr are the pressure and radius changes shown, and r_o is the tube diameter, then

$$F = -\Delta r/r_o$$

Clearly, positive values of F refer to pellets which fit without necessarily requiring deformation in the lubricating zone, while negative-F pellets need such deformation; for these pellets, we expect elastic properties to play a large part in determining the mechanics of motion. We shall show that negative or very small positive values of F are expected for red cells in narrow capillaries.

Fig. 2 shows a typical pressure profile for a negative-clearance lubrication zone. The physical significance of the profile has been fully discussed elsewhere

(6, 16). Notice particularly that the mean pressure gradient across the lubrication region is much greater than that in the plasma 'bolus' separating neighbouring cells. This suggests that the red cells play a dominant role in determining resistance (and hence velocity) in narrow capillaries.

The three equations described above may be solved to give relationships between velocity, pressure gradient, film thickness and clearance. It is also interesting to discuss the resistance at various velocities, expressed as a ratio of the (constant) resistance of a corresponding homogeneous Newtonian fluid (c.h.N.f.)) 'corresponding' in the sense of having a viscosity typical of whole blood in the bulk, and a mean velocity a little less than red cell velocity. We call this ratio D_*(a slightly different definition was used in (6)). Another useful parameter is the 'velocity reduction factor' R_v, which expresses the ratio of pellet velocity for a given pressure gradient to the expected velocity for c.h.N.f. All important symbols are listed for convenience in the table opposite. Several interesting results emerge:

(i) Velocities are much smaller than those expected if the pellet-fluid character of the flow were ignored. Values of R_v range from 0.4 for zero and small positive-

clearance conditions (corresponding to capillaries of 7.5 -9 μm diameter) to 0.15 for F = -0.1 (6 μm capillary). These values are for normal flow conditions; they become much lower at reduced velocities.

(ii) R_v depends sensitively on the pressure gradient, indicating that the velocity depends non-linearly on the pressure gradient. It is important to distinguish this characteristic from the previous one - not only are velocities much smaller than for c.h.N.f., they decrease more rapidly as the pressure gradient is reduced. Curves of R_v against pressure gradient for red cells in capillaries are given later (Fig. 5). For 5-7 μm capillaries, it is found that, approximately,

$$R_v \propto (\text{pressure gradient})^{\frac{1}{2}}$$

(iii) For positive clearances, film thickness is rather insensitive to velocity, and takes larger and larger values as F increases. Hence little possibility of 'seize-up' occurs under these conditions (8-9 μm capillaries and above) unless pressure gradients are reduced virtually to zero.

(iv) For negative clearance, film thickness decreases markedly with velocity (or pressure gradient); computations show that, approximately,

$$\text{film thickness} \propto (\text{velocity})^{\frac{1}{2}}$$

(v) For a given (negative) clearance, D increases as velocity decreases. Consequently, if pressure gradient is reduced, the velocity must fall more than would velocity of c.h.N.f., in order that the equilibrium of forces is maintained, and this effect is greater for smaller velocities. It is found that, approximately,

$$D \propto (\text{velocity})^{-\frac{1}{3}}$$

(vi) For a given velocity, D increases as clearance decreases. Consequently, there is more disparity (in pressure-velocity terms) between two tubes of slightly different diameter than for c.h.N.f.

Pellet asymmetry

The above theory was developed for an axisymmetric pellet. It is possible (6) to discuss the effect of small asymmetries; the results strongly indicate that the same behaviour holds for larger ones. It might be expected that the fluid would tend to 'take the line of least resistance' and flow, as far as possible, through regions where the gap thickness is greatest. This would enhance the effect of the asymmetry, and cause local 'high spots' in the lubrication layer, producing greater resistance and leading to more rapid seize-up. Rather surprisingly, this does not

happen; the deformability of the membrane allows the fluid pressures to reduce the effect of the asymmetry, and 'flatten out' the gap profile around the circumference. This 'symmetrization' increases as clearance decreases, i.e. under conditions where we might expect asymmetrical effects to seriously hamper lubrication, the large pressure peaks generated in the thin film are more able to smooth the irregularities. The arguments apply equally well to asymmetries in the tube cross-section; we may therefore confidently discuss, for example, flow in pulmonary capillaries which have been distorted from circularity by tension in the alveolar wall.

Capillary filtration

Since the pressure-flow relationships depend to a large extent on lubrication film thickness, it has been suggested (16) that fluid loss through the walls of the capillary may enhance the resistance effects, and increase the possibility of seize-up, by causing reductions in film thickness. A study of a fairly simple model, involving uniform filtration per unit length of capillary, has been made (6), taking typical filtration coefficients (14). Although both film thickness and velocity (for a given clearance and pressure gradient) were reduced by filtrat-

ion, the effect was very small. Even for glomerular capillaries, with high rates of filtration (.03 $\mu m^3/sec/\mu m^2/cm\ H_2O$), film thicknesses at normal velocities were reduced by only about 6%, and velocities even less. The physical explanation for the behaviour is not clear, because of the complexity of the system. Perturbations in leakback produced by the filtration modify the equation of continuity rather than the balance of forces, and it appears that the continuity equation has relatively less importance in determining flow characteristics.

The magnitude of the effect increases as the pressure gradient is reduced; we might expect cessation of flow to occur at slightly higher pressure gradients. This is likely to be the principal effect of filtration, unless abnormally high filtration rates occur, in pathological conditions such as tissue damage. In normal conditions, however, it is remarkable that the system is able to produce movement of metabolites by transport through the capillary walls, over a wide range of filtration rates, without interfering unduly with pressure-flow characteristics of the narrow capillaries.

Mechanics of the red cell

We now obtain approximate values for the clearance

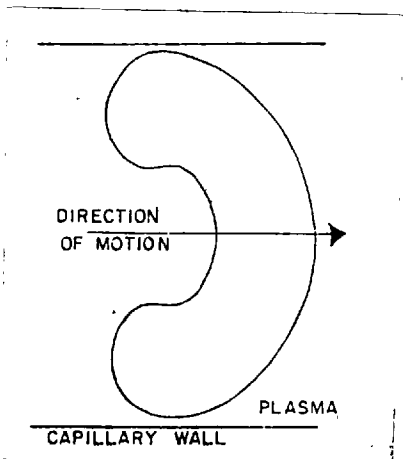


FIG. 3. Parachute configuration of the red cell in a narrow capillary.

and elastic compliance of the erythrocyte. Treating the rim of the cell as a flexible membrane, Fitz-Gerald (6) has shown that the elastic compliance β of the rim, defined as the local deformation produced by unit change of local pressure, is approximately of the form

$$\beta = r_o^2/(15S)$$

where r_o is the capillary radius, and S is the 'resistance to deformation' of the membrane, approximately .0185 dynes /cm (22). Values of β are of the order of 6.5 μm/cm H_2O computed for a 6 μm capillary); this parameter determines the amount of 'squashing' produced by the lubrication pressures.

Calculations of the clearance depends on the mode of deformation as well as relative diameters. For the 'parachute' configuration (Fig. 3), the amount of 'bowing' produced by the pressure difference and viscous drag may be theoretically derived for a geometrically simplified model, and the clearance parameter obtained approximately (6) as

$$F = 1 - k_1 S/r_o(\delta p)\left[\sin(k_2(\delta p)/S)\right]$$

where (δp) is the pressure difference across the faces of the cell, and k_1, k_2 are geometric constants. This relationship is valid only for capillaries whose diameters are

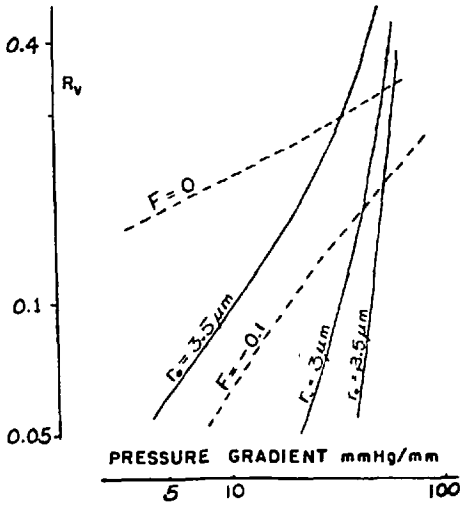


FIG. 5. Velocity reduction factor as a function of pressure gradient for various capillary radii. Broken lines indicate hypothetical curves for constant-clearance pellets. (Both scales are logarithmic.)

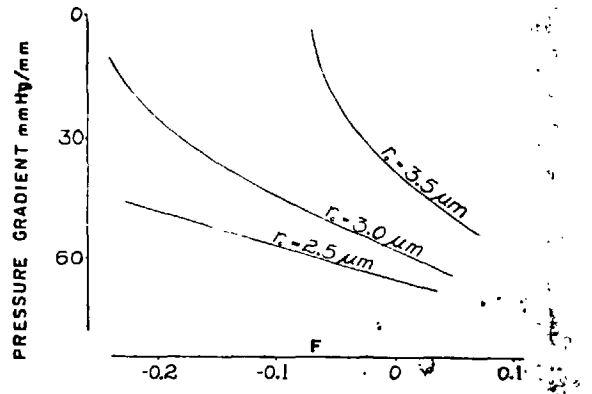


FIG. 4. Clearance as a function of pressure gradient for various capillary radii.

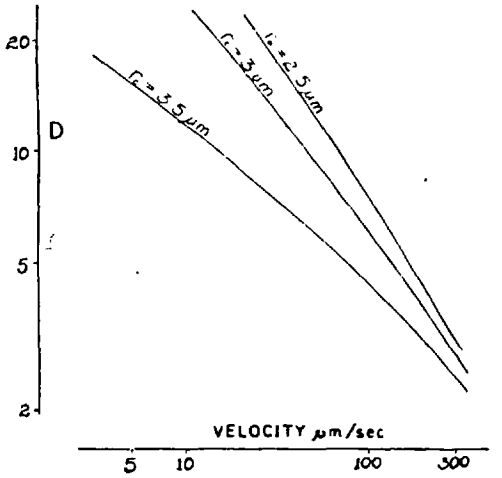


FIG. 6. Resistance enhancement against velocity for various capillary radii. (Scales are logarithmic.)

greater than about 5 μm; for smaller capillaries, the rolled-up 'crepe-suzette' shape described by Burton (2) predominates.

Theoretical values of F for red cells in capillaries are shown in Fig. 4. Under physiological conditions, F depends sensitively on pressure gradient; as this (and velocity) increases, the amount of 'bowing' increases, giving a larger clearance (easier fit). Conversely, we expect the decreasing clearance for decreasing pressure gradient to make the velocities fall even faster than for a pellet whose clearance is independent of pressure gradient. Fig. 5 shows curves of velocity reduction factor R_v; for comparison, some constant-clearance curves are also shown. Plots of the resistance enhancement parameter are shown in Fig. 6. All of the numerical predictions of the following sections include the above effects of the functional dependence of cell bending on pressure gradient, and no specific mention is made in the applications of the particular role played by cell deformation.

The enhanced resistances predicted here do not seem to be in accord with the findings of Prothero and Burton (20), who consider friction between capillaries and erythrocytes to be negligible, and find the resistance offered by whole blood in narrow capillaries to be perhaps

only 30% greater than that of plasma alone. It is difficult to accept, however, that their experimental results are indicative of flow in the narrow capillaries where this friction might be present. Their erythrocyte velocities are of the order of 30 cm/sec; the relatively large pressure gradients associated with these extreme velocities would considerably reduce the effective radius of the red cell (increase its clearance); and although their capillary diameters averaged about 8.4 μm, tapering to 5 μm, we might expect their results to apply to flow regimes typical of somewhat larger capillaries, and not to conflict with the predictions of the present theory. This is confirmed by Whitmore (25), who points out that these results of Prothero and Burton are in good agreement with his theoretical calculations for blood flow in capillaries a little larger than red cells.

It is interesting that for larger capillaries (10-40 μm), Whitmore predicts red cell velocities considerably in excess of mean velocities expected for c.h.N.f., and resistances less than for c.h.N.f.; this effect, together with that of recruitment, may help to explain the large increases in perfusion (up to 15 times) during exercise.

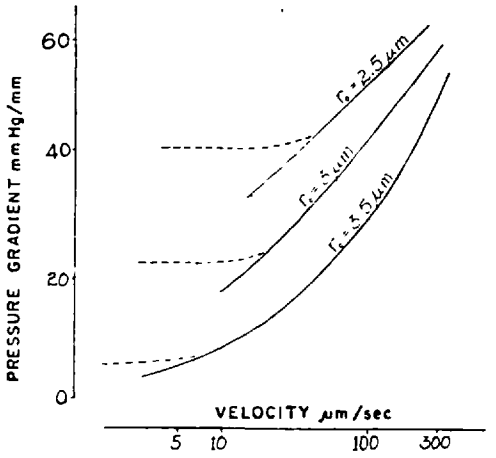


FIG. 7. Erythrocyte velocity as a function of pressure gradient for various capillary radii. Broken lines indicate seize-up due to lubrication failure. (Velocity scale is logarithmic.)

Pressure-flow relationships in the capillaries

We may now plot predicted velocities (in microns per second) against pressure gradient (in mm Hg/mm) for red cell movement in capillaries of various diameters (Fig. 7). In a 7 μm capillary, probably quite small by systemic standards, a typical velocity of the order of 100-200 μm/sec (8) corresponds to a predicted pressure gradient of 30-45 mm Hg/mm. Actual measurements of capillary pressure gradient are extremely difficult; however, it is thought that a pressure drop of 20-25 mm Hg occurs in the systemic capillaries (19), over distances of the order of 0.1-1.0 mm (9). A rough estimate of pressure gradient based on these figures is in reasonable agreement with the sort of values predicted by the theory, provided that the measured estimate is typical of individual narrow-capillary elements.

In the pulmonary circulation, a larger proportion of the pressure drop occurs in the capillary networks (7), even though the total drop is relatively small (say 15 mm Hg). More of the capillaries fall in the range of diameters treated by the lubrication theory (24), and more of the pressure-flow effects (compared with systemic capillaries) are probably due directly to the mechanical behaviour of the system. The theory is therefore most relevant

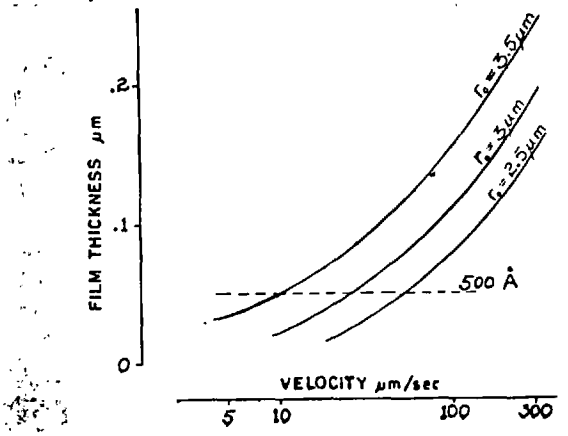


FIG. 8. Lubrication film thickness against velocity for various capillary radii. Broken line denotes 500 A thickness, at which seize-up may occur. (Velocity scale is logarithmic.)

to the pulmonary microcirculation, although there are apparently important flow regulation phenomena in narrow systemic capillaries to which it applies.

Fig. 7 illustrates the previously-mentioned dependence of red cell velocity on pressure gradient, and the greater sensitivity of flow in narrower capillaries. Film thickness also depends on pressure gradient; Fig. 8 plots film thicknesses for various capillary diameters. These are calculated for a 'normal' red cell of 8 μm diameter. Lubrication theory shows that for very thin films, a few hundred Å thick, the lubricant behaves in a non-Newtonian manner, and film breakdown, with consequent sudden increase in resistance, rapidly occurs. The thin muco-polysaccharide coating on the endothelium (18) probably forms such a limiting layer, and 'seize-up' might be expected when this coating fills most of the lubrication region. The broken lines in Fig. 7 show possible modification due to seize-up, if the critical thickness of the coating is assumed to be 500 Å. Thus the theory predicts, for example, that flow in a 7 μm capillary element would cease at a pressure gradient of about 6 mm Hg/mm.

Critical pressure gradients for smaller capillaries are much higher, and seem to conflict with the results of Prothero and Burton (21), who find that red cells will

pass readily through a 5μm millipore filter under a pressure of less than 4 cm water. The blood used in the experiments, however, was diluted about 1000 times; and calculation shows that the effective pressure difference available to act on each red cell is several times greater than the theoretical minimum required to avoid seize-up.

Erythrocyte structure and perfusion control

If the RBC clearance depended on absolute pressure rather than on pressure gradient, its clearance would decrease as it moved down the capillary. This could be caused by distensible capillary walls, as well as by a hypothetical compressible nature of the RBC. A critical pressure would exist, below which motion would seize up. Consequently, downstream pressure would need to be maintained above this critical value; serious limitations on perfusion control would exist if upstream pressure were close to the critical value. Furthermore, the response of a capillary segment to changes in perfusing pressure would be non-uniform, since the resistance of a cell would depend on its position in the capillary.

The 'bendable' structure of the erythrocyte and rigidity of the capillary eliminates these difficulties. Control of velocity can be achieved with equal facility,

over wide ranges, by pressure changes at either end of the capillary; this control is effected uniformly over the whole length, since resistance (and therefore pressure gradient) will be reasonably constant at all parts of a capillary of given diameter. Pressure changes at some point proximal to a capillary network will effect control at all sections of the network (although the response may be different in different sections). All of these statements refer, of course, only to capillary segments in the diameter range of the theory.

The dependence of clearance (and hence flow) on pressure gradient may explain a phenomenon noted by Glazier et al (12) concerning the RBC counts in alveolar septa. They showed that capillary blood seemed to 'see' arterial pressure (in any region where flow was occurring), irrespective of how far the pressure had dropped towards venous level - the RBC count per unit length of septum, which was found to be a good 'manometer' of pressure, depended only on vertical distance down the lung, and not on position in the capillary network. The comments above on RBC structure indicate that once flow has been initiated, pressure gradient (and hence flow and RBC count) will remain fairly constant along the capillary. The uniform distribution of RBC's therefore probably indicates that the

uniform blood flow at all points at a given height is responding to a uniform pressure gradient, rather than 'seeing' a constant (arterial pressure. It also provides confirmation that capillary diameters in the lung are sensibly unaffected, once flow has developed, by the relatively small pressure changes needed for red cell movement (see later).

Vasomotion and autoregulation

The concept of perfusion control by vasomotion or congestion involves resistance changes principally in the vessels at the site of the constriction. Capillary resistance, which is under normal conditions of flow in the systemic circulation fairly small compared with arteriolar resistance, is largely ignored. At the low Reynolds' numbers characteristics of the microcirculation, however, local constriction is less efficient than might be supposed in reducing flow velocity, particularly in the case of precapillary sphincters. Dynamic head is virtually non-existant, so that the only velocity-reducing mechanism available is increased local viscous resistance. Since in some cases this occurs over only a relatively small length of the vesses, it is perhaps difficult to accountfor all variations in perfusion on this basis alone.

The non-linear dependence of narrow-capillary resistance on pressure gradient, and the possibility of 'seize-up', may well provide the answer. Only a moderate change in arteriolar pressure is required to cause a relatively large change in capillary resistance, so that under certain conditions the capillary may act as a sensitive amplifier of resistance changes in the muscular sphincter or arteriole. Similar considerations apply to pressure increases in the veins mediated by external constriction, although the situation may be complicated by venous distension and capillary recruitment. Autoregulation involving vasomotion in response to myogenic or chemical action may well be augmented by what may be called a 'passive autoregulation' effect in the capillaries, although this term is normally reserved for effects of venous distension tending to maintain near-uniform end-capillary pressure. This must also be the reason for the 'stick-slip' mode of progress of RBC's in narrow capillaries, caused by random contractions in pre-capillary sphincters; and there may well be some connection with the cessation of flow at small but positive perfusing pressures.

Uneven filling of the pulmonary capillaries

The striking feature of the morphology of the pul-

monary circulation is the mesh of very short, narrow vessels which form the capillary 'marsh' of the alveolar septa. This is thought to be responsible for the 'patchy' filling of the vessels in the septa; clearly, the flow characteristics of red cells must play an important role. Transient capillary deformation due to passage of red cells has been discussed in (6), and shown to be negligible.

In such a complex network, some pathways will offer less resistance to flow than others because of greater diameter and/or shorter path length. These preferred channels will open first in response to an increasing pressure difference. Two mechanisms operate: (i) for a shorter channel, pressure gradients are greater for a given pressure difference; (ii) RBC clearance is higher in larger vessels, so that a smaller pressure gradient is needed to initiate lubrication and hence motion. As channels open up, pressure changes are transmitted to more distant parts of the network, and less direct routes are recruited as the pressure gradient in them exceeds their 'threshold' for commencement of motion. Computer simulation using an analogous electrical network, and a potential-current curve very similar to RBC pressure-flow relationships, seems to predict the same characteristics.[1]

(1) Private communication on a preliminary study by Dr J. West.

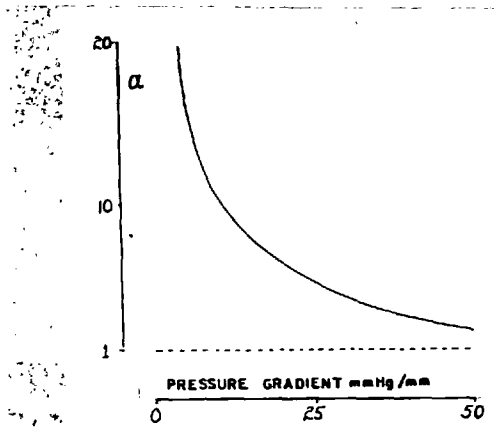


FIG. 9. Relative apparent viscosity α as a function of pressure gradient, for a 6-μm diameter capillary.

The flow pattern is highly dependent on the morphology, and on interactions between the various sections. Since flows in smaller capillaries are more sensitive to changes in pressure gradient, we expect the non-preferred channels to show the greater variations of flow. Any obstruction on a small capillary may cause a critical reduction in pressure gradient, below the level at which lubrication is just possible. This may also occur because of pressure changes, at either end of the segment, due to flow variarions in other parts of the network. We expect to find, therefore, that a flow irregularity at some point could cause whole patches of the mesh to seize up.

Apparent blood viscosity in capillaries

The non-linear resistance effect described above may be expressed in terms of a variable apparent viscosity for the cell-plasma suspension in a narrow capillary. We define α, the 'apparent viscosity coefficient', to be the ratio of actual resistance to that expected for a Newtonian fluid having a similar bulk viscosity. Fig. 9 shows as a function of velocity for a 6 μm capillary. This definition may be extended to a network of such capillaries, but the viscosity cannot be regarded as being a property of the blood alone, since it depends to a large extent on

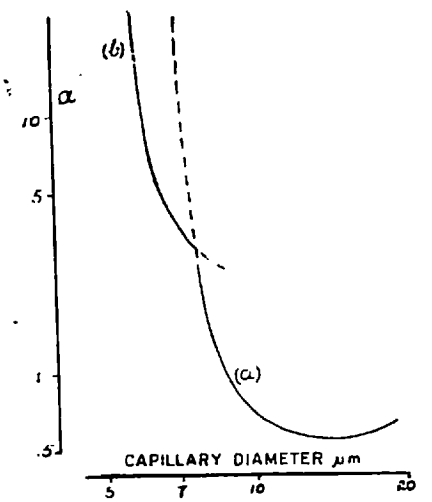


FIG. 10. Relative apparent viscosity as a function of capillary diameter, for a pressure gradient of about 40 mm Hg/mm. Curve a: Whitmore; curve b: Fitz-Gerald. (Both scales are logarithmic.)

the morphology.

The dependence of viscosity on capillary diameter may be viewed as a velocity-dependent extension to Whitmore's results (25) for larger vessels. Fig. 10 combines the two theories, illustrating well the much-enhanced viscosity in narrow capillaries; viscosity α is plotted for a fixed pressure gradient (about 40 mm Hg/mm) against 'effective cell radius/capillary radius', measured in the case of the present theory in terms of the film thickness. We might expect the Fahreus-Lindquist effect to occur down to capillary diameters of about 15 μm; viscosity should then rise slightly from 15-9 μm, and then increase rapidly for capillaries with diameters equal to or less than that of the red cell.

Djojosugito et al (5) find that apparent viscosity *in vivo* for blood perfusing the maximally-vasodilated calf muscle of the cat, measured by comparison with a Newtonian fluid of known viscosity, increases (and almost doubles) as flow rate decreases. At high perfusion rates, *in vivo* apparent viscosity is about half the *in vitro* value (at high shear rate); this effect is probably due to axial concentration of red cells, with consequent lowering of resistance, in the larger vessels of the microcirculation. Although some of the viscosity increase may be ex-

plained in terms of a reduction of this axial concentration, it is not unlikely that increased capillary resistance plays a significant role.

Dintenfass (4) has studied the apparent viscosity of blood in a parallel-sided glass viscometer; he worked with blood at a haematocrit of very nearly 50%, and a pressure gradient of 0.5-2.0 mm Hg/mm. He found that the viscosity decreased with decreasing capillary width down to about 12 μm, as predicted by the Fahreus-Lindquist effect. It then increased, gradually at first, more rapidly below about 10 μm, and reaching enormous values (10^3 - 10^4) below about 8 μm. These experiments confirm both Whitmore's results and the present work; and the effective 'seize-up' below 8 μm at these low pressure gradients is also very much in line with the predictions of the lubrication theory.

Conclusion

It is again stressed that the results of the theory were derived in non-dimensional form. Several fairly crude approximations (values of membrane compliance, clearance, pressure drop in individual capillary elements) are necessary to express these results in physiological terms; therefore, the numerical values for velocity, pressure

drop, and film thickness predicted by the theory should be taken as being merely indicative, rather than as exact results to be compared with observed physiological data. It is the qualitative behaviour predicted for various situations that is most important at present.

It would be extremely interesting if experimental results were obtained for comparison with predictions. To the author's knowledge, no direct measurements of red cell velocity at physiological pressure gradients in narrow-bore capillaries (5-9 μm) have been made, nor has the effect of altered haematocrit and cell elasticity been studied, again for individual narrow-capillary elements. Observation of a critical pressure gradient for flow cessation would be valuable, as would a study of apparent viscosity for a range of velocities and (narrow) capillary diameters.

Acknowledgements

The author has great pleasure in acknowledging the generous assistance and constant encouragement of Professor M.J. Lighthill during the preparation of this work. He is also indebted to Dr. C.G. Caro for many enjoyable and stimulating discussions on the physiological aspects of the theory, and similarly to the other members of the Physio-

logical Flow Studies Unit, Imperial College.

The financial support of a Gowrie Travelling Scholarship, during the tenure of which this work was completed, is also gratefully acknowledged.

References

(1) Bloor, M.I.G. The flow of blood in the capillaries Med. Biol. 13: 443-450, 1968.

(2) Burton, A.C. Role of geometry, of size and shape, in the microcirculation. Federation Proc. 25: 1753-1760, 1966.

(3) Cameron, A. Principles of lubrication. pp 126-128. (Longmans, 1966).

(4) Dintenfass, L. Viscosity of blood at high haematocrits measured in microcapillary (parallel-plate) viscometer at r = 3-30 microns. Proc. First International Conference on Haemorheology. 197-209, 1966.

(5) Djojosugito, A.M., B. Folkow, B. Oberg and S. White. Comparison of *in vitro* and *in vivo* viscosity in the cat. International Conference on Microcirculation, Gotoborg, Sweden, 1968. European Society Microcirc.

(6) Fitz-Gerald, J.M. Mechanics of red cell motion in very narrow capillaries. Proc. Roy. Soc. B. (in the press).

(7) Fowler, K.T., J.B. West and J.C.F. Pain. Pressure-flow characteristics of horizontal lung preparations of minimal height. Respiration Physiol. 9: 88-98, 1966.

(8) Fulton, G.P. and B.R. Lutz. The use of the hamster

check pouch and cinephotomicrography for research on the microcirculation and tumour growth, and for teaching purposes. Boston Medical Quart. 8: 1-7, 1957.

(9) Fung, Y-C. Biomechanics: its scope, history, and some problems of continuum mechanics in physiology. Appl. Mech. Revs. 21: 1-20, 1968.

(10) Fung, Y-C. Theoretical considerations of the elasticity of red cells and small blood vessels. Federation Proc. 25: 1761-1772, 1966.

(11) Gabe, I.S. and L. Zatz. Studies of plasma viscosity under conditions of oscillatory flow. Biorheology 5: 86, 1968.

(12) Glazier, J.B., J. .B. Hughes, J.E. [illegible] and J.B. West. Measurements of capillary dimensions and blood volume in rapidly frozen lungs. CIBA Conference on Mass Transport, London, 1968.

(13) Landis, E.M. Capillary pressure and capillary permeability. Physiol. Revs. 14: 404-481, 1934.

(14) Landis, E.M. and J.R. Pappenheimer. Exchange of substances through the capillary walls. In: Handbook of Physiology, Section 2: Circulation, Vol. 1. American Physiolobical Soc., Washington, D.C., 1963.

(15) Lighthill, M.J. Motion in narrow capillaries from the standpoint of lubrication theory. CIBA Conference on Mass Transport, London, 1968.

(16) Lighthill, M.J. Pressure-forcing of tightly-fitting pellets along fluid-filled elastic tubes. J. Fluid Mech. 34: 113-143, 1968.

(17) Lubrication and Wear in Living and Artificial Human Joints. I. Mech. E. and British Orthopaedic Assoc., London, 1967.

(18) Luft, J.H. Fine structure of capillary and endocapillary layer as revealed by ruthenium red. Federation Proc. 25: 1773-1783, 1966.

(19) Prothero, J. and A.C. Burton. The physics of blood flow in capillaries: I. The nature of the motion. Biophys. J. 565-579, 1961.

(20) Prothero, J. and A.C. Burton. The physics of blood flow in capillaries: II. The capillary resistance to flow. Biophys. J. 2: 199-212, 1962.

(21) Prothero, J. and A.C. Burton. The physics of blood flow in capillaries: III. The pressure required to deform erythrocytes in acid-citrose-dextrose. Biophys. J. 2: 213-222, 1962.

(22) Rand, R.P. and A.C. Burton. Mechanical properties of the red cell membrane. Biophys. J. 4: 115-135,

1964.

(23) Wang, H. and R. Skalak. Viscous flow in a cylindrical tube containing a line of spherical particles. Office of Naval Research, Project No. NR-063-393, Technical Report No. 1.

(24) Weibel, E.R. and D.M. Gomez. Architecture of the human lung. Science 137 (3530): 577-585, 1962.

(25) Whitmore, R.L. A theory of blood flow in small vessels. J. Appl. Physiol. 22 (4): 767-771, 1967.

Chapter IV

Plasma Flow in Inter-Erythrocyte Spaces

1. Introduction

The previous two chapters have been principally concerned with the mechanics of red cell motion, and how these depend on factors such as capillary diameter, applied pressure gradient, and erythrocyte structure. In the present chapter, interest will be centred on the flow of plasma around the erythrocytes. As mentioned in the introductory chapter, the principal motivation for such analysis lies in the need to understand the relative effec of convection and diffusion on mass transport in the capillaries. In the last section of the chapter, therefore, a discussion of transport mechanisms for oxygen and protein, in particular, will be given in some detail.

Previous numerical solutions, described in Chapter I (Bugliarello et al., 1966; Gross, 1969; Bloor, 1968), while agreeing broadly with Prothero and Burton's (1961) suggestion of a circulating bolus flow, differ amongst themselves in their descriptions of the details of the flow. Since it might be expected that transport will depe significantly on velocity gradients near the interfaces, particularly for slowly-diffusing species such as protein,

it will be of considerable importance to determine how shear rates and velocities near the surfaces of erythrocytes and capillaries depend, for example, on cell spacing and plasma 'leakback' - which is a measure of the disparity between the mean velocities of red cells and plasma. Further, the flow near the points where the plasma emerges from and enters the lubrication zones may well be influenced by the emergent velocity profile; it is of some importance, therefore, to match the flow obtained in the cell-free space with that found earlier for the lubrication layer.

In capillaries, plasma is flowing at very low Reynolds' number (10^{-2} - 10^{-3}); the detailed geometry of the inter-erythrocyte space will, therefore, probably not greatly affect the type of flow occurring. This supposition is supported by the similarity between the streamline patterns found by Wang and Skalak for spheres in a fluid-filled tube, and those obtained in the numerical analyses using plane-ended red cells.

For the present analysis, the red cells will be assumed to have plane ends. The ellipsoidal shape used in the discussion of Chapter II will be terminated at some convenient distance z_o from the centre of the lubrication zone, chosen so that the region where the important elastic

effects occur lies well within the interval $(-z_o, z_o)$, but so that the assumptions made for the lubrication theory are reasonably valid in this interval; i.e. the thickness of the fluid layer at z_o should still be small compared with the red cell radius $r_c(z)$.

At z_o, the longitudinal velocity profile is given by the lubrication theory (equation II: 3.1) to be

$$u(r) = \frac{1}{4\mu}\cdot\frac{dp}{dx}\left[r^2 - r_c^2 - \frac{2r_c h + h^2}{\ln(1+h/r_c)}\cdot\ln\frac{r}{r_c}\right] - \frac{U\ln(r/r_c)}{\ln(1+h/r_c)} \qquad (1.1)$$

where $h(z)$ is the thickness of the lubrication film, U is the red cell velocity, and

$$\frac{dp}{dx} = \frac{aQ - U\left[\frac{(r_c+h)^2}{2} - \frac{2r_c h + h^2}{\ln(1+h/r_c)}\right]}{\frac{1}{4\mu}\cdot\frac{2r_c h + h^2}{4}\left[2r_c^2 + 2r_c h - \frac{2r_c h + h^2}{\ln(1+h/r_c)}\right]} \qquad (1.2)$$

Here a is the capillary radius, and Q the 'leakback' (negative flux of plasma per unit length of capillary circumference). It will be recalled that these formulae were obtained for a coordinate system in which the red cell was stationary and the capillary was moving backwards with velocity -U; the same frame of reference will be used throughout the present discussion.

Since z_o has been chosen to ensure elastic effects there on $h(z_o)$ to be negligible, the cell radius $r_c(z_o)$ may be obtained from the geometrical formula expressing the

'undistorted' red cell profile. This will here be assumed spherical, i.e.

$$r_c^2 = a^2 - z^2 \qquad (1.3)$$

Clearly, an elliptical profile with arbitrary curvature at the midpoint of the lubrication zone could equally well be chosen; in the non-dimensional coordinates defined in Chapter II, however, the value of r_c obtained will be independent of this curvature, provided z_o is consistently defined in some convenient way. In this analysis, z_o will be chosen as $\frac{1}{8}a$, a value which may be shown to satisfy the first requirement (by an examination of the pressure profile in the lubrication region); the corresponding fluid film thickness is $.14a$, so that the second condition is satisfied also.

Equations (1.1), (1.2) and (1.3) define a longitudinal velocity profile $u(r)$ at $z = z_o$, which will be used as part of the boundary conditions for the flow in the cylindrical, inter-erythrocyte space. The no-slip requirement continues the definition of the longitudinal velocity condition on the capillary wall $r = a$, and finally, $u(r)$ must be zero at the solid boundary of the cell, $0 \leq r \leq r_c(z_o)$. The radial velocity $v(r,z)$ will be taken to be zero on the boundaries; this is clearly true at the capillary wall and red cell surface, and agrees in the lubrication gap with a

similar assumption made for the lubrication theory of Chapter II. If desired, an approximate radial velocity in the gap could be computed from the continuity equation, containing an arbitrary function f(z); this could then be defined to allow v(r,z) to take the correct values at $r = r_c$ and $r = a$. Unfortunately, the radial velocity so obtained does not necessarily satisfy the Navier-Stokes equation, because of the approximations needed to obtain the longitudinal velocity u(r,z); in any case, the radial velocities will be small compared with u(r,z) and will therefore have little influence on the inter-erythrocyte flow.

If the origin of z is redefined to be the midpoint of the inter-erythrocyte space, then the required flow in the space may be obtained in terms of the usual Stokes' stream function ψ, as the solution of the biharmonic equation, with prescribed values of $\frac{\partial \psi}{\partial r}$, $\frac{\partial \psi}{\partial z}$ at $z = \pm \ell \; (0 \leq r \leq a)$ and at $r = a \; (-\ell \leq z \leq \ell)$; here 2ℓ represents the inter-erythrocyte spacing.

In the next section, an analytic solution of this problem is presented in the form of a truncated series of eigenfunctions superimposed on the basic Poiseuille stream function. Results are shown in section 4 for several values of the various parameters involved, and these are discussed in section 4 with reference to the mass transport problem.

The coefficients in the series solution are obtained using a least squares technique for minimizing the error in matching the boundary conditions; such an approach seems preferable to the more naive collocation matching used, for example, by Zidan (1969) in his solution (using similar eigenfunctions) for the slow extrusion of a jet of fluid from a nozzle in the spin-process for the manufacture of artificial fibres.

An interesting feature of the flows obtained is the presence of a region of relatively high shear, extending along the entire length of the capillary wall; the effect is virtually independent of cell spacing and lubrication film thickness. Interesting also is the intrusion of part of the circulating bolus flow into the entry and exit regions of the lubrication zone, and the continuation, in some cases, of a zone of relatively high shear for some distance up the rod cell face.

2. Mathematical Formulation

An analytic solution for the slow viscous flow of an incompressible fluid in the absence of body forces will now be obtained in a finite, circular tube, of radius a and length 2ℓ. The usual axisymmetric cylindrical coordinates r', z' are used, with origin at the midpoint of the axis.

Since the flow is axisymmetric, a Stokes stream function ψ' may be utilized; it is defined by the formulae

$$\frac{\partial \psi'}{\partial r'} = r'u', \quad -\frac{\partial \psi'}{\partial z'} = r'v', \quad \psi'(0,x') = 0 \tag{2.1}$$

where u', v' are respectively the axial and radial components of the fluid velocity. It may readily be shown that the equations of motion expressed in terms of ψ' reduce to the single equation $(D')^4\psi' = 0$, explicitly

$$\left(\frac{\partial^2}{\partial(r')^2} - \frac{1}{r'}\frac{\partial}{\partial r'} + \frac{\partial^2}{\partial(z')^2}\right)^2\psi' = 0 \tag{2.2}$$

As discussed in section 1, the tube will be considered to be moving with velocity -U (with the red cells stationary); the boundary conditions at $r' = a$ are therefore

$$\left.\begin{aligned} &\frac{\partial \psi'}{\partial r'} = -aU \\ \text{and} \quad &\frac{\partial \psi'}{\partial z'} = 0 \text{ , or } \psi' = \text{constant} = A', \text{ say} \end{aligned}\right\} \tag{2.3}$$

Here $2\pi A'$ is the net flux of fluid past any plane perpendicular to the axis.

At the ends of the tube, general boundary conditions will be allowed, viz.

$$\left.\begin{aligned} \frac{\partial \psi'}{\partial z'} &= \pm r'g'(r') \\ \frac{\partial \psi'}{\partial r'} &= r'f'(r') \end{aligned}\right\} \text{ at } z' = \pm \ell \tag{2.4}$$

Clearly, $u'(r', \pm\ell) = f'(r')$, $v'(r', \pm\ell) = \mp g'(r')$; the second condition of (2.4) may be re-expressed as

$$\psi'(r', \pm\ell) \int_0^{r'} tf'(t)dt = F'(r') \quad , \text{ say} \qquad (2.4a)$$

The only restriction made here is that the boundary conditions be symmetric at the two ends, i.e. that the flow is symmetric about $x' = 0$. This restriction is prompted by the application to capillary flow, to which particular attention will be directed later; antisymmetrical solutions may, of course, be included in an exactly analogous manner, but with a considerable increase in algebraic and computational complexity.

It will be convenient to work in non-dimensional variables; these are defined, in an obvious way, as

$$z = z'/a, \quad r = r'/a, \quad \varphi = \varphi'/(Ua^2).$$

The stream function satisfies

$$D^4\varphi = 0 \qquad (2.2a)$$

and the boundary conditions are now

$$\left.\begin{aligned} \frac{\partial\varphi}{\partial r} &= 1, \quad \varphi = A \quad \text{on } r = 1 \\ \frac{\partial\varphi}{\partial z} &= \pm\, rg(r), \quad \varphi = F(r) \quad \text{on } z = \pm\epsilon \end{aligned}\right\} \qquad (2.3)$$

where $A = A'/(Ua^2)$, $g(r) = (g'(r'))/U$, $F(r) = (F'(r')/(Ua^2)$, $\epsilon = \ell/a$.

The stream function will be expressed as

$$\varphi = \varphi_p + \varphi_a$$

where φ_p is a Poiseuille solution having the required vel-

ocity at r = 1 and the required net flux, and ψ_a is an additional solution selected to match the boundary conditions at $z = \pm \epsilon$. Clearly

$$\psi_p = (\tfrac{1}{2} - A)r^2 - (\tfrac{1}{2} - 2A)r^4,$$

and ψ_a must satisfy

$$\frac{\partial \psi_a}{\partial r} = \psi_a = 0 \quad \text{on } r = 1 \tag{2.6}$$

and

$$\left.\begin{aligned} \psi_a &= F(r) - \psi_p = F_1(r), \text{ say} \\ \frac{\partial \psi_a}{\partial z} &= \pm\, r g(r) = G(r), \text{ say} \end{aligned}\right\} \text{ on } z = \pm\epsilon \tag{2.7}$$

The additional part ψ_a may conveniently be obtained as a series of separated solutions of (2.2a), which may be written as

$$(\mathcal{E} + \frac{\partial^2}{\partial z^2})^2 \psi = 0$$

where the operator

$$\mathcal{E} \equiv \frac{\partial^2}{\partial r^2} - \frac{1}{r}\cdot\frac{\partial}{\partial r}$$

Explicitly, this is

$$\mathcal{E}^2\psi + 2(\mathcal{E}\frac{\partial^2}{\partial z^2})\psi + \frac{\partial^4}{\partial z^4}\psi = 0 \tag{2.8}$$

Separated solutions may be obtained by requiring that either

$$\frac{\partial^2 \psi}{\partial z^2} = \alpha^2 \psi \tag{2.9}$$

or

$$\mathcal{E}\psi = \beta^2 \psi \tag{2.10}$$

Equation (2.9) gives rise to solutions of (2.8) of the form

Table 4.1

n	$Re(\alpha_n)$	$Im(\alpha_n)$
1	4.46629854858	1.46747037233
2	7.69410395105	1.72697153719
3	10.87457448839	1.89494334623
4	14.03889131024	2.02006279875
5	17.19556531553	2.11994518794
6	20.34796817781	2.20312418032
7	23.49772381627	2.27440623630
8	26.64571748890	2.33677882616
9	29.79247539953	2.39222622061
10	32.93833107994	2.44213486876

$$Ae^{\pm\alpha z} r^2 J_0(\alpha r) + Be^{\pm\alpha z} rJ_1(\alpha r) \qquad (2.11)$$

while (2.10) gives solutions

$$Ae^{\pm\beta z} rJ_1(\beta r) + Bze^{\pm\beta z} rJ_1(\beta r) \qquad (2.12)$$

Clearly, a solution of the form (2.12) cannot simultaneously satisfy both the conditions (2.6); (2.12) is therefore irrelevant to the present problem and will be ignored. Application to (2.11) of the boundary conditions (2.6), which are to be satisfied by each separated solution independently, gives simultaneous linear equations for A and B;

$$\begin{pmatrix} J_0(\alpha) & J_1(\alpha) \\ 2J_0(\alpha) - \alpha J_1(\alpha) & \alpha J_0(\alpha) \end{pmatrix} \begin{pmatrix} A \\ B \end{pmatrix} = \begin{pmatrix} 0 \\ 0 \end{pmatrix}$$

which have non-trivial solutions only if

$$\alpha\left[J_0^2(\alpha) + J_1^2(\alpha)\right] = 2J_0(\alpha)J_1(\alpha) \qquad (2.14)$$

Solutions of (2.14) form a set $\{\alpha_n\}$ of discrete eigenvalues for the separation constant α. They are all complex; those of large modulus (large n) may be shown to have the asymptotic form

$$\alpha_n \simeq (2n + 1)\pi/2 + i.\ln\left[(4n + 2)\pi\right] \;;$$

the first few eigenvalues (α_1 to α_{10}) are tabulated (Table 4.1); the trivial solution $\alpha_0 = 0$ corresponds to the z-independent Poiseuille solution.

Corresponding eigenfunctions (even in z), may be written down, and are of the form

$$\chi_n(r,z) = \frac{\cosh(\alpha_n z)}{\cosh(\epsilon\alpha_n)}\left[r^2 J_0(\alpha_n r) - S_n r J_1(\alpha_n r)\right] \qquad (2.15)$$

(ignoring the singular Bessel functions of the second kind), where $S_n = J_0(\alpha_n)/J_1(\alpha_n)$, and χ_n has been defined so that at $z = \pm\epsilon$,

$$\chi_n(r,\pm\epsilon) = \psi_n(r) = r^2 J_0(\alpha_n r) - S_n r J_1(\alpha_n r) \qquad (2.16)$$

Since the eigenfunctions are now all even in z, the boundary condition only at $z = +\epsilon$ need be satisfied.

The required additional solution ψ_a may be expressed as the real part of a series of these eigenfunctions:

$$\psi_a = \text{Real}\ (\sum_1^\infty B_n \chi_n). \qquad (2.17)$$

Since the equation (2.2a) and the boundary conditions (2.6) are linear in ψ, both real and imaginary parts of χ_n will separately be solutions; at $z=\epsilon$, therefore, (2.17) may be written in the form

$$\psi_a(r,\epsilon) = \Sigma B_n^R \psi_n^R - \Sigma B_n^I \psi_n^I \quad , \qquad (2.18)$$

where

$$\psi_n = \psi_n^R + i\psi_n^I$$

$$B_n = B_n^R + iB_n^I$$

It seems plausible that both $\{\psi_n^R\}$, $\{\psi_n^I\}$ constitute complete

sets over the function space satisfying (2.6). All relevant eigenvalues have been obtained, so that no other eigen-solution, having a different z-dependence, is possible. Physically, it is possible to specify arbitrary boundary conditions at $z=\epsilon$, which must be expressible in terms of the above eigenfunctions.

The radial velocity at $z=\epsilon$ corresponding to any eigenfunction is given by

$$v(r,\epsilon) = -\frac{\partial \chi_n}{\partial z}\bigg|_{z=\epsilon} = -\alpha_n \tanh(\epsilon\alpha_n)\,\psi_n \;;$$

writing

$$\alpha_n \tanh(\epsilon\alpha_n) = a_n + ib_n \;,$$

the radial velocity at $z=\epsilon$ for the solution (2.18) is

$$\frac{\partial \psi_a}{\partial z}\bigg|_{z=\epsilon} = \Sigma B_n^R\left[a_n\psi_n^R - b_n\psi_n^I\right] - \Sigma B_n^I\left[b_n\psi_n^R + a_n\psi_n^I\right] \quad (2.19)$$

Truncated forms of the series (2.17) or (2.18) are now used to match the prescribed functions in (2.7). A simultaneous least square error fit will be obtained. Define I to be the integral

$$\int_0^1 \omega(r)\left[\left\{F_1(r) - \sum_1^N B_n^R\psi_n^R + \sum_1^N B_n^I\psi_n^I\right\}^2 + \left\{G(r) - \sum_1^N B_n^R(a_n\psi_n^R - b_n\psi_n^I) + \sum_1^N B_n^I(a_n\psi_n^I + b_n\psi_n^R)\right\}^2\right]dr \;,$$

where N is the number of terms in the truncated series, and $\omega(R)$ is a convenient weighting function; then $\left\{B_n^R\right\}$, $\left\{B_n^I\right\}$

may be obtained as solutions of the 2N equations

$$\left.\begin{aligned}\frac{\partial I}{\partial B_n^R} &= 0\\ \frac{\partial I}{\partial B_n^I} &= 0\end{aligned}\right\} \quad n = 1, \ldots\ldots, N, \qquad (2.20)$$

which are derived explicitly in Appendix 1.

Examination of the form of the eigenfunctions suggests that $\omega(r) = r^{-1}$ is a suitable, convenient weighting function; this makes the integrals

$$\int_0^1 \omega(r)\psi_n^R\psi_m^R dr, \quad \int_0^1 \omega(r)\psi_n^R\psi_m^I dr, \quad \int_0^1 \omega(r)\psi_n^I\psi_m^I dr$$

decrease rapidly as $|n-m|$ increases from zero, giving a matrix for the equations which is strongly diagonally dominated (i.e. well-conditioned). This is of importance when error propagation in the numerical solution of (2.19) is being considered.

For the plasma flow case described in section 1, the functions F(r), G(r) take the forms (derived from (1.1), (1.2), (1.3)):

$$G(r) = 0$$

$$F(r) = \begin{cases} 0 & (r \le \sqrt{1-z_0^2}) \\ 4\left[\dfrac{r^4+(1-z_0^2)^2}{4} - \dfrac{r^2}{2} + \dfrac{z_0^2}{\ln(1-z_0^2)}r^2\ln r\right]\left[\dfrac{c-1}{2} - \dfrac{z_0^2}{2\ln(1-z_0^2)}\right] \cdot \\ \left[z_0^2(2 - z_0^2 + \dfrac{2z_0^2}{\ln(1-z_0^2)}\right]^{-1} + \dfrac{r^2(\ln r - \frac{1}{2})}{\ln(1-z_0^2)} + \dfrac{1-z_0^2}{2\ln(1-z_0^2)} - \dfrac{r^2}{2} \\ (\sqrt{1-z_0^2} < r \le 1). \end{cases}$$

The constant A has the value $\frac{1}{2}C$ (shown either by substitution of r=1 into the above formula, or by direct comparison of net flux in lubrication and inter-erythrocyte regions); and as discussed in section 1, z_o may be taken as $\frac{1}{2}$ in this non-dimensional form.

Finally, it may be noted that although this solution was developed primarily to examine the case of flow in narrow capillaries, eigenfunction expansions similar to those developed here may be used to solve problems such as viscous entry flow in a pipe, and the flow of gases in a simplified model of the terminal bronchioles and arterioles of the lung.

3. Numerical Details

Using the University of London CDC 6600 computer, with single precision accuracy to 14 significant figures, the eigenvalues α_n were obtained to 12 significant figures; the resulting eigenfunctions ψ_n, computed with a complex Bessel function routine accurate to 13 significant figures in the sector of interest, satisfied the boundary conditions (2.6) also to 12 significant figures. The number of operations required to compute the integral coefficients defined in Appendix 1 (using a 10-point Gaussian quadrature with successive halving of the interval) to 10-figure accur-

acy was of order 10^3; accuracy to at least 9 significant figures may then be expected for the matrix entries, and right-hand-side vector, in the set of equations (2.20). Round-off errors here would lead to an error at worst in the 11th place, and may be ignored.

The equations (2.20) were solved using Gaussian elimination with scaling, partial pivoting, and iterative improvement of the initial results. For values of ε greater than about 0.001, precision to at least 12 significant figures was obtained in the initial (unimproved) solution. The condition of the matrix was therefore approximately of the order of 10^2; so that relative errors of 10^{-9} in the matrix entries and right-hand-sides would lead to relative errors in the solution of order 10^{-7} at most. These are negligible compared with errors introduced by truncation of the series.

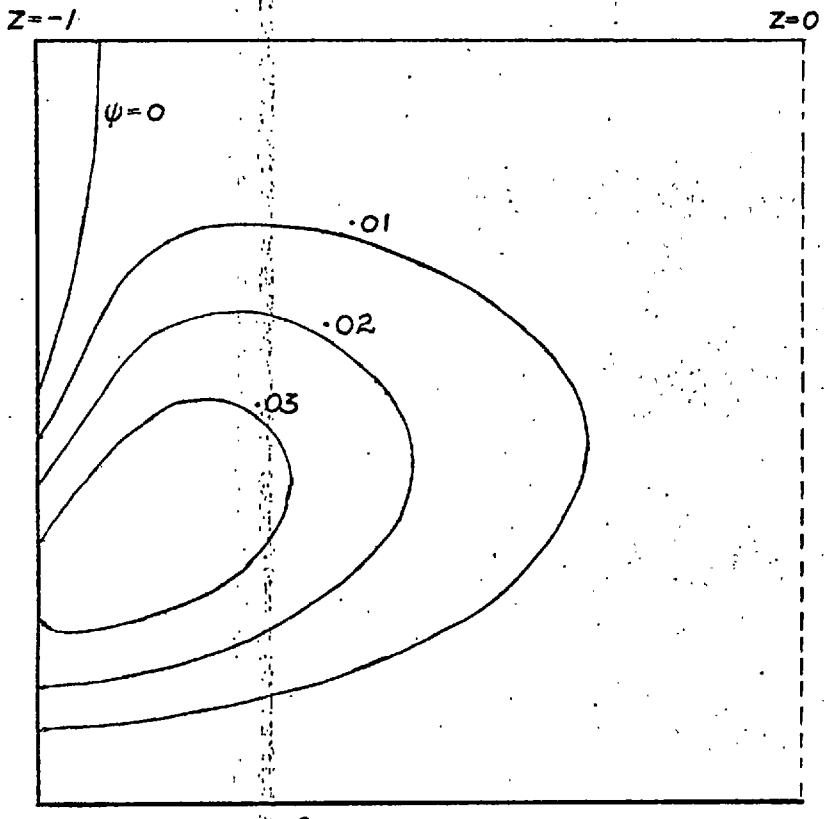
Sixty terms were used; as might be expected, the condition that the radial velocity be zero at $z = \varepsilon$ was satisfied to good accuracy, because of the absence of discontinuities of any kind in the function G(R). On the other hand the stream function boundary condition (F(R)) has a discontinuity, at the edge of the rod cell face, in the second derivative. It might therefore be anticipated that convergence of the series expansion would be slow, and that

considerable errors would occur in matching the function F(R). However, calculations showed that the coefficients of the dominant, slowly-decaying terms were obtained with excellent accuracy, and were stable to variations in the level of truncation. Any errors in matching the boundary condition, therefore, decay extremely rapidly with decreasing z.

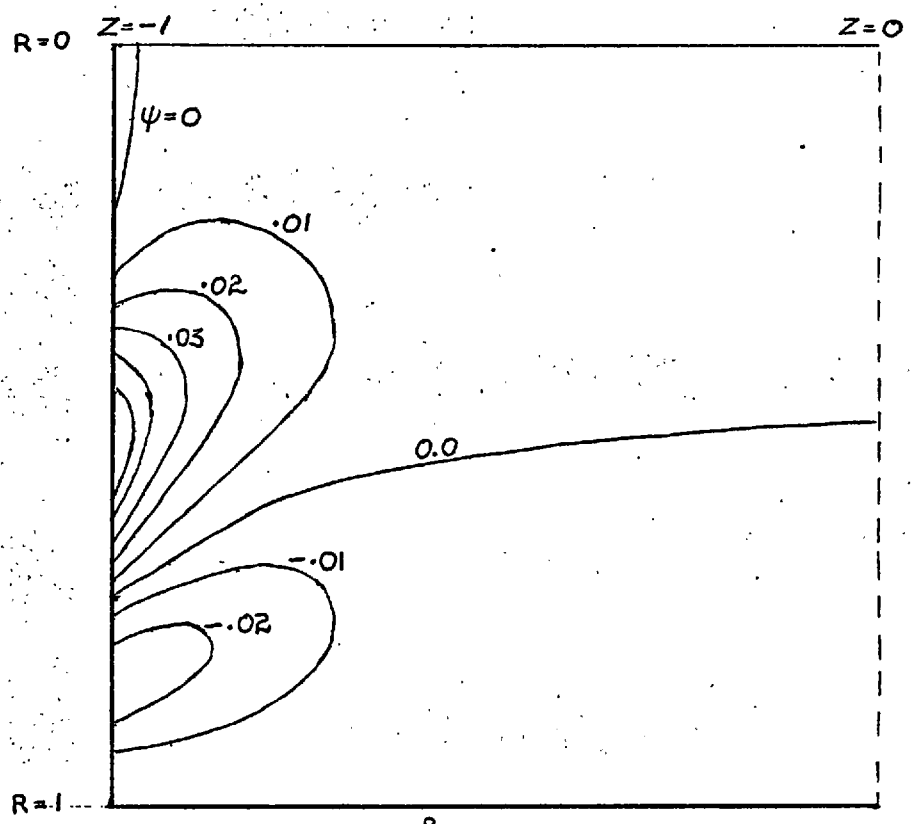
4. Results

It is of interest, before discussing particular solutions of the plasma flow problem, to examine the properties of the eigenfunctions. Accordingly, streamlines for the real and imaginary parts of χ_1 and χ_2 are shown in Figs. 1a and 1b, for $\varepsilon = 1$. As expected, the functions tend to decay from $z = \varepsilon$ to $z = 0$, the rate of decay increasing as the order of eigenfunction increases. However, the streamlines of the real parts, χ_1^R and χ_2^R, are inclined to the axis. For a given r, the functions need not exhibit a monotonic decay, and local increases may occur. In the case of χ_1^R this effect is so marked that the maximum value of the function occurs off the line $z = \varepsilon$.

The behaviour of χ_1^R as ε decreases is illustrated in Fig. 1c; similar plots for χ_1^I are given for purposes of comparison. The maximum value achieved by χ_1^R actually in-



ψ_1^R : $\epsilon = 1.0$



ψ_2^R : $\epsilon = 1.0$

Fig. 1a

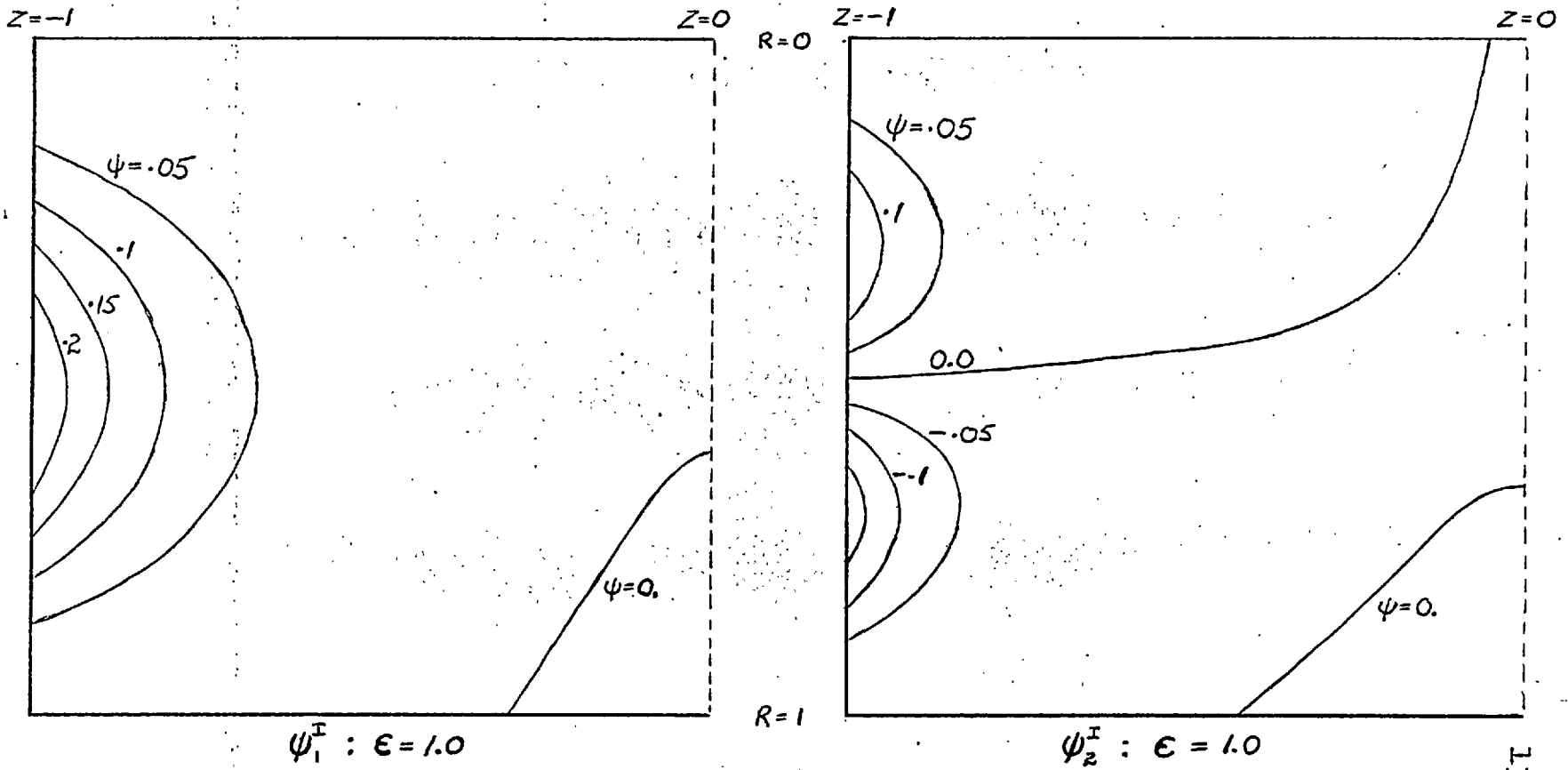


Fig. 1b

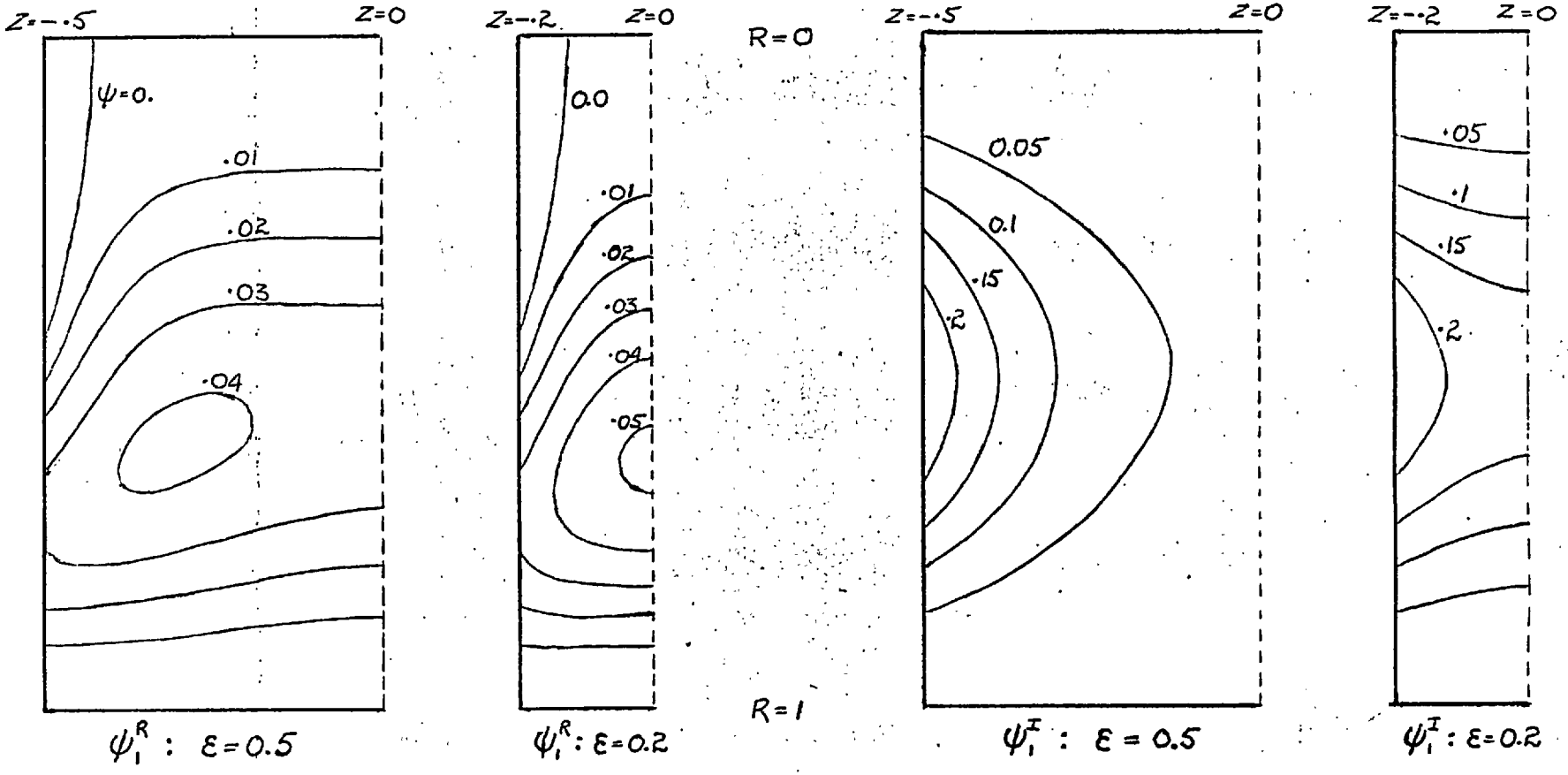

Z=-.5
Z=0
ψ=0.
.01
.02
.03
.04
Z=-.2
Z=0
0.0
.01
.02
.03
.04
.05
R=0
R=1
Z=-.5
Z=0
0.05
0.1
.15
.2
Z=-.2
Z=0
.05
.1
.15
.2
ψ_1^R : ε=0.5
ψ_1^R : ε=0.2
ψ_1^I : ε=0.5
ψ_1^I : ε=0.2

Fig. 1c

I36c.

creases as ε decreases, and for $\varepsilon = 0.2$, this maximum occurs at $z = 0$; over most of the region, therefore, χ_1^R increases markedly, rather than decreases, from $z = \varepsilon$ to $z = 0$. This somewhat unexpected feature of the first eigenfunction has important consequences for the flow patterns in inter-erythrocyte plasma spaces.

Fig. 2 shows streamlines for flow corresponding to a fairly small value of the film thickness parameter, $C = 0.025$, and three values of ε. There are several important features. Firstly, there is a region of relatively high shear near the capillary wall, extending the length of the plasma bolus, and continuing on into the lubrication zone. This region is comparatively unaffected by variations in ε; and similar calculation with $C = 0.05$ show that film thickness in the lubrication zone (or amount of leakback) also has little influence on the high-shear wall region.

There is in some cases a second high-shear region on the outer parts of the red cell face. Unlike that on the capillary wall, this is very dependent on ε, increasing in intensity as ε decreases. The maximum value taken by the stream function also increases as ε decreases. This is due to the anomalous behaviour of the real part of the first eigenfunction, which is the dominant member of the series particularly for small ε. Ultimately, of course, as ε be-

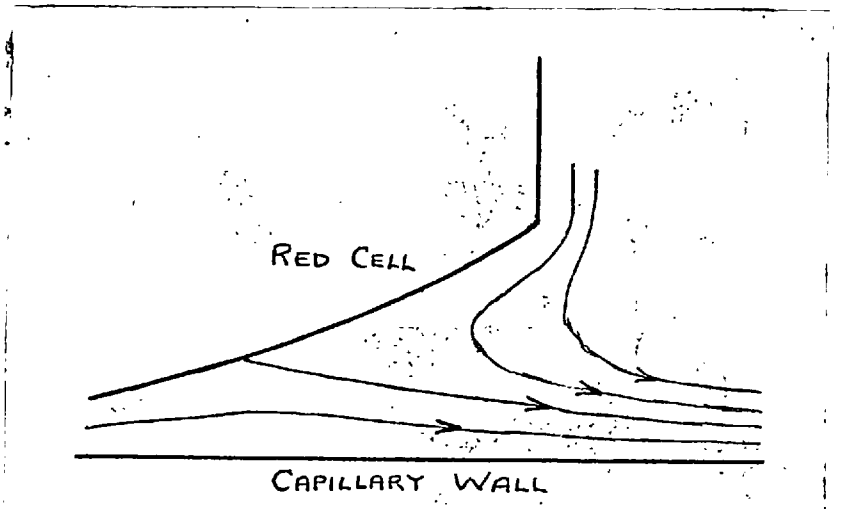


Fig. 4.

comes very small, and the eigenfunctions vary little in the region of the flow, the shear and stream function values decrease again, and tend to zero with ε (except near the capillary wall).

The unexpected form of the streamlines for $\epsilon = 1.0$, with a 'necking' of the main circulation, and a secondary circulation near the middle of the red cell face, seems to be dependent on the amount of leakback through the lubrication zone. Fig. 3 shows the streamlines for $\epsilon = 1$, $C = 0.05$; for this case there is much less disturbance from the simple, toroidal circulation found by Gross (1969) and Bloor (1968) for the fixed-leakback, rigid red cell model, with no intrusion of fluid from bolus to lubrication region. For completeness, a schematic diagram of the streamline patterns around the entry to the lubrication zone is shown in Fig. 4; and in Fig. 5, streamlines for the flows of Fig. 2 are plotted in a coordinate system with the capillary stationary and red cells in motion.

A final remark concerns the dependence of the pressure drop in the plasma bolus on ε, the cell spacing. Both Bugliarello and Bloor found the pressure drop to increase as ε decreased, rapidly for ε less than about 0.5; similar experimental findings were obtained by Prothero and Burton. These results are confirmed by the increasing

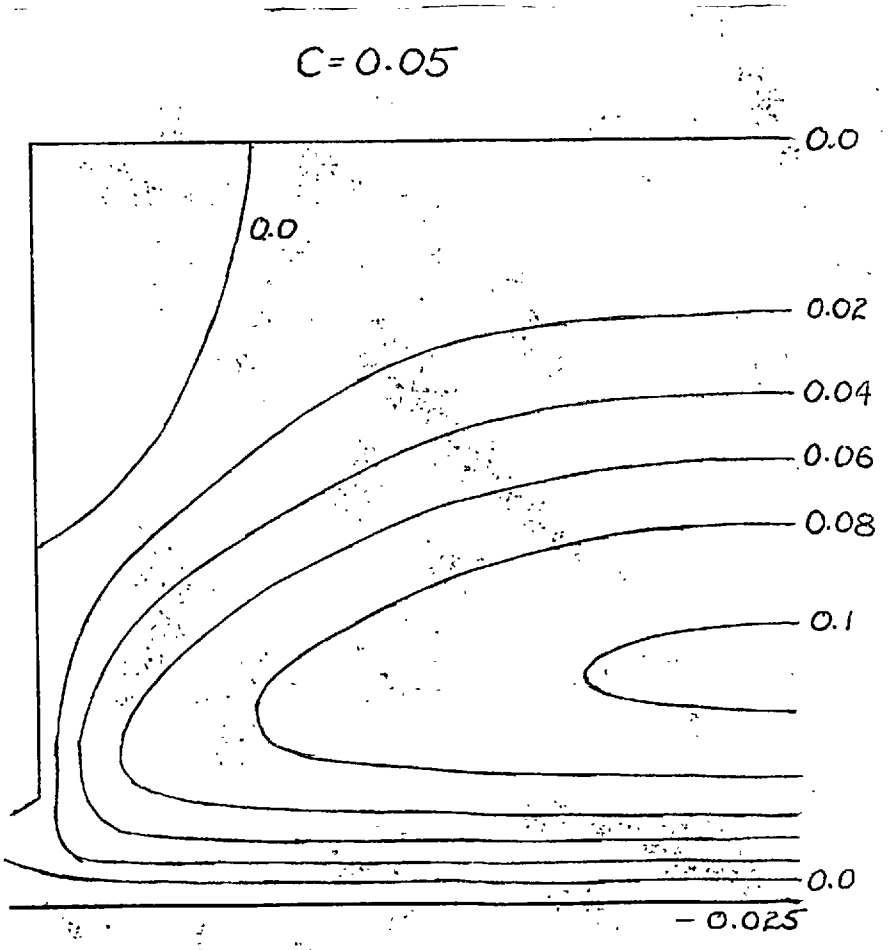


Fig. 3.

shear rates on the red cell face found in this analysis; such an increase will lead to an increased energy dissipation and larger pressure drop. It is possible to show, in fact, that the pressure drop on the capillary wall from one cell face to the next is

$$\Delta p = -4 \sum_{1}^{\infty} B_n \alpha_n J_0(\alpha_n) \tanh(\varepsilon \alpha_n).$$

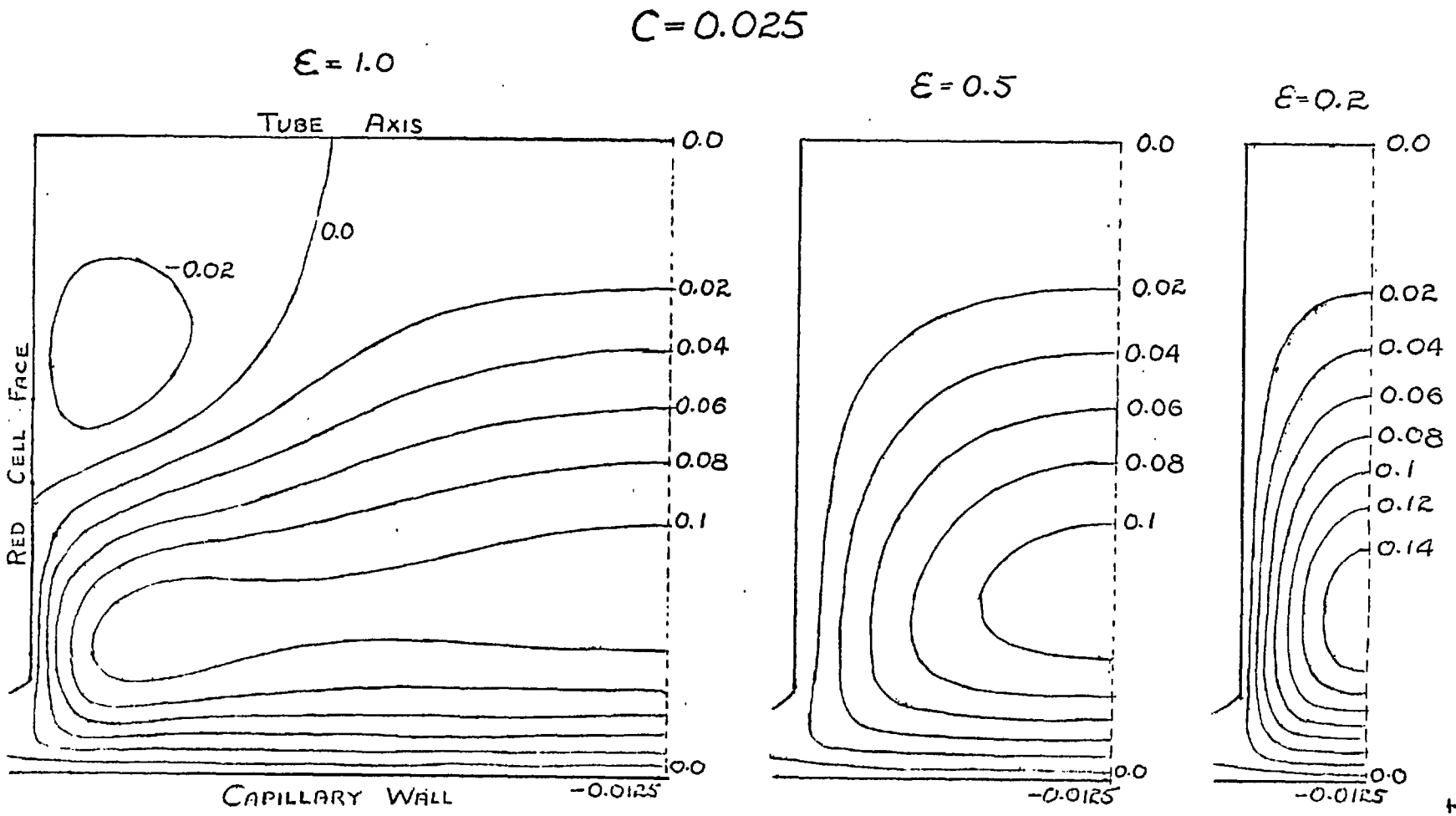

C = 0.025
ε = 1.0
TUBE AXIS
0.0
-0.02
0.0
0.02
0.04
0.06
0.08
0.1
RED CELL FACE
0.0
CAPILLARY WALL
-0.0125
ε = 0.5
0.0
0.02
0.04
0.06
0.08
0.1
0.0
-0.0125
ε = 0.2
0.0
0.02
0.04
0.06
0.08
0.1
0.12
0.14
0.0
-0.0125

Fig. 2.

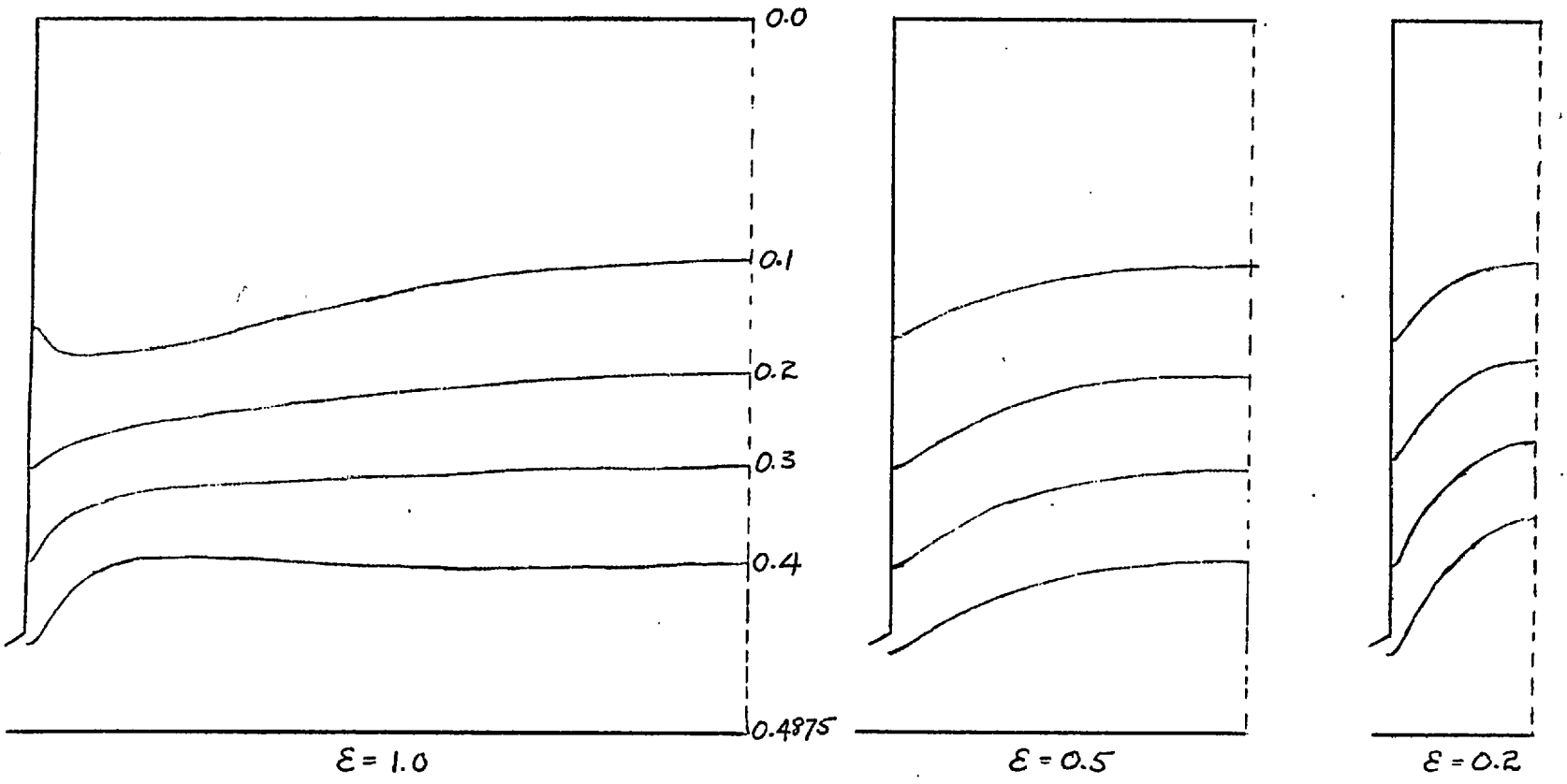


Fig 5.

5. Implications for Mass Transport

The relevance of these flow phenomena to mass transport are now considered. In capillaries, typical cell velocities are of order 100-1000 μm/sec, and diameters are of order 5-10 μm. The kinematic diffusivity for oxygen in plasma may be estimated as 1.5×10^{-5} cm^2/sec, and for a large molecule such as albumin about 0.085×10^{-5} cm^2/sec (Landis & Pappenheimer 1963).

For oxygen, therefore, Péclét numbers are of order unity ($0.35 < Pe < 7$ for values given), and convection may be expected to be at least as important as diffusion for transfer between red cells and endothelium. This is only true in the inter-erythrocyte space; in the lubrication layer, mean diffusion distances are so small (of the order of 0.25 μm) that convection will be relatively unimportant for the transfer process. The high-shear region near the endothelium in the inter-erythrocyte space is a continuation of the lubrication layer, and will be well supplied with oxygen; diffusion paths in the plasma may therefore be relatively short, even to those parts of the capillary wall not in close proximity to a red cell. In the same context, the high-shear region on the face of the red cell may also play some part in increasing the oxygen transport to and from the cell membrane. Similar considerations will apply to the

transport of other gases such as CO_2.

Péclét numbers for proteins such as albumin lie in the range 10-100; convection will therefore be even more important in controlling the supply to tissue of such a high-molecular-weight, slowly-diffusing species than for gases. Furthermore, the available protein contained in blood is stored principally in the plasma; the rotation of the inner 'bolus', bringing large portions of the plasma near the highly-sheared layer adjacent to the endothelium, will ensure that diffusion path lengths for protein are minimized. Such a mechanism may be viewed as an analogue of the diffusion of oxygen across the lubrication layer from the concentrated oxygen 'pool' in the haemoglobin-rich red cells.

It might be thought that since protein transfer occurs very slowly (for example, about 16 hours are required for a sample of labelled protein introduced to the blood to come to equilibrium with the protein pool of the tissues), effects which enhance or retard the process will be of relatively little importance. However, since transfer processes are linear in the concentration terms, and depend only on concentration gradients, absolute concentrations are unimportant when transfer is being considered. Thus even though the relative concentrations of protein in different

parts of capillary plasma may differ by insignificant amounts during transfer, the Nusselt number at the surface, which expresses the enhancement of transfer rate over that expected solely for diffusion, may be considerably greater than unity (Nu = 1 for purely diffusive transfer in the usual definition).

In this context, it is interesting to note that recent theories (discussed, e.g. by Luft, 1966) of mechanisms of transport of lipid-insoluble molecules such as protein through the endothelium consider that movement can occur only through the narrow 'gaps' at the junctions of endothelium cells (although pinocytosis may play some subsidiary role). These gaps, approximately 100Å wide, are estimated to occupy only 0.1% of the total endothelial area. The necessity for the concentration of diffusion paths at these widely-spaced exit points underlines still further the importance of convection for assisting the transfer of slowly-diffusing nutrients and metabolites to and from the tissues.

Appendix 1

Introduce the notations

$$\binom{RR}{ij} = \int_0^1 \frac{1}{r}\psi_i^R \psi_j^R dr \,, \qquad \binom{RI}{ij} = \int_0^1 \frac{1}{r}\psi_i^R \psi_j^I dr \,,$$

$$\binom{II}{ij} = \int_0^1 \frac{1}{r}\psi_i^I \psi_j^I dr \,, \qquad F_i^R = \int_0^1 \frac{1}{r} F \psi_i^R dr \,,$$

$$F_i^I = \int_0^1 \frac{1}{r} F \psi_i^I dr \,, \qquad G_i^R = \int_0^1 \frac{1}{r} G \psi_i^R dr \,,$$

$$G_i^I = \int_0^1 \frac{1}{r} G \psi_i^I dr \,;$$

then the equations (2.20) may be represented explicitly in matrix form as

$$\underset{\sim}{\underset{\sim}{S}} \cdot \underset{\sim}{X} = \underset{\sim}{D}$$

where D_n

$$\begin{cases} F_n^R + a_n G_n^R - b_n G_n^I & (n = 1, \ldots\ldots, N) \\ F_{n-N}^I + a_{n-N} G_{n-N}^I - b_{n-N} G_{n-N}^R & (n = N+1, \ldots, 2N) \end{cases}$$

and

$$\left\{ \begin{aligned} S_{ij} &= (1 + a_i a_j)\binom{RR}{ij} - a_j b_i \binom{RI}{ji} - a_i b_j \binom{RI}{ij} + b_i b_j \binom{II}{ij} \\ -S_{i,j+N} &= a_i b_j \binom{RR}{ij} - b_i b_j \binom{RI}{ji} + (1+a_i a_j)\binom{RI}{ij} - a_j b_i \binom{II}{ij} \\ S_{i+N,j} &= a_j b_i \binom{RR}{ij} + (1+a_i a_j)\binom{RI}{ji} - b_i b_j \binom{RI}{ij} - a_i b_j \binom{II}{ij} \\ -S_{i+N,j+N} &= b_i b_j \binom{RR}{ij} + a_i b_j \binom{RI}{ji} + a_j b_i \binom{RI}{ij} + (1+a_i a_j)\binom{II}{ij} \end{aligned} \right\}$$

all for $i = 1, \ldots\ldots, N$; $j = 1, \ldots\ldots, N$. The solutions B_n^R, B_n^I are related to the solutions X_n by

$$\left\{ \begin{aligned} B_n^R &= X_n & n &= 1, \ldots\ldots, N \\ B_n^I &= X_{n+N} & n &= 1, \ldots\ldots, N \end{aligned} \right\}$$

References

Bloor, M.I.G. 1968 Phys. Med. Biol., 13, 443.

Bugliarello, G., H.J.Day, A. Brant, A.J. Eggenburger & G.C.C. Hsiao 1966 Proc. First Int. Conf. Haemorheology, Reykjavik, p305 (Pergamon, 1968).

Gross, J.F. 1969 Euromech 12, Jablonna.

Landis, E. & J.R. Pappenheimer 1963 In: Handbook of Physiology, Section 2, I. (Amer. Physiol. Soc., Washington, D.C., 1963).

Luft, J.H. 1966 Federation Proc., 25, 1773.

Prothero, J. & A.C. Burton 1962 Biophys. J., 2, 213.

Wang, H. & R. Skalak 1969 J. Fluid Mech., 38, 75.

Zidan, von M. 1969 Rheologica Acta, 8, 89.

Chapter V

A Model Capillary Flow Experiment

1. Introduction

The results obtained from the lubrication theory in Chapters II and III are perhaps somewhat surprising, particularly in view of established concepts involving relative ease of movement of red cells even in narrow capillaries. It seemed, therefore, desirable to test these findings experimentally, particularly the enhancement and non-linearity of resistance offered by the deformable erythrocytes to an applied pressure gradient.

In vivo measurements of capillary pressures and pressure gradients are very difficult - no satisfactory techniques have been developed which do not interfere unduly with the flow (although the null-flow, micropipette method of Wiederhielm (1966) seems to offer hope for the future). Qualitative and *in vitro* observations have been made which tend to confirm the theoretical predictions. The work of Dintenfass (1966) has already been mentioned; Krueger (1969) investigated the effects of increase of plasma viscosity (by lipid injection) on capillary flows. He found that on reduction of pressure gradient red cell velocities decreased gradually to a certain limit (for any individual

narrow capillary), when flow suddenly ceased (seize-up); the limiting velocity was raised by lipid injection. Furthermore, the velocities of cells in wider capillaries, where an appreciable plasma gap existed between cell and endothelium, were affected less than those for deformed cells in narrow capillaries. This work, however, does not provide convincing evidence that the approximate quantitative results are reasonable; neither do they give any indication of possible flaws in the assumptions of the theory.

Accordingly, a model experiment was devised, on a large scale, to investigate the behaviour of red cell analogues under approximate capillary flow conditions. The materials and apparatus were designed on the basis of the non-dimensional analyses of Chapter II; details of their selection and construction are described in sections 2 and 3. Results obtained verified the predictions remarkably well; in addition, observations enabled qualitative confirmation of the plasma flow patterns described in Chapter IV, and interesting new phenomena were brought to light.

2. Design of the Experiment

Two rather obvious considerations need to be borne in mind here: the apparatus should allow easy observation of the phenomena under discussion, and the Reynolds' numbers involved should simulate actual values as closely as

possible. Furthermore, the red cell models should be selected with some care; it is clearly desirable to have, not merely 'flexible' red cells, but models which quantitatively mimic the elastic behaviour of actual cells, in some suitable non-dimensional sense. This consideration is discussed later in some detail.

In view of the comments in Chapter II on the relative lack of distensibility of the capillary wall, a perspex tube (one inch in diameter (internal)) was used as a 'capillary'; the diameter was chosen to facilitate manufacture of 'red cells'; in addition, such a large diameter has the attraction of enabling easy observation of fluid flow fields. A 1.25 meter (approximately) length of tubing was fixed between 3-litre aspirator bottles, attached to a pressure source and manometer; the arrangement allowed application of a variable pressure difference in either direction. Provision was made for tilting the assembly, to allow smaller, accurately-measureable hydrostatic pressure differences to be applied. In all, a range of steady pressure differences from 0.5 to 20 cms Hg was obtainable.

The selection of a suitable 'plasma' was governed by the availability of a compatible red cell model. For example, the use of glycerol (kinematic viscosity about 10^3 centistoke) restricts the range of velocities to below

about 0.1 cms/sec, if Reynolds numbers are to be maintained below 10^{-2}. As demonstrated later, this requires a cell model with a membrane having a resistance to deformation little greater than the surface tension of water in air (about 70 dynes/cm), if values of the non-dimensional velocity parameter A are to be in the capillary-flow range. Such a model would obviously be quite difficult to manufacture; and 'haemolysis' would be a severe problem for any conceivable membrane material.

A silicone fluid supplied by ICI (FF 111/10000) was finally chosen; its kinematic viscosity was specified as 10^{4} centistoke. Accompanying data charts showed that the viscosity varied negligibly over a wide range of temperature, and that, for shear rates in the range required for the experiment, variation of viscosity was of the order of only one or two percent. For practical purposes, then, the fluid was virtually Newtonian.

The 'red cell' consisted of a thin latex membrane containing a mixture of water and glycerol, the proportions being selected to give virtually neutral bouyancy in the silicone fluid. The relatively low viscosity of the cell interior liquid was unimportant, since virtually no changes of shape were observed during the experiments; motions of the intracellular fluid must therefore have been minimal.

Plasticine moulds were coated with prevulcanized liquid latex; the moulds were of typical red cell shape and had a diameter of 3.5 cm. Variations in diameter and thickness were within the limits observed (e.g. Rand and Burton 1964) for normal human red cell populations. The coating was achieved by dipping, followed by judicious rotation to give a uniform final deposit. Any number of coats could be applied to avoid excessive fragility of the membrane. It was found that the internal volume of the 'red cells' averaged about 8 cc; this gives a gratifying agreement with the 'shape factor' (defined by Burton, 1966) for human red cells.

In principle, the resistance to deformation S (defined in Chapter II) can be measured in essentially the same way as was used by Rand and Burton for actual red cells. The pressure difference δp required to suck a hemisphere of membrane inside a small tube of radius r is obtained, and S is calculated from the formula

$$\delta p = \frac{2S}{r} \quad .$$

In practice, however, the relatively large pressure differences needed for this operation mean that severe frictional artifacts are introduced into the measurements - the membrane tends to stick to the end of the tube. Lubrication of the surface is ineffective, since the lubricating films are rapidly extruded. When frictional restraints are large, el-

astic resistance to the formation of a membrane hemisphere will become disproportionately large, compared with the bending moment contribution.

Consequently, only a very approximate value of S can be obtained; this is perhaps most consistantly done by observing the pressure difference when a curved 'dome' begins to appear in the membrane inside the tube, and estimating an effective radius of curvature for the dome. Smaller pressure differences are required, and errors caused by friction are reduced.

Measurements made in this way indicate that the value of S characteristic of the red cells used was of the order of 10^{4} dyne/cm; this value was for the most flexible membrane attainable which did not rupture during the course of the experiment. A corresponding order-of-magnitude value for β, the red cell compliance in the capillary (computed from $\beta = r_o^2/15S$, r_o the capillary radius) is 10^{-5} cc/dyne, or 10^{-2} cms/cm H_2O.

3. Selection of Material Parameters

The radius of the capillary has already been specified; further, the choice of cell deformability has been determined by fragility limitations. The red cell diameter is, of course, constrained by the need to make the tube

represent a capillary of some required size; for the diameter used here (3.5 cms), flow in a 6 μm capillary (approx.) is simulated. Two further parameters (plasma viscosity μ and cell velocity U) may be selected to give accurate model similarity.

Two considerations govern this selection; firstly, the Reynolds' number should be no greater than about 10^{-2} for the maximum velocity (U_{max}) envisaged:

$$\frac{r_o U_{max}}{\nu} \sim 10^{-2} , \qquad (3.1)$$

where $\nu = \mu/\rho$; here $\rho = .975$ gm/cc. Secondly, the non-dimensional velocity parameter A, defined in Chapter II as

$$A = \mu U \beta / r_o^2 (\kappa r)^{\frac{1}{2}},$$

should take a value appropriate to typical capillary flow (say 10^{-3}) for $U = U_{max}$; since $(\kappa r_o)^{\frac{1}{2}}$ is approximately unity, this requirement becomes

$$\frac{\mu U_{max} \beta}{r_o^2} \sim 10^{-3} \qquad (3.2)$$

Essentially, A compares the viscous resistance of the lubricating fluid with the elastic resistance of the cell membrane, and is clearly the important parameter to consider when making a selection of compatible values for μ, U, and β.

Substitution of $\beta = 10^{-5}$, $r = 1.27$ cms shows that

should be approximately 100 poise, and U_{max} of the order of 1 cm/sec. It is interesting that if a less viscous, but still plausible, plasma simulator such as glycerol (μ = 10 poise) is used, U_{max} is of the order 0.1 cm/sec, and a compatible value of S for the membrane is about 100 dyne/cm, little greater than the surface tension of water. The absurdity of such a requirement underlines the necessity for careful consideration of the deformability factors in the design of a model experiment of this kind.

It was found that about 10 cells in the tube gave good results with a minimum of experimental difficulty; measurements were taken in two series, one with 12 cells, one with 9. These correspond to 'haematocrits' of 28% and 20% respectively. With these numbers of cells, pressure gradients needed for velocities in the desired range were within the available limits.

4. Qualitative Observations

Before detailed quantitative results are presented, a brief discussion will be given of several interesting features of the model, observed in the course of the experiments.

(i) The predominant mode of deformation of the cells was some variant of the rolled-up, 'crepe-suzette' configuration;

very few had orientations even approaching the 'parachute' mode discussed in Chapter II. The importance of this for cell clearances is discussed later. Furthermore, the geometry of the region of constriction was considerably more complicated than the single smooth narrowing and widening assumed in the theory. This is not necessarily a severe problem, since each of the local lubrication zones could be considered separately; however, the existance of relatively resistance-free, 'dimpled' regions, in association with constrictions, on the cell rim introduces some difficulties in interpretation of the results in terms of the parameter E defined in Chapter II see (later).

Furthermore, in some cases there were sections of the rim with no constricted lubrication zone; fluid could be observed leaking forward in such regions. This forward flow is due to the relatively high pressure gradient across the red cell, determined in the regions where lubrication is occurring; in unconstricted regions this pressure gradient must be balanced by the viscous dissipation associated with a relatively large, forward, fluid flux. Under certain conditions, this may give a net forward flux of plasma instead of the leakback necessary for fully lubricated cells. In vivo circumstances may be envisaged where plasma from a labelled bolus of blood emerges from a capillary before the

labelled cells.

(ii) Successive application of pressure differences in alternate directions produced a gradual separation of the line of cells; this became a problem during the experiments, reducing the available traverse, and was the principal reason for limiting the haematocrit to below 30%. The phenomenon may have some connection with the observation of Monro (1966) that (actual) red cells tend to become uniformly spaced in narrow capillaries; it will be recalled that such capillaries are subject to random fluctuations in pressure gradient due to vasomotion in arterioles or closure of precapillary sphincters.

(iii) Streamlines in the plasma were observed with the aid of small bubbles (which proved to be stable for some hours) and impurities (actually tiny globules of water-glycerol from the accidental haemolysis of one of the cells). The concentration of these indicators was small, and it was assumed that they had no appreciable effect on the viscosity of the plasma.

Toroidal motions in the plasma boli were strikingly apparent, even when the inter-erythrocyte distance was comparatively small. The intrusion of some streamlines into the entry and exit regions of the lubrication zones was also clearly observable. Bubbles in such streamlines re-

mained in close proximity to the cell membrane for considerable periods of time, indicating that fluid velocities in these areas were comparatively small (as might be expected in view of their close approach to the stagnation point separating the intruding flow from the leakback flow of the lubrication). This feature of the flow may well be of importance for the transport of oxygen.

Leakback of fluid through the lubrication zones was evident from the behaviour of indicator particles very close to the tube wall. It is interesting that when bubbles passed through a lubrication zone, they frequently 'stuck' with their trailing edges just at the end of the constriction. This may be interpreted as evidence of the existence of a 'necking', and a local pressure minimum, at that point. For a bubble to be able to pass through such a constriction, the free energy required for deformation of the bubble surface is supplied by the (positive) pressure gradient in the central part of the lubrication region doing work on the bubble; this gradient runs from the peak between entry and central zones to the minimum at the boundary between central and exit zones. As the leading edge of the bubble enters the (adverse) pressure gradient in the exit zone, free energy is lost; when the last of the bubble approaches the neck, there may not be enough energy left for the trailing edge

to deform sufficiently to pass through.

5. The Quantitative Experiment

The principal motivation for the experiment was to test the pressure-flow relationships for such a system. The cell velocity U was measured for a range of applied pressure differences Δp, using two techniques: firstly, tilting of the assembly (see Fig. 1), enabling hydrostatic pressure differences up to about 50 cms H_2O (3.5 cms Hg) to be attained; secondly, by pressurization of the apparatus using compressed nitrogen, followed by release of pressure at one end. The pressures were recorded on a manometer; differences of some 20 cms Hg were obtainable.

While the first method provides an accurate means of measuring the applied pressure difference, the second may be subject to error, owing to the use of a compressible fluid as the pressurizing medium. In practice, it was found to be quite difficult to maintain a steady pressure at the pressurized end of the system while motion was occurring in the capillary. The following procedure was adopted: for any given setting of the needle valve controlling the gas flow, the limiting value to which the pressure tended during motion was obtained by trial and error. The entire system was then pressurized, the pressure at one end being re-

leased as the limiting pressure was reached at the manometer. It was found that the pressure, measured at the manometer, subsequently remained stationary during flow, and did not do so for any other initial pressure. Although this technique gave reasonably consistent results for various pressures and velocities, it is still not certain that the pressure measured at the manometer is equal to that at the plasma surface. Consequently, the results obtained by this method should perhaps be viewed with some caution; the region of greatest interest, however, is that where pressure differences are obtained by tilting.

The results are most conveniently displayed in terms of the non-dimensional parameters defined in Chapter II. Firstly, the resistance enhancement parameter D compares pellet resistance to that for Poiseuille flow in the same length of the fluid alone, for which D=16. The value of D corresponding to a measured pair of values of U and Δp may be obtained as follows. Suppose the length of the tube is ℓ, and that the cells occupy a fraction γ of the length (haematocrit $100\gamma\%$). Then the pressure drop for flow of plasma alone, at the same mean velocity U, is

$$\Delta p_f = \frac{8\mu U \ell}{r_o^2} \quad ; \qquad (5.1)$$

the drop for the length occupied by cells is $\gamma \Delta p_f$, and for

the remainder $(1-\gamma)\Delta p_f$. Evidently, D may now be calculated from the formula

$$D = 16\left[\Delta p - (1-\gamma)\Delta p_f\right] / \gamma \Delta p_f \quad , \qquad (5.2)$$

where the term in square brackets is the pressure drop across the cells. If there are N cells present, the pressure drop across each is clearly

$$\delta p = (\Delta p - (1-\gamma)\Delta p_f)/N \quad . \qquad (5.3)$$

Denote the length of each cell by b; this is equal to $2(Kr_o)^{-\frac{1}{2}} r_o$ for the model used in Chapter II; and clearly a calculation of D based on the formula

$$D = \frac{\delta p . r_o}{\mu U (Kr_o)^{\frac{1}{2}}} = \frac{2r_o^2\left[\Delta p - (1-\gamma)\Delta p_f\right]}{\mu U b N}$$

of Chapter II (p63) is equivalent to the definition (5.2). Simmilarly, values for the non-dimensional velocity parameter A can be obtained from the formula

$$A = \frac{\mu U \beta}{r_o^2 (Kr_o)^{\frac{1}{2}}} = \frac{\mu U \beta b}{2r_o^3} \qquad (5.4)$$

It will be useful to compute values of E also; these are most readily obtained by observing, from the formulae on p65, that

$$E = A.D \quad . \qquad (5.5)$$

Experimental results are presented in Fig. 2, as a graph of D against A; the dots show experimental points.

The rapid increase of D with decreasing A is very striking, and extremely satisfying from the point of view of confirming the predictions of Chapter II. Accurate measurements of smaller velocities and pressure gradients than those recorded was very difficult; and at a pressure difference of 3.65 mm Hg, complete seize-up was observed. (The pressure difference corresponding to the lowest velocity measured is 4.04 mm Hg.)

The somewhat surprising shape of the curve, with a point of inflection near $A = 10^{-4}$, may be due to an artifact introduced by errors of measurement of the higher pressure differences. If not, however, the inflection may be evidence of two separate resistance-increasing mechanisms. Variations of large-scale deformation, affecting clearances, produce increases in D which would be more apparent at high pressure gradients, and would account for the steeper slope of the D-A curve at larger values of A. At the smaller velocities, the increasing effect of elastic control over the lubrication process would again produce a more rapid increase of D.

It is interesting that, due to non-uniformity of manufacture, one of the cells offered less resistance than the others, and moved at a slightly higher velocity. This effect became more marked at low velocities, as would be

expected from the non-linearity predictions of the theory; the disparity was negligible for D< 200, while for D∼900 the value of A for the less resistant cell was about 1.7 times the mean A.

The dependence of resistance on capillary diameter was demonstrated as the cells approached the ends of the capillary, where the diameter decreased, over a distance of about 1.2 cms, to 1.6 cms. It was possible, by application of a sufficiently high ~~high~~ pressure difference, to force one or more cells through the narrow portion; the accompanying increase of resistance, and reduced velocity, were clearly apparent. Confirmation was obtained also of Burton's (1966) observation that (actual) red cells haemolysed when forced through capillaries of diameter smaller than some critical value. In this case, one of three cells accidentally forced into the reservoir haemolysed in the 1.6 cm diameter section.

Although the main purpose of the experiment was to demonstrate the applicability of the theoretical pressure-flow relationships to blood-capillary systems, it is instructive to compare the results obtained with the quantitative predictions for actual red cells in a 6 μm capillary. Ths comparison is made on the basis of the pressure gradient-clearance 'compatibility curves' of Fig. 3, Chapter II. A

similar curve may be plotted from the experimental results, using (5.5) to compute values for E. Fig. 3 of this chapter illustrates both theoretical and measured curves, on the same E-F axes as in Chapter II.

A striking feature of the comparison is that the model apparently exhibited clearance characteristics considerably more positive than the theoretical system. Two reasons for this can be advanced; firstly, uncertainties in the measurement of the 'resistance to deformation' of the model membrane will introduce errors into the calculation of the non-dimensional parameters A and E from the measured data. Although the form of the important velocity-resistance curve (Fig. 2) is not affected, the position of the origin for the A-scale is in some doubt.

Of more profound significance are the effects of the crepe-suzette mode of deformation observed for the models, as opposed to the parachute deformation assumed in Chapter II to facilitate analysis. In contrast to the above error in measurements of S, these effects are likely to be of importance when the theory is being applied to phenomena of red cell movement <u>in vivo</u>, since it is expected that the behaviour of the model closely parallels that of actual red cells.

It was found much easier to insert the red cell

models into the tube in the crepe-suzette shape than to try to force them in with a parachute configuration; in fact, one cell haemolysed when such forcing was attempted. This indicated that the clearance of the cells in the capillary was larger (i.e. easier fit) than for hypothetical cells in the parachute mode. Moreover, it is reasonable to expect a constriction-free section of the membrane to have a large, positive, local clearance; this would produce a larger mean value for the clearance parameter F.

The complex geometry of the lubrication zones, with 'dimples' and constricted sections juxtaposed, also needs consideration. The theory of Chapter II assumed that all of the cell length was involved in a single constricted lubrication region, and calculated values for the pressure drop across the cell on this assumption. Here, however, only part of the cell length is involved in the lubricating mechanism. Computations of D for comparison with the theory should be based, not on the haematocrit as in (5.2), but on the fraction of the total tube length actually occupied by a region of constriction.

Clearly, both of the effects of cell deformation geometry will tend to shift the experimental curve of Fig. 3 away from the predicted one in the manner shown; however, it is significant that the pressure gradient-clearance com-

patibility curves for experiment and theory are similar in form, demonstrating the decrease of clearance with decreasing pressure gradient. The rapid levelling off of the experimental curve as E falls below 10^{-2} is an indication of the onset of seize-up, although this may be due partly to the presence of surface asperities.

The significance of the experiment may be briefly summarized. It has been demonstrated that the elasto-hydrodynamic lubrication theory forms an excellent basis for a discussion of blood flow phenomena in narrow capillaries. However, for the detailed application of the numerical results to specific situations, the large-scale deformations of the red cells need to be more closely examined.

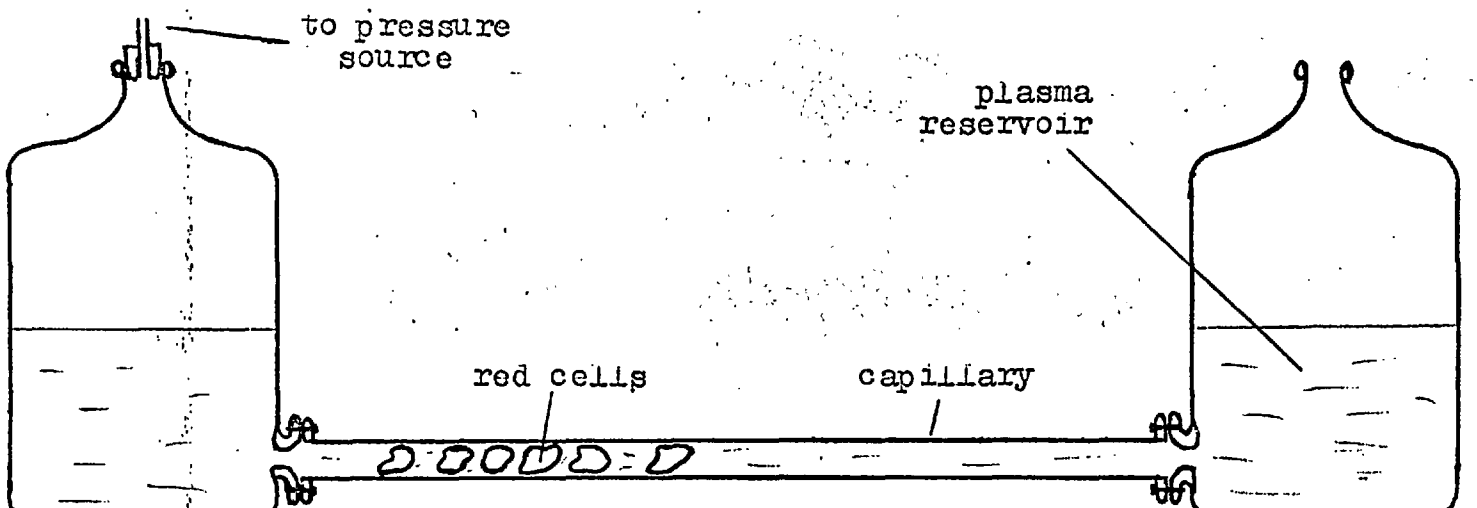


Fig. 1. Schematic diagram of apparatus.

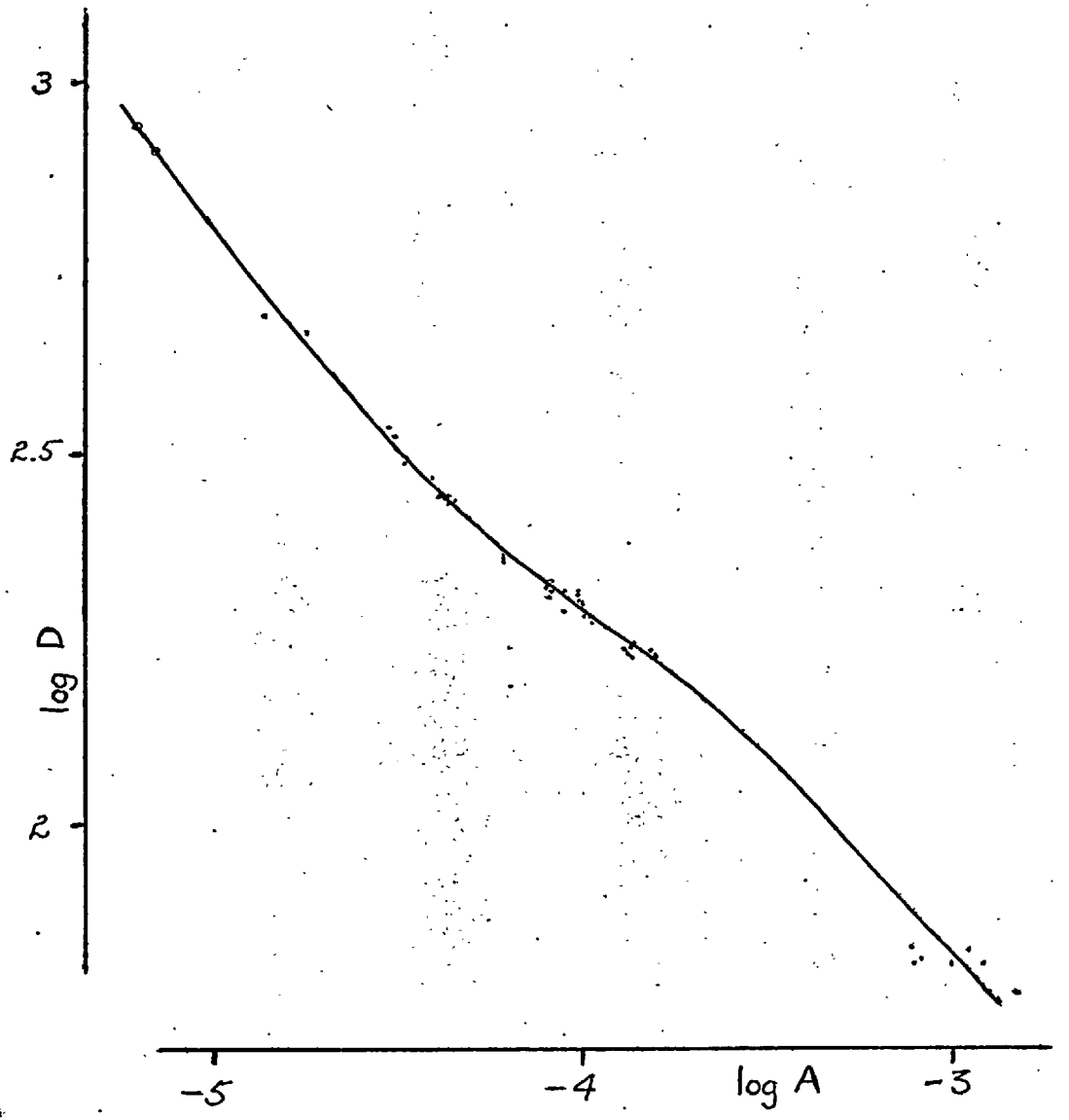


Fig. 2. Experimental velocity-resistance curve

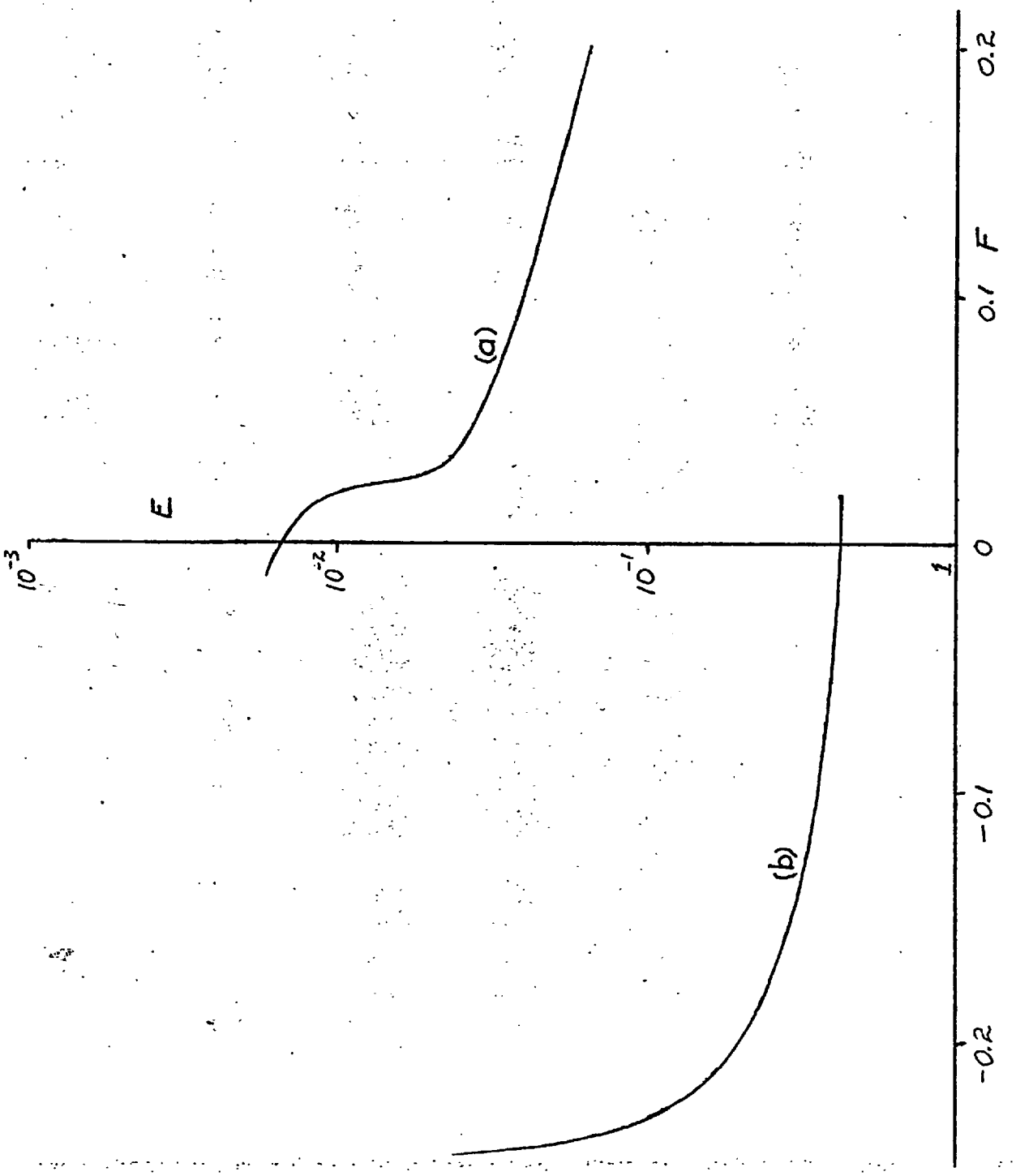


Fig. 3. Comparison of experimental (curve a) and theoretical (curve b) clearance characteristics.

References

Burton, A.C. 1966 Federation Proc., 25, 6, 1753.

Dintenfass, L. 1966 Proc. First Int. Conf. Haemorheology, Reykjavik, p297 (Pergamon, 1968).

Krocger, A. 1969 Euromech 12, Jablonna.

Monro, P.A.G. 1963 Biorheology, 1, 239.

Rand, R.P. & A.C. Burton 1964 Biophys. J., 4, 115.

Wiederhcilm, C.A., J.W. Woodbury, S. Kirk & R.F Rushmer 1964 Am. J. Physiol., 207 (1), 173.